



Calhoun: The NPS Institutional Archive

Theses and Dissertations

Thesis and Dissertation Collection

2016-06

Methodology to distinguish features in complex and congested underwater environments

Mitchelson, Matthew Arthur

Monterey, California: Naval Postgraduate School

<http://hdl.handle.net/10945/49717>



Calhoun is a project of the Dudley Knox Library at NPS, furthering the precepts and goals of open government and government transparency. All information contained herein has been approved for release by the NPS Public Affairs Officer.

Dudley Knox Library / Naval Postgraduate School
411 Dyer Road / 1 University Circle
Monterey, California USA 93943

<http://www.nps.edu/library>



NAVAL POSTGRADUATE SCHOOL

MONTEREY, CALIFORNIA

THESIS

**METHODOLOGY TO DISTINGUISH FEATURES IN
COMPLEX AND CONGESTED UNDERWATER
ENVIRONMENTS**

by

Matthew Arthur Mitchelson

June 2016

Thesis Advisor:

Noel du Toit

Second Reader:

Timothy H. Chung

Approved for public release; distribution is unlimited

THIS PAGE INTENTIONALLY LEFT BLANK

REPORT DOCUMENTATION PAGE			Form Approved OMB No. 0704-0188	
Public reporting burden for this collection of information is estimated to average 1 hour per response, including the time for reviewing instruction, searching existing data sources, gathering and maintaining the data needed, and completing and reviewing the collection of information. Send comments regarding this burden estimate or any other aspect of this collection of information, including suggestions for reducing this burden to Washington headquarters Services, Directorate for Information Operations and Reports, 1215 Jefferson Davis Highway, Suite 1204, Arlington, VA 22202-4302, and to the Office of Management and Budget, Paperwork Reduction Project (0704-0188) Washington DC 20503.				
1. AGENCY USE ONLY (Leave Blank)		2. REPORT DATE 06-17-2016	3. REPORT TYPE AND DATES COVERED Master's Thesis 07-04-2015 to 06-17-2016	
4. TITLE AND SUBTITLE METHODOLOGY TO DISTINGUISH FEATURES IN COMPLEX AND CONGESTED UNDERWATER ENVIRONMENTS			5. FUNDING NUMBERS	
6. AUTHOR(S) Matthew Arthur Mitchelson				
7. PERFORMING ORGANIZATION NAME(S) AND ADDRESS(ES) Naval Postgraduate School Monterey, CA 93943			8. PERFORMING ORGANIZATION REPORT NUMBER	
9. SPONSORING / MONITORING AGENCY NAME(S) AND ADDRESS(ES) N/A			10. SPONSORING / MONITORING AGENCY REPORT NUMBER	
11. SUPPLEMENTARY NOTES The views expressed in this document are those of the author and do not reflect the official policy or position of the Department of Defense or the U.S. Government. IRB Protocol Number: N/A.				
12a. DISTRIBUTION / AVAILABILITY STATEMENT Approved for public release; distribution is unlimited			12b. DISTRIBUTION CODE	
13. ABSTRACT (maximum 200 words) The underwater community involves researchers who conduct various work and experiments below the surface of Earth's oceans. Today's high-frequency sonar limitations do not provide sufficient information for the underwater community. There is a pressing need to increase the accuracy of detection, identify items detected and obtain knowledge of missing details. Currently, no standard methodology exists to evaluate the accuracy and completeness of sonar and detection algorithms; this is critical because both are required to use sonar effectively. Such a methodology is required for the evaluation and comparison of sensors and algorithms. This research investigated a proposed methodology to evaluate effectively underwater perception in complex underwater environments. This methodology considered the challenges of underwater localization and other design factors during the use of a mobile autonomous underwater vehicle and high-frequency sonar, and the employment of underwater signal and image processing techniques. The focus of this research and contribution to the underwater community is an initial robust methodology the underwater community may use to obtain relevant data sets. Furthermore, researchers can apply those data sets to custom perceptrons and algorithms, and evaluate whether or not these custom methods are capable of detecting the known features while quantifying the missed features. Ultimately, the results of the signal and image processing, compared to the defined ground truth, demonstrated that the use of the high-frequency sonar was not capable in distinguishing all smaller features and gaps between underwater structures.				
14. SUBJECT TERMS enhanced methodology, acoustic baseline, autonomous underwater vehicle, image processing algorithm, high-frequency sonar			15. NUMBER OF PAGES 139	
			16. PRICE CODE	
17. SECURITY CLASSIFICATION OF REPORT Unclassified	18. SECURITY CLASSIFICATION OF THIS PAGE Unclassified	19. SECURITY CLASSIFICATION OF ABSTRACT Unclassified	20. LIMITATION OF ABSTRACT UU	

NSN 7540-01-280-5500

Standard Form 298 (Rev. 2-89)
Prescribed by ANSI Std. Z39-18

THIS PAGE INTENTIONALLY LEFT BLANK

Approved for public release; distribution is unlimited

**METHODOLOGY TO DISTINGUISH FEATURES IN COMPLEX AND
CONGESTED UNDERWATER ENVIRONMENTS**

Matthew Arthur Mitchelson
Lieutenant, United States Navy
B.S., United States Naval Academy, 2009

Submitted in partial fulfillment of the
requirements for the degree of

MASTER OF SCIENCE IN SYSTEMS ENGINEERING

from the

**NAVAL POSTGRADUATE SCHOOL
June 2016**

Approved by: Noel du Toit
Thesis Advisor

Timothy H. Chung
Second Reader

Ronald Giachetti
Chair, Department of Systems Engineering

THIS PAGE INTENTIONALLY LEFT BLANK

ABSTRACT

The underwater community involves researchers who conduct various work and experiments below the surface of Earth's oceans. Today's high-frequency sonar limitations do not provide sufficient information for the underwater community. There is a pressing need to increase the accuracy of detection, identify items detected and obtain knowledge of missing details. Currently, no standard methodology exists to evaluate the accuracy and completeness of sonar and detection algorithms; this is critical because both are required to use sonar effectively. Such a methodology is required for the evaluation and comparison of sensors and algorithms. This research investigated a proposed methodology to evaluate effectively underwater perception in complex underwater environments. This methodology considered the challenges of underwater localization and other design factors during the use of a mobile au-tonomous underwater vehicle and high-frequency sonar, and the employment of underwater signal and image processing techniques. The focus of this research and contribution to the underwater community is an initial robust methodology the underwater community may use to obtain relevant data sets. Furthermore, researchers can apply those data sets to custom perceptors and algorithms, and evaluate whether or not these custom methods are capable of detecting the known features while quantifying the missed features. Ultimately, the results of the signal and image processing, compared to the defined ground truth, demonstrated that the use of the high-frequency sonar was not capable in distinguishing all smaller features and gaps between underwater structures.

THIS PAGE INTENTIONALLY LEFT BLANK

Table of Contents

1	INTRODUCTION	1
1.1	Motivation	1
1.2	Needs Analysis and Capability Gaps.	2
1.3	Literature Review	4
1.4	Community Contribution	6
2	FUNDAMENTALS OF PERCEPTION IN THE UNDERWATER COMMUNITY	9
2.1	Underwater Acoustic Sensors	10
2.2	Underwater Electro-Optical Sensors	20
2.3	Environment	23
2.4	Perception	29
3	EXPERIMENTAL DESIGN	37
3.1	Rig Design.	38
3.2	ACQUAS	41
3.3	Measures of Performance	43
3.4	Data Collection Methodology	44
4	ANALYSIS	51
4.1	Sonar Theory Applied to the BlueView P900	51
4.2	Sonar Image Interpretation	52
4.3	Results	54
5	CONCLUSION	83
5.1	Summary	83
5.2	Near-Term Improvements	84
5.3	Recommendation for Future Work	88
	Appendix: EXAMPLE FIGURES AND DATA ANALYSIS TABLES	89

A.1	Data Set 11-51-36 Sample Analysis	89
A.2	Data Set 12-09-07 Sample Analysis	91
	List of References	101
	Initial Distribution List	107

List of Figures

Figure 1.1	Systems engineering waterfall model	3
Figure 2.1	Wenz acoustic ambient noise in the ocean curves	14
Figure 2.2	Snell's Law applied to multiple layers	16
Figure 2.3	Inertial measurement unit	24
Figure 2.4	Inertial navigation system	24
Figure 2.5	Ground truth compared to sonar detections	27
Figure 2.6	Step 1 of the ground truth overlay	27
Figure 2.7	Verification of rig outline alignment	28
Figure 2.8	Defined starting point	28
Figure 2.9	Ground truth defined	29
Figure 2.10	Raw image	30
Figure 2.11	The effects of Gaussian blurring	31
Figure 2.12	Thresholding applied	32
Figure 2.13	Eroded image	32
Figure 2.14	Algorithm I final image	33
Figure 2.15	Image example of edge detection	34
Figure 2.16	Example of dilating an image	34
Figure 2.17	Final product through the use of Algorithm II	35
Figure 3.1	BlueView P900 sonar	40
Figure 3.2	Finished Platform Golf in CAVR bay	40
Figure 3.3	Finished Platform Tango in CAVR bay	41

Figure 3.4	Modified (tethered, autonomous) SeaBotix ACQUAS	43
Figure 3.5	Location of Initial - US Coast Guard Pier Monterey, CA	44
Figure 3.6	Location of Contingency - Stevenson School aquatics facility Pebble Beach, CA	45
Figure 3.7	Initial setup position of the vehicle on Platform Tango	46
Figure 3.8	ACQUAS positioned to begin lateral data extraction on Platform Tango	47
Figure 3.9	ACQUAS sweeping Platform Tango	48
Figure 3.10	ACQUAS data extraction on Platform Golf	49
Figure 4.1	Example of errors within sonar signal processing	52
Figure 4.2	Raw sonar image - forward insonification at 5 meter standoff; Platform Tango	57
Figure 4.3	Example of Algorithm I based on the applied forward insonification at 5 meter standoff; Platform Tango	57
Figure 4.4	Example of Algorithm II based on the applied forward insonification at 5 meter standoff; Platform Tango	58
Figure 4.5	Average probability of feature detection based on the applied forward insonification at 5 meter standoff; Platform Tango	58
Figure 4.6	Example of raw sonar image based on the applied lateral movement at 5 meters standoff; Platform Tango	60
Figure 4.7	Example of Algorithm I based on the applied lateral movement at 5 meters standoff; Platform Tango	61
Figure 4.8	Example of Algorithm II based on the applied lateral movement at 5 meters standoff; Platform Tango	61
Figure 4.9	Average probability of feature detection based on the applied lateral movement at 5 meters standoff; Platform Tango	62
Figure 4.10	Sonar image based on image processing of Algorithm II applied to the sweeping movement at 5 meters standoff; Platform Tango	63

Figure 4.11	Example of raw sonar image based on the applied sweeping movement at 5 meters standoff; Platform Tango	64
Figure 4.12	Example of Algorithm I based on the applied sweeping movement at 5 meters standoff; Platform Tango	64
Figure 4.13	Example of Algorithm II based on the applied sweeping movement at 5 meters standoff; Platform Tango	65
Figure 4.14	Average probability of feature detection based on the applied sweeping movement at 5 meters standoff; Platform Tango	65
Figure 4.15	Example of raw sonar image based on the applied forward insonification at 7 meters standoff; Platform Tango	67
Figure 4.16	Example of Algorithm I based on the applied forward insonification at 7 meters standoff; Platform Tango	67
Figure 4.17	Example of Algorithm II based on the applied forward insonification at 7 meters standoff; Platform Tango	68
Figure 4.18	Average probability of feature detection based on the applied forward insonification at 7 meters standoff; Platform Tango	68
Figure 4.19	Example of raw sonar image based on the applied forward insonification at 1.5 meters standoff; Platform Tango	69
Figure 4.20	Sonar image with ground truth defined based on the applied lateral movement at 5 meters standoff; Platform Golf	70
Figure 4.21	Example of raw sonar image based on the applied lateral movement at 5 meters standoff; Platform Golf	71
Figure 4.22	Example of Algorithm I based on the applied lateral movement at 5 meters standoff; Platform Golf	71
Figure 4.23	Example of Algorithm II based on the applied lateral movement at 5 meters standoff; Platform Golf	72
Figure 4.24	Average probability of gap detection based on the applied lateral movement at 5 meters standoff; Platform Golf	72
Figure 4.25	Example of raw sonar image based on the applied forward insonification at 7 meters standoff; Platform Golf	73

Figure 4.26	Example of Algorithm I based on the applied forward insonification at 7 meters standoff; Platform Golf	74
Figure 4.27	Example of Algorithm II based on the applied forward insonification at 7 meters standoff; Platform Golf	74
Figure 4.28	Average probability of gap detection based on the applied forward insonification at 7 meters standoff; Platform Golf	75
Figure 4.29	True negatives produced via Algorithm I based on the applied sweeping movement at 5 meters standoff; Platform Golf	76
Figure 4.30	Example of raw sonar image based on the applied sweeping movement at 5 meters standoff; Platform Golf	77
Figure 4.31	Example of Algorithm I based on the applied sweeping movement at 5 meters standoff; Platform Golf	77
Figure 4.32	Example of Algorithm II based on the applied sweeping movement at 5 meters standoff; Platform Golf	78
Figure 4.33	Average probability of gap detection based on the applied sweeping movement at 5 meters standoff; Platform Golf	78
Figure 4.34	Example of raw sonar image based on the applied lateral movement at 1.5 meters standoff; Platform Golf	80
Figure 4.35	Example of Algorithm I based on the applied lateral movement at 1.5 meters standoff; Platform Golf	80
Figure 4.36	Example of Algorithm II based on the applied lateral movement at 1.5 meters standoff; Platform Golf	81
Figure 4.37	Average probability of gap detection based on the applied lateral movement at 1.5 meters standoff; Platform Golf	81
Figure 5.1	Example of corrected gap reestablishment in Platform Golf . . .	87
Figure A.1	Example of raw sonar image 0 - forward insonification at 7 meter standoff - Platform Tango	89
Figure A.2	Example of Algorithm I applied to image 0 - forward insonification at 7 meter standoff - Platform Tango	90

Figure A.3	Example of Algorithm II applied to image 0 - forward insonification at 7 meter standoff - Platform Tango	90
Figure A.4	Example of raw sonar image 50 - forward insonification at 7 meter standoff - Platform Tango	91
Figure A.5	Example of Algorithm I applied to image 50 - forward insonification at 7 meter standoff - Platform Tango	91
Figure A.6	Example of Algorithm II applied to image 50 - forward insonification at 7 meter standoff - Platform Tango	92
Figure A.7	Example of raw sonar image 303 - forward insonification at 7 meter standoff - Platform Tango	92
Figure A.8	Example of Algorithm I applied to image 303 - forward insonification at 7 meter standoff - Platform Tango	93
Figure A.9	Example of Algorithm II applied to image 303 - forward insonification at 7 meter standoff - Platform Tango	93
Figure A.10	Example of raw sonar image 0 - forward insonification at 7 meter standoff - Platform Golf	95
Figure A.11	Example of Algorithm I applied to image 0 - forward insonification at 7 meter standoff - Platform Golf	95
Figure A.12	Example of Algorithm II applied to image 0 - forward insonification at 7 meter standoff - Platform Golf	96
Figure A.13	Example of raw sonar image 25 - forward insonification at 7 meter standoff - Platform Golf	96
Figure A.14	Example of Algorithm I applied to image 25 - forward insonification at 7 meter standoff - Platform Golf	97
Figure A.15	Example of Algorithm II applied to image 25 - forward insonification at 7 meter standoff - Platform Golf	97
Figure A.16	Example of raw sonar image 50 - forward insonification at 7 meter standoff - Platform Golf	98
Figure A.17	Example of Algorithm I applied to image 50 - forward insonification at 7 meter standoff - Platform Golf	98

Figure A.18 Example of Algorithm II applied to image 50 - forward insonifica-
tion at 7 meter standoff - Platform Golf 99

List of Tables

Table 3.1	Building Material Information	42
Table A.1	Sample of Data Set 11-51-36 Sonar Analysis	94
Table A.2	Sample of Data Set 11-51-36 Algorithm Analysis - binary step . .	94
Table A.3	Sample of Data Set 12-09-07 Sonar Analysis	95
Table A.4	Sample of Data Set 12-09-07 Algorithm Analysis - binary step . .	100

THIS PAGE INTENTIONALLY LEFT BLANK

List of Acronyms and Abbreviations

2D	two-dimensional
3D	three-dimensional
AA	Achieved Availability
ACQUAS	Agile Close-Quarters Underwater Autonomous System
AOI	areas of interest
AO	area of operation
AUV	Autonomous Underwater Vehicle
CAVR	Center for Autonomous Vehicle Research
DC	Direct Current
DOD	Department of Defense
DVL	Doppler Velocity Logs
EKF	Extended Kalman Filter
EO	electro optical
FBN	feature-based navigation
FLS	forward-looking sonar
FOM	figure of merit
FOV	field of view
FSW	feet seawater
GPS	Global Positioning System
Hz	hertz

hd	high definition
IAW	in accordance with
INS	inertial navigation systems
IOP	inherent optical properties
kHz	kilohertz
LED	Light Emitting Diode
LBL	long baseline
MATLAB	Matrix Laboratory
MCM	Mine Counter Measure
MHz	megahertz
Mk	Mark
MOE	measures of effectiveness
MOP	Measures of performance
MPa	mega pascals
MSW	meters seawater
NASA	National Aeronautics and Space Administration
NEEMO	NASA Extreme Environment Mission Operations
NOAA	National Oceanic and Atmospheric Administration
NODC	National Oceanographic Data Center
NPS	Naval Postgraduate School
PMS	preventative maintenance system
PCR	pulse compression ratio

PD	Parameter design
POI	point of interest
ppt	parts per thousand
PVC	Polyvinyl Chloride
PW	pulse width
RANSAC	Random Sampling and Consensus
REMUS	Remote Environmental Monitoring UnitS
RFI	Request for Information
RL	reverberation level
ROC	receiver operating characteristics
ROV	remote operated vehicle
SA	situational awareness
scuba	self-contained underwater breathing apparatus
SE	systems engineering
SEP	systems engineering process
SL	source level
SLAM	Simultaneous Localization and Mapping
SNR	signal-to-noise ratio
sonar	sound navigation and ranging
SOP	standard operating procedure
SoS	system of systems
TAN	terrain-aided navigation

THAUS	Tethered Hovering Autonomous Underwater System
TOF	time of flight
TS	target strength
U.S.	United States
USA	United States of America
USBL	ultra-short baseline
USP	Underwater Staging Platforms
UUV	Unmanned Underwater Vehicle
WWI	World War I
WWII	World War II

Executive Summary

Light (and other electro-optical signals) does not travel far through water. The underwater community involves researchers who conduct various work and experiments below the surface of Earth's oceans. Today, the underwater community utilizes sonar as one of the primary tools to sense the environment and produce underwater maps. The production of underwater maps enable researchers to minimize the risk of underwater collisions and enhances the ability to interpret the smaller details within the operational environment. A pressing need within the underwater community is to increase the accuracy of detection and know what is seen, or greater yet, what details are missed due to today's high-frequency sonar limitations. Currently, no standard methodology exists to evaluate the accuracy and completeness of sonar and detection algorithms; this is critical because both are required to use sonar effectively. Thus, a methodology is required for the evaluation and comparison of sensors and algorithms. This research established a proposed methodology to evaluate underwater perception in complex underwater environments. This methodology considered the challenges of underwater localization and other design factors during the use of a mobile autonomous underwater vehicle, a high-frequency sonar, and employing underwater signal and image processing techniques. Furthermore, this methodology includes two example perceptors for the analysis of data sets collected from the Stevenson School aquatics facility located in Pebble Beach, CA. The focus of this research and contribution to the underwater community is an initial robust methodology to obtain relevant data sets, apply those data sets to custom perceptors and algorithms, and evaluate whether or not these custom methods are capable of detecting the known features while quantifying the missed features.

The emergence of unmanned underwater systems is exciting yet also challenging. In such an alien environment, understanding where one is becomes quite challenging. The requirement to understand what is present in the sea and how that affects those individuals within it was first understood by Leonardo Da Vinci in 1490 when he proposed that an individual could hear the sounds of approaching maritime vessels by listening to sounds underwater. For centuries, this concept was investigated until Mr. Lewis Dixon successfully invented a sonar system for the detection of icebergs in 1906 [1]. Soon thereafter, the application of sonar was used during World War I (WWI) for submarine detection.

Today, the use of sound navigation and ranging (sonar) has many applications to the underwater community. As seen through the tragedy that struck the RMS Titanic in April 1912, the use of shipboard sonar had and still has its limitations in regards to accurate object detection and obstacle avoidance [2]. It is not merely a question as simple as what one can detect, but rather a question of how one uses the data extracted from the sonar. In the underwater community today, a plethora of processing algorithms and perceptrons exist, but none precisely depict what the environment actually is [3]. From the standpoint of industry and the military, the loss of life and resources is undesirable, especially through a correctable methodology. During World War II (WWII), the United States (U.S.) Navy submarine force suffered the highest casualty percentage of all American armed forces at the time, losing roughly one in five deployed boats, largely due to the unfortunate limitations of underwater identification [4]. Should the same horrific numbers surface in today's operational environment, the aftermath would certainly warrant elevating the urgency of enhanced undersea technologies. Thus, it behooves the underwater community to continue to seek out an accurate methodology that not only enables current sonar to capture what is there but also enable a standardized methodology to evaluate the data obtained and information extracted.

Although there are many sophisticated processing methods utilized commercially and within the Department of Defense (DOD), none claim to provide a ground truth: the actuality of the area of operation (AO) [5]. The ability to define the ground truth data allows for the calibration of sonar and assists in the understanding of what is actually being observed or missed. More specifically, ground truth involves a process in which detections in the sonar image are compared to what is physically present in order to verify the sonar detections. For example, in the case of a sonar frame, ground truth aids in determining the accuracy of the detection performed by sensing software, and allows for the classification of the detections, including both the error rates of the sensor and of the detection algorithms [6].

In an attempt to determine a methodology to utilize for the work of this thesis, many methods were considered. However, with regard to object detection, no standardized data sets or methodology have currently been established as the underwater community standard. The direction of this thesis then deviated to address this gap, and concluded that the underwater community requires a standardized methodology in order to evolve the application of

object detection and enhanced mapping. The contribution of this work to the underwater community is an initial robust methodology with which the community may obtain relevant data sets, apply those data sets to custom preceptors and algorithms, and evaluate whether or not these custom methods are capable of detecting the known features while quantifying the missed features.

What does it take to build a representation of the underwater environment? In an attempt to answer this question, the community needs to enhance its understanding of the three factors which make underwater sensing difficult to then allow the researcher to build an accurate representation; these three factors are the underwater environment, sensor used, and the perception capability.

1. *Environment*: The environment refers to knowing what a researcher is looking at (ground truth) and from where (localization).
2. *Sensing*: Sensing refers to the mechanism to measure the environment.
3. *Perception*: Extracting useful information from measurements obtained in the environment from the sensor data.

Whether it be through the use of active sonar or electro optical (EO) cameras, imaging the details of underwater objects remains a challenge [7]. The trifecta required for map production requires knowledge of two factors to provide the inference of the third; the effectiveness of the trifecta is demonstrated through its application within the Mine Counter Measure (MCM) community [8]. However, although many perception methodologies are utilized in the community today, none is recognized as the community standard for accurate map production [9].

What must be considered when designing an experiment that allows for the accurate representation of the underwater environment? The underwater community's capability gap is the inability to accurately distinguish features, specifically those too small to detect using common methods, within congested environments. The trifecta drove the development of the experimental design and consideration of what targets the underwater community, specifically naval divers, tend to encounter in the littorals. Thus, two similar yet distinct targets were constructed to provide the ground truth element while an Autonomous Underwater Vehicle (AUV) carried a high frequency sonar providing the sensor element.

1. The motivation of Platform Golf is to establish a baseline of the forward-looking sonar (FLS) ability to observe and extract information of spaces between objects (i.e., gaps).
2. The motivation of Platform Tango is to establish a baseline of the sonar's ability to detect equally spaced features of increased thickness.

What follows is a brief description regarding specific environment and sensor considerations.

1. *Size of a target:* Distinguishing smaller underwater features through sonar signal processing and then detecting them through image processing is difficult, particularly those features that are set on the sea floor where high levels of clutter and noise exists. Additionally, smaller targets are more difficult to insonify due to the target's low target strength (TS) [8]. Similarly, small gaps between features are hard to detect.
2. *Sensor localization:* The initial insonification of the entire target was conducted which then provided the knowledge of the structure. From that knowledge, the ability now existed to eliminate the concerns of sensor localization and ground truth for most trials; this was based upon the sonar range from the target.
3. *Field of View:* The high frequency sonar utilized in this work provides a horizontal field of view (FOV) of 45 degrees. Using the calculated frame length of 3.048 meters, a standoff distance of approximately 3.65 meters is required in order to insonify the entire width of the platform. Should this distance decrease, the ability to insonify the entire frame would be lost. However, the ability to resolve within the target may be enhanced.

What is reasonable to expect in the experimental results for the sonar used in this work: the BlueView P900 sonar? The physics of sonar can now be used to explicitly calculate the sizes of features that is expected to be detectable as a function of range.

1. The vehicle and sonar were placed at the minimum range of 1.5 meters from the rigs during two of the trials. Applying this range to the theory, the expected smallest resolvable distance that the sonar may distinguish between objects is 0.0313 meters. If the horizontal spacing between the pylons or the thicknesses of the pipes are less than 0.0313 meters, the sonar will not be able to distinguish them.
2. The vehicle and sonar were placed at the mid-range of five meters from the rigs

during five of the trials. Applying this range to the theory, the expected smallest resolvable distance that the sonar may distinguish between objects is 0.104 meters. If the horizontal spacing between the pylons or the thicknesses of the pipes are less than 0.104 meters, the sonar will not be able to distinguish them.

3. The vehicle and sonar were placed at a long range of seven meters from the rigs during two of the trials. Applying this range to the theory, the expected smallest resolvable distance that the sonar may distinguish between objects is 0.146 meters. If the horizontal spacing between the pylons or the thicknesses of the pipes are less than 0.146 meters, the sonar will not be able to distinguish between them.

Image processing extracts the feature data through the use of various operations on the images. Typically, image processing approaches require that features be well defined in the sonar images, either through factors such as pixel intensity or texture variation, in order to reliably distinguish them from their surroundings. Not only can image processing be used to detect these features or targets, it may also use the information to classify or recognize the targets and track them [10]. Once the image processing algorithms have been applied, the probability of detection can be calculated by comparing the detected features to the ground truth data. The probability of detection is a measure of how likely detection of a feature is to occur and is a function of both the obtained sonar image and the image processing algorithm used.

The goal of the image processing algorithms is to reliably extract information from the sonar images. However, this is complicated due to various factors that arise such as low update rates and the low resolution of images; both are due to the physics of utilizing acoustic signals. Furthermore, sonar images tend to have high noise content, complicating the image processing task. In general, a higher sensitivity level of the image processing algorithm, the higher the probability of detection. This comes at the expense of detecting more clutter or false positives in the sonar image [11]. Conversely, a low sensitivity level of the image algorithm, the lower probability of detection. This comes at the benefit of the reduced number of false positives produced in the sonar image. Three distinct but related objectives with sonar image processing can be identified; these are the detection, classification, and tracking of underwater targets [12].

1. *Detection:* Detection is the discovery of underwater objects. The detection of small

features, specifically, through the use of image processing is critical for building accurate representations of complex underwater environments. Based on the algorithm sensitivity level, the image processing will detect a varying number of features.

2. *Classification:* Classifying is the act of categorizing the detected underwater objects. For example, the texture or pixel intensity variations of the objects on the sonar image may be used to classify the detected objects as opposed to merely discovering a number of objects on the frame. Generally, the classification of an object is based on its type or shape. For example, the classification type may include arranging the detected objects based on material composition or whether they remain static or dynamic. Classifying an object based on its shape is also common. In the case of mine warfare, distinguishing the shapes of underwater mines aid in determining the lethality of their explosive capability [8]. The information used to classify an object differs from that of merely detecting an object. Although the element of classifying objects is not within the scope of this thesis, it is an important underwater environmental objective and one that should be considered for future work.
3. *Tracking:* The process of tracking an underwater target may be described as repeatedly recognizing an object. In order to track an object, that object must first be detected and classified. Based on the sensitivity of the algorithm, the ability to track the classified object then becomes time dependent. For example, submarines first detect and classify the targets they encounter and will repeatedly plot the position of the contact over a period of time. Although the process of tracking objects is not within the scope of this thesis, it is also an important underwater environmental objective that should be considered for future work.

Based on the results of the trials, the following conclusions are presented:

1. The sonar signal processing and algorithms are not able to distinguish the 0.0098 meter diameter feature of Platform Tango at any of the previously stated ranges, which was expected. However, the second smallest feature (0.0215 meters) of Platform Tango was consistently distinguished throughout the trials when the vehicle was positioned at a range to insonify the whole rig, at five and seven meters. This was additionally unexpected based on the shortest vehicle range of 1.5 meters when the expected feature to be distinguished was 0.0313 meters or greater.
2. Algorithm I provides the greater average probability of detecting individual features

- (57%). However, upon reviewing all results presented by the algorithm, positioning the vehicle and sonar is not necessarily conducive distinguishing all the expected features. For example, the features typically compile at the 1.5 meter range. This occurrence might be the result of acoustic interference between features spaced adjacent to each other, as seen in Platform Golf, or that of numerous larger features not spaced far enough apart (seen in Platform Tango).
3. Algorithm II provides the greater average probability of detecting gap spacing (53%). Presumably, this is due to the algorithm specifics and especially, erosion. By eroding the image in this manner, the minimum value assigned to each pixel's surroundings allows the researcher to distinguish the features as opposed to viewing a compilation. This is important regarding the gap spacing in Platform Golf where same sized features were positioned at minimal distances which were expected to provide numerous more compilations during image processing.
 4. False positives occur more frequently when the sonar maintains a range to target of five meters than at any other range or movement.

The goal of this work was to provide the underwater community with a methodology to compare the data extraction and representation of complex underwater environments using different sensors and image processing algorithms. Based on the results of this work, there remains an inability to accurately distinguish congested spacing and small features. However, through the systems engineering process (SEP), this work presented an initial attempt to address the pressing capability need for the establishment of a standardized methodology that not only evaluates acoustic sensors but also provides evaluation of the associated processing algorithms. This work is therefore the initial baseline to address this community requirement.

The most important recommendation for future work is to enhance the image processing algorithms. The processing algorithms utilized in this thesis were established as the baseline for extracting data in very congested underwater environments. However, the surrounding medium in which the data was extracted was benign and without much noise and clutter; this is not a realistic setting in which the underwater community typically operates. It can then be assumed that in an open water environment, the amount of false positives, true negatives, and compilations would increase significantly. Therefore, it may behoove researchers to improve on the algorithm threshold establishment that might mitigate the amount of noise compiled on the sonar images [13].

List of References

- [1] S. De and A. Tomer, "Mapping the floor," *Science*, vol. 42, pp. 31–34, 2005.
- [2] R. Eustice, H. Singh, J. J. Leonard, M. Walter, and R. Ballard, "Visually Navigating the RMS Titanic with SLAM Information Filters." in *Robotics: Science and Systems*, Cambridge, MA, 2005, pp. 57–64.
- [3] R. J. Vaccaro, "The past, present, and the future of underwater acoustic signal processing," *Signal Processing Magazine, IEEE*, vol. 15, no. 4, pp. 21–51, 1998.
- [4] N. Friedman, *US Submarines Through 1945: An Illustrated Design History*, 1st ed. Naval Institute Press, 1995.
- [5] H. M. South, D. C. Cronin, S. L. Gordon, and T. P. Magnani, "Technologies for sonar processing," *Johns Hopkins APL Technical Digest*, vol. 19, no. 4, p. 459, 1998.
- [6] J. Pickles, *Ground truth: The social implications of geographic information systems*, 1st ed. Guilford Press, New York, 1995.
- [7] J. S. Jaffe, K. D. Moore, J. McLean, and M. P. Strand, "Underwater optical imaging: Status and prospects," *Oceanography*, vol. 14, no. 3, pp. 66–76, 2001.
- [8] A. D. Waite and A. Waite, *Sonar for Practicing Engineers*, 3rd ed. London: Wiley, 2002.
- [9] C. Kunz and H. Singh, "Map building fusing acoustic and visual information using autonomous underwater vehicles," *Journal of Field Robotics*, vol. 30, no. 5, pp. 763–783, 2013.
- [10] J. C. Russ and R. P. Woods, "The image processing handbook," *Journal of Computer Assisted Tomography*, vol. 19, no. 6, pp. 979–981, 1995.
- [11] P. Corke, *Robotics, vision and control: Fundamental algorithms in MATLAB*, 73rd ed. Springer Science & Business Media, Berlin, 2011.
- [12] H. Peyvandi, H. Roufarshbaf, M. Farrokhrooz, and S.-J. Park, *SONAR systems and underwater signal processing: Classic and modern approaches*. INTECH Open Access Publisher, 2011.
- [13] J. T. Juriga, "Terrain aided navigation for REMUS autonomous underwater vehicle," master's thesis, NPS, Monterey, CA, 6 2014. [Online]. Available: <http://oai.dtic.mil/oai/oai?verb=getRecord&metadataPrefix=html&identifier=ADA608055>

Acknowledgments

I would like to first thank the Lord for teaching me perseverance and humility throughout this rigorous academic achievement. My gratitude is extended to my thesis advisers, Dr. Noel Du Toit and Dr. Timothy Chung, for very different reasons. Dr. Du Toit offered me the technical expertise and practical techniques when designing, building, and understanding the various technical works in discussion here. Dr. Chung provided the stalwart leadership in ensuring that the project remained on schedule and within the scope of Systems Engineering.

I would like to acknowledge Professor Mark Gondree, Professor Barbara Berlitz, Professor James Calusdian, LT Robert Fauci, USN, and LT Forrest Bush, USN, of NPS for their technical expertise and guidance, and also to thank Mr. David J. Desrosiers, III, and Mr. Josh Arnett for their assistance while conducting research alongside NASA during the NEEMO XX project.

Lastly, but most importantly, my wife, Brianna Mitchelson, deserves my gratitude. There were many long days and nights when the above named professors' projects kept me from coming home, and her tolerating that time alone is no easy task. I love you, Brianna.

It is for discipline that you have to endure. God is treating you as sons. For what son is there whom his father does not discipline? - Hebrews 12:7

THIS PAGE INTENTIONALLY LEFT BLANK

CHAPTER 1:

INTRODUCTION

1.1 Motivation

The underwater community involves researchers who conduct various work and experiments below the surface of Earth's oceans. Currently, this community utilizes sound navigation and ranging (sonar) as one of the primary tools to produce underwater maps. The production of underwater maps enables researchers to minimize the risk of underwater collisions and enhances the ability to detect the smaller details within the operational environment. The pressing need within the community is to increase the accuracy of detection, to "see" obstructions or details that are missed due to today's sonar limitations. Furthermore, *no standard methodology exists to evaluate the accuracy and completeness of sonar and detection algorithms; this is critical because both are required to use sonar effectively.*

The emergence of unmanned underwater systems is exciting yet also challenging. In such an alien environment, understanding where one is remains challenging. The requirement to understand what is present in the sea and how that affects those individuals within it was first understood by Leonardo Da Vinci in 1490 when he proposed that an individual could hear the sounds of approaching maritime vessels by listening to sounds underwater. For centuries, this concept was investigated until Mr. Lewis Dixon successfully invented a sonar system for the detection of icebergs in 1906 [1]. Soon thereafter, the application of sonar was used during World War I (WWI) for submarine detection.

Today, the use of sonar has many applications to the underwater community. As seen through the tragedy that struck the RMS *Titanic* in April 1912, the use of shipboard sonar had and still has its limitations in regards to accurate object detection and obstacle avoidance [2]. In practice, no mechanical device has ever proven to be error-free. Thus, one of the motivational aspects of this work is not to produce an error-free sonar but rather to convey to those within the community that sonar has limitations in correctly understanding what is or is not observed. It is not merely a question as simple as what one can detect, but rather a question of how one uses the information extracted from the sonar. In the un-

derwater community today, a plethora of processing algorithms exist, but none precisely depict what the environment actually is [3].

From the standpoint of industry and the military, the loss of life and resources is undesirable, especially through a correctable methodology. During World War II (WWII), the United States (U.S.) Navy submarine force suffered the highest casualty percentage of all American armed forces at the time, losing roughly one in five deployed boats, largely due to the unfortunate limitations of underwater identification [4]. Should the same horrific numbers surface in today's operational environment, the aftermath would certainly warrant elevating the urgency of enhanced undersea technologies. Thus, it behooves the underwater community to continue to seek out an accurate methodology that not only enables current sonar to capture what is there but also enable a standardized methodology to evaluate the data obtained and information extracted.

1.2 Needs Analysis and Capability Gaps

In 1970, Mr. Winston W. Royce published a paper regarding the enhancement of software development [5]. The result of this work is what is now commonly referred to as the systems engineering (SE) waterfall model; this model is represented in Figure 1.1.

The initial step in this process is to address the stakeholder requirement. In the case of sonar limitations, the pressing capability need is for the establishment of a methodology that not only evaluates acoustic sensors but also provides evaluation of the associated processing algorithms. The following is a brief yet descriptive needs analysis.

1. *Identify the audience and purpose for analysis:* The underwater community has concerns in regards to how to accurately represent the underwater environment [6]. Though many tools and sensors are available, from sonar to electro optical (EO) technology, no standardized methodology regarding the use or accuracy of such tools currently exists.
2. *Describe the target population and service environment:* The need for a standardized methodology to evaluate and compare underwater mapping techniques, including sonar and processing algorithms, is emphasized by the National Oceanic and Atmospheric Administration (NOAA) in their 2005 study of restoring the Eastern North Pacific Southern Resident killer whale population [7]. Such community spe-

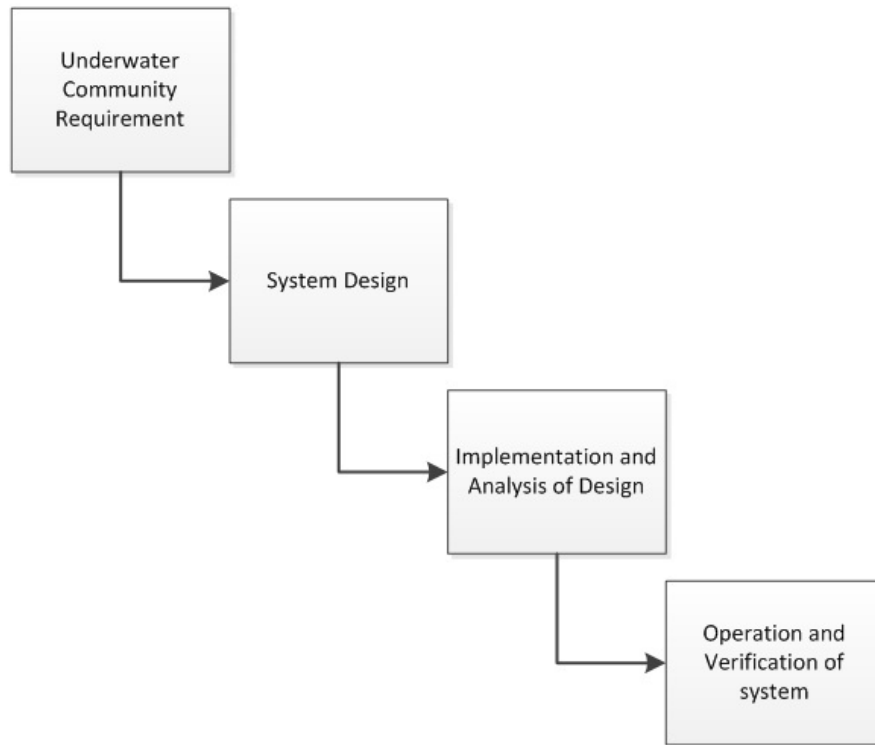


Figure 1.1: Systems engineering waterfall model

Adapted from [5]. B.S. Blanchard and W.J. Fabrycky, *Systems Engineering and Analysis*, vol.5, pp. 50-51, 2011

cific needs include the establishment of a standardized data set and data processing methodology.

3. *Need identification:* Industry and military stakeholders have long seen the benefits of Dixon's work in 1906, specifically in the evaluation of what can and cannot be detected [1]. In today's ever booming maritime transportation industry, for example, pilots and captains depend on accurate charts of sea lanes, underwater obstructions, and varying depths in order to mitigate groundings, collisions with other vessels, and enabling determination of the quickest and safest route possible. Additionally, the increased complexity of the operating environments within which modern systems are deployed, further increase the need for accurate mapping. Those trusted charts that sailors cherish when deployed are produced through the meticulous and precise work of researchers and their underwater acoustic systems. Thus, the need for precise

and accurate mapping methodologies is imperative to the survivability of vessels and their global impacts.

4. *Needs assessment:* The underwater community would greatly benefit from a methodology that accurately evaluates acoustic sensors and algorithms commonly utilized to evaluate the underwater environment. As seen throughout the history of detection techniques using remotely-sensed data, an evaluation of results has indicated that various procedures of change detection produce different maps of change even in the same environment [8]. Such an agreeable methodology is thus required to be implemented in the field of underwater acoustics and evaluation of sensors and algorithms.

In general, the capability gap that exists in the underwater community has been established above. However, it is important to note further that although there are many sophisticated processing methods utilized commercially and within the Department of Defense (DOD), none claim to provide a ground truth: the actuality of the area of operation (AO) [9]. The ability to define the ground truth data allows for the calibration of sonar and assists in the understanding of what is actually being observed or missed. More specifically, ground truth involves a process in which detections in the sonar image are compared to what is physically present in order to verify the sonar detections. For example, in the case of a sonar frame, ground truth aids in determining the accuracy of the detection performed by sensing software, and allows for the classification of the detections, including both the error rates of the sensor and of the detection algorithms [10]. Further discussion of ground truth and its application to this work will be shown in the analysis of Chapter 2.

1.3 Literature Review

The limitations of sonar and its inability to accurately process the returned acoustic data is continuously being addressed by researchers around the globe. A central concern for the community surrounds the utilization of a mobile sonar, its obtained data sets, and how researchers may use the returns to produce a usable underwater map, especially in a complex or unknown underwater environment [11]. This concern can be applied on a much grander scale. The mishap that occurred on January 8, 2005, when the USS *San Francisco* (SSN-711) struck an undersea mountain, is a recent example of current mapping technology failing the submarine's collision avoidance system. At the time of the incident, the sea mount

was not accurately represented on the navigator's charts. Given the relatively uncharted AO that the nuclear submarine was operating within, an operator would have undoubtedly preferred a map that accurately represented the most dominant of geographical features, at the very least, in order to avoid such obstacles [12]. As a result of incidents such as this, more advanced maps and mapping methodologies are needed in order for underwater systems to accurately detect and evaluate the environment [13]. Clearly, the enhancement of underwater mapping remains a priority and is critical to successful operations of the underwater community. Further, the incident involving the USS *San Francisco* provides motivation to consider the outcomes of a system that would not only outline what features are presently known but also incorporate those features that were previously missed through current methodologies.

Mapping the underwater environment is difficult, however. Similar to space missions conducted by National Aeronautics and Space Administration (NASA), the underwater world provides a challenging task to operators in that they must rely on an Autonomous Underwater Vehicle (AUV) or remote operated vehicle (ROV) to venture into areas in which they themselves can not maneuver. This means that not only are the operators physically removed from the AO but that their situational awareness (SA) is greatly diminished [14]. In order to combat such a loss, bathymetric surveys are conducted in areas of interest (AOI). As an example, researchers and environmentalists sympathetic to the declining numbers of the Nassau grouper in Belize recently conducted bathymetric surveys enabling comprehensive oceanographic data collection in remote locations. Through the use of an AUV, the team was able to accurately map the bathymetry of the reef and shelf break enabling the addition of previously undetected features to new underwater charts [15]. This research exemplifies how the tedious collection of accurate data may uncover previously undiscovered features detrimental to safe navigation within the underwater environment.

In order to maneuver in underwater regions, an AUV must rely on some sort of navigational system. The most common of navigational systems for vehicles that map the underwater environment utilize acoustic beacons (which require infrastructure deployment) and dead reckoning; the benefits and limitations of these methods will be further discussed in Chapter 2. In this work, the AUV uses an inertial navigation system combined with aiding sensors such as Doppler Velocity Logs (DVL). These advanced methods include terrain-aided navigation (TAN) and feature-based navigation (FBN) which use detected environmental

features to aid in the safe navigation of the vehicle. These software based navigational systems are required due to the fact that Global Positioning System (GPS) communication signals cannot travel through a water medium in order to guide vehicles at depth [16]. Further, these methods rely on sonar's ability to detect features in the environment. The use of TAN, specifically, requires the system to utilize a previously built map of the region, unlike the related field of Simultaneous Localization and Mapping (SLAM) which will be discussed shortly [17]. Therefore, in order to capture the finer details that are critical to the population of an enhanced mapping methodology, a low-speed platform able to maintain a constant relative pose (position and orientation) is needed [18]. This consistent pose allows the focus on an AOI more accurately than simply sweeping over an AOI at high speed and missing critical features.

Shown through operational experience, capturing the critical details within the underwater environment is obtainable only when moving precisely and systematically. In terms of yet another critical maritime mission, the U.S. Navy conducts Mine Counter Measure (MCM) operations in various complex underwater environments that include restricted straits and within the littorals. In these instances, naval operators typically understand the dimensions of their targets and conduct surface vessel or undersea passes at low speeds in order to detect the objects of interest. Although mines may be secured to the sea floor, the manipulation of applicable sonar frequency, previous maps, and complete processing algorithms encompass a naval standard operating procedure (SOP) that allows these operators to identify and localize threats, thereby preventing accidents and the loss of life [19]. Furthermore, in February 1991, the U.S. Navy lost control of the northern Arabian Gulf due to the placement of over thirteen hundred mines deployed by Iraqi forces. During this time, not only were two U.S. Navy warships damaged but numerous amphibious missions were aborted in fear of further mine contact [20]. These events provide increased motivation to ensure that U.S. naval personnel obtain the most accurate and up-to-date information and methods to process real-time acoustic data in order to understand what may be detected and ensure no sea-based mines are potentially missed in the future.

1.4 Community Contribution

As has been discussed, the stakeholder requirement for an enhanced underwater mapping system is clear, whether it be for the U.S. Navy or commercial use. However, the previ-

ous examples have been focused on the wide area acquisition of data to populate maps. The work of this thesis focuses on the application of capturing the finer details missed by the same stakeholders that would benefit from this refinement. Stakeholders utilize ROVs and AUVs for underwater applications such as the inspection of pipelines, structures, and coral reefs; all are targets that require the understanding and inspection of the finer details. Three dimensional mapping is currently gaining popularity among academics in order to depict these finer details. Further, some have been successful processing the acquired data and building extremely detailed three-dimensional (3D) maps through the use of refined SLAM algorithms [21]. SLAM attempts to fulfill the need of building an underwater map while at the same time localizing the AUV within that underwater map. In practice, these dilemmas cannot be solved independently. Before an AUV can answer the question of what the underwater environment looks like, given an observational data set, the AUV requires information regarding at which locations these observations have been made [22].

Chiefly, localization and algorithms are important; however, neither can operate properly without field-acquired data sets to process. Data sets provide researchers with accessible benchmarks in order to refine their existing algorithms and allow for the testing of new methods [23]. Although data sets continue to evolve in their ability to contain even more data than ever, the focus has remained on processing static and passive information [23]. Within the underwater community the extraction of data sets occurs continuously while operators utilize a plethora of methodologies and algorithms to process collected data in order to yield desired results. However, as it is throughout the fields of underwater robotics and sonar data processing, the decision as to what methodology to utilize becomes a daunting task [24].

In an attempt to determine which methodology to utilize for the work of this thesis, many methods were considered. However, with regards to object detection, no standardized data sets or methodology have currently been established as the community standard. The direction of this thesis then deviated to address this gap, and concluded that the underwater community requires a standardized methodology in order to further evolve the application of object detection and enhanced mapping. Based on the examples and motivations previously described, the contribution of this work to the underwater community is an initial robust methodology with which the community may obtain relevant data sets, apply those data sets to custom preceptors and algorithms, and evaluate whether or not these custom

methods are capable of detecting the known features while quantifying the missed features.

CHAPTER 2:

FUNDAMENTALS OF PERCEPTION IN THE UNDERWATER COMMUNITY

What does it take to build a representation of the underwater environment? In an attempt to answer this question, the community needs to enhance its understanding of the three factors which makes underwater sensing difficult. The three factors that enable a researcher to build an accurate representation are the underwater environment, sensor used, and the perception capability.

1. *Environment*: The environment refers to knowing what a researcher is looking at (ground truth) and from where (localization). During this thesis work, the physical location of the target is approximately known relative to the sensor while the ground truth data is obtained from accurate knowledge of the sensed environment by designing and constructing a target with known features.
2. *Sensing*: Sensing refers to the mechanism to detect the environment. A discussion of the sensing techniques used in this work will follow in Chapter 3.
3. *Perception*: Extracting useful information from measurements obtained in the environment from the sensor data.

Whether it be through the use of active sonar or EO cameras, imaging the details of underwater objects remains a challenge [25]. The trifecta required for map production requires knowledge of two factors to provide the inference of the third; the effectiveness of the trifecta is demonstrated through its application within the MCM community [19]. However, although many perception methodologies are utilized in the community today, none is recognized as the community standard for accurate map production [26]. All methodologies in use are governed by the laws of physics and those physical truths are discussed in the following detail.

2.1 Underwater Acoustic Sensors

2.1.1 Operational Description

Electromagnetic energy does not propagate underwater effectively. However, acoustic energy propagates well underwater [27]. Active sonar, simply put, is the intentional transmission of acoustic energy, a *ping*, so that the echo is reflected back from the target [28]. This echo is then processed into a representation of the environment.

1. An active sonar system consists of a transmitter, transducer, receiving array, and a display which presents the raw intensity images.
2. An electrical impulse is generated from the transmitter and converted into a wave of sound outputted into the underwater environment.
3. When the sound wave strikes the feature, it then reflects back to the transducer.
4. The transducer then converts the sonar signal back to an electric signal which is then amplified by the receiving array and presented for visual interpretation.
5. It is this visual assimilation that allows researchers to view detectable features obtained by this sonar signal processing. [29]

The use of an array of projectors to transmit acoustic pulses through the water allows underwater targets to be detected, localized, and classified by these return echoes. Also of importance, the use of an array of detectors associated with an array of projectors allows the determination of range and bearing. Further, the time it takes for the echo to return to the receiver array is also used to determine the range and bearing of a target. In order to calculate the range to an underwater target, the speed of sound in salt water must be known. The speed of sound in water is a function of the waters temperature, salinity, and depth and may be shown through the functional dependencies

$$c = f(T, S, z), \quad (2.1)$$

where c is the speed of sound in water, T is the temperature of the water measured in degrees Celsius, S is the salinity of the water measured in parts per thousand (ppt), and z is the depth of interest measured in meters [30]. The range, R , to a target can now be determined by

$$R = \frac{c \times t}{2}, \quad (2.2)$$

where t is the time required for the signal to reach the target and the echo to return to the receiving array [19].

However, the focus of this work is not to enhance the range at which a sonar may insonify a target. The focus of this work is to enhance the community's ability to distinguish features. Thus, the understanding of range and bearing resolution of the sonar remains at the core of this thesis.

Range resolution is the ability of a sonar to distinguish between multiple targets on the same line of bearing, but at slightly different ranges. The degree of range resolution depends greatly on the pulse width (PW) as well as on the physical characteristics of the target, and ability of the receiving array. The PW of a sonar output is merely a measure of the time between a high and low of a single acoustic pulse generated by the system. In order to mitigate the negative effects of an increased PW, the signal-processing technique called pulse compression utilizes the high energy of a sustained pulse in order to enhance the detection capability of the sonar yet maintaining a high range resolution of shorter pulsed outputs [28]. This ability of the receiving array to improve the range resolution over traditional sonar systems is referred to as the pulse compression ratio (PCR). This means that should the sonar system have the PCR of fifteen to one, the range resolution of the system is reduced to one-fifteenth of those traditionally used systems. This improvement factor is incorporated when calculating the range resolution, R_r , of a sonar and allows the receiving array to slightly delay acoustic signals returning simultaneously causing each echo to become shorter, increasing their amplitude, and ultimately providing increased resolution [28]. This improvement factor is determined by

$$R_r = \frac{c \times PW}{2 \times PCR}, \quad (2.3)$$

The horizontal azimuth, or bearing resolution, is the ability of a sonar to distinguish objects at the same range but at slightly varied bearings [19]. Somewhat similar to the concept of range resolution, the degree of bearing resolution is based upon the beamwidth and range

of the targets. The beamwidth is fixed and based upon the physical construction of the sonar, such as the type or number of staves within the sonar head. Traditionally, targets at the same range must be apart by one beamwidth in order to be distinguished as separate targets; this is a concept discussed further in Chapter 3 and tested in Chapter 4 [31]. The bearing resolution of a sonar may be determined by

$$R_b = \frac{k \times \lambda}{D_{sonar}}, \quad (2.4)$$

where R_b is the bearing resolution, k is the constant factor derived from a Bessel function which in the case presented shall be approximated at a value of one due to a sonar's diffraction pattern [32], λ is the wavelength of the acoustic signal in the water medium, and D_{sonar} is the physical diameter of the sonar aperture in meters [33] and [32].

2.1.2 Noise

The underwater environment is filled with sound sources that interfere with the acoustic sensors; this interference is commonly referred to as noise [34]. Two equations presented by Payne are required in the discussion of the noise associated with active sonar. The first equation describes the instance in which active sonar encounters an ambient noise-limited situation; the second equation describes a reverberation-limited scenario. Ambient noise is described as background noise in the underwater environment caused by hydrodynamics, seismic activity, maritime traffic, or biologic activity while reverberations are the unwanted echoes from the sea surface or bottom and from scatterers within the volume of the sea [19]. Further, the successful performance of active sonar requires that the ping minus noise is greater than the detection threshold in order to receive the desired return data for processing [28].

Noise Limited Once a ping is directed towards a target within this restricted environment, the pulse will suffer a transmission loss resulting in a smaller percentage of the original output to be transmitted back to the receiving array. This loss in target strength (TS) can be modeled as the following return signal equation to the sonar

$$S = SL - 2TL + TS, \quad (2.5)$$

where SL is the target active source level, TL is the transmission loss of the acoustic signal, TS is the target strength, and S is the ultimate acoustic signal return to the receiving array; these factors are experienced when the source of the radiated energy and receiver for the echo are located together.

Once the return signal is received, the reverberation background due to the initial ping will have dispersed resulting in only ambient noise being present. The fundamental relationship between ambient noise and the transmitted signal is

$$SL - 2TL + TS - NL + DI \geq DT, \quad (2.6)$$

where NL is the ambient noise level, DI is the receiving directivity index, and DT is the detection threshold initially established [28]. Thus, this basic active sonar equation holds true when the system is operating in a noise-limited environment.

A practical example, pertinent to the underwater community, of this scenario occurs when a U.S. submarine or surface vessel is patrolling for an enemy submarine. If the enemy submarine is known to be underway and producing sound at a frequency of 300 hertz (Hz) and the AO is currently experiencing six foot seas, an operator may utilize Figure 2.1 in order to determine the appropriate value of ambient noise level in decibels [28]. From Figure 2.1, the ambient noise level due to shipping is approximately sixty-five decibels while the ambient noise level due to the six foot seas is approximately sixty-six decibels. Using a nomogram to calculate and combine decibel levels, the total ambient noise level being produced within the AO is approximately sixty-eight decibels. This scenario allows for not only the determination of noise within the AO but also the understanding of important factors to be considered in determining the sonar performance within the fixed frequency range of interest [28].

Reverberation Limited Should the transmission return to the sonar sensor suite when the reverberation background has not fallen to a level below ambient noise, the background noise is then referred to as the reverberation level (RL) representing returns reflected by objects other than the desired point of interest (POI) [28]. A practical example, again pertinent to the underwater community, includes sonar returns from entrained air bubbles or that of underwater marine life activity. The noise due to these objects limits the maximum

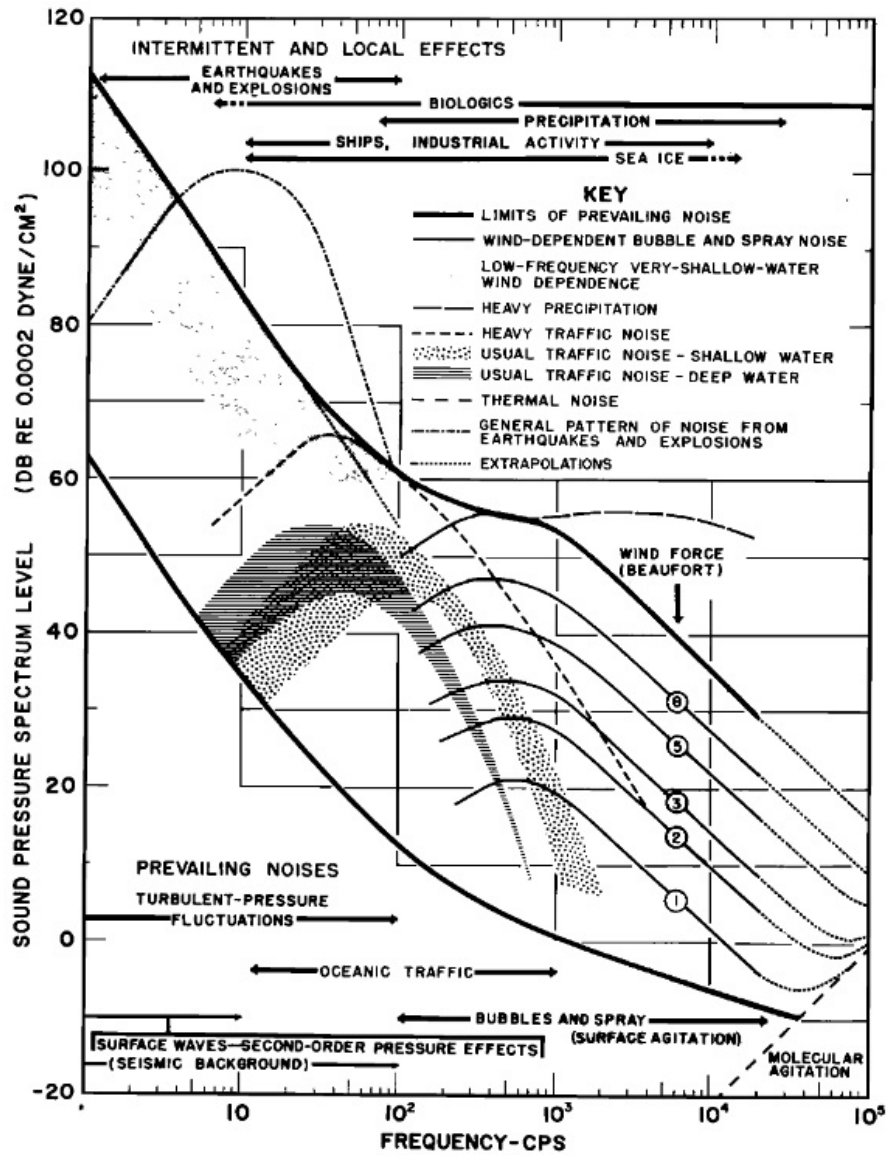


Figure 2.1: Wenz acoustic ambient noise in the ocean curves

Source: G.M. Wenz, *Acoustic ambient noise in the ocean: spectra and sources*, *The Journal of the Acoustical Society of America*, vol. 34, no. 12, pp. 1936-1956, 1962

source level (SL) thus increasing the RL in an AO. This is undesirable for sonar operations because reverberation is then directed back in the same direction from which the sonar is

pinging. In this case, the RL observed by the sonar transducer terminals forms the equation

$$SL - 2TL + TS - RL \geq DT, \quad (2.7)$$

thus diminishing the resolution of the desired target [28].

Acoustic Sensor Noise and this Thesis Although the underwater environment is typically filled with sound sources that interfere with acoustic sensors, the facility that was ultimately utilized to conduct the experiments was assumed to not produce significant noise or reverberation limited effects. For example, unlike those shallow water environments found off the California coast, an aquatics facility does not house the marine life or foliage that may cause reverberation limited effects. Based on the targeted applications of the sonar and the chlorinated environment of the aquatics facility, the only noise that was expected to be present were that caused by the reflection and refraction of the acoustic signals off the target or surrounding walls of the pool. By setting a reasonable threshold level in Algorithm I, for example, the assumption was that the sensitivity of the algorithm would minimize or negate the noise entirely displaying only the relevant extracted data. Additionally, the detection range of the sonar was limited in order to minimize the effects of reverberation for the data sets.

2.1.3 Limitations

Active sonar has many limitations, thus, the incentive to fill the capability gaps are pressing within the community. For this research project, the immediate concern involves the determination of an acoustic sensor's range and bearing resolution while providing details of the finer features. Should no modification in the system occur, the overall sonar's resolution might prove insufficient based upon the ever changing sea water environment and noise present. Simply put, sonar systems require researchers to establish a detection threshold in order to receive the desired intensity of sound. The resolution from which that set sound intensity arrives is ultimately dependent upon the amount of signal lost en route to and back from the target [28].

Other limitations or performance factors that may inhibit the full utilization of active sonar include:

1. *Propagation of sound:* Water's bulk modulus and mass density determine the speed of sound propagation. This is based upon the mathematical model of refraction more commonly referred to as Snell's law which describes how the propagation of sound will bend from one point in the medium to the next [35]. A practical example of this occurs immediately after the sonar emits a ping. For example, in Figure 2.2 the sound wave passes through horizontal layers or strata causing the sound wave to be refracted and ultimately decreasing the original speed, direction, and intensity of the signal [28]. In the case of sonar, Snell's Law may be represented as

$$\frac{c_1}{\cos \theta_1} = \frac{c_2}{\cos \theta_2} = \frac{c_n}{\cos \theta_n}, \quad (2.8)$$

where c_1 , c_2 , and c_n are the varying quantities of sound speed as they pass through the different strata [28].

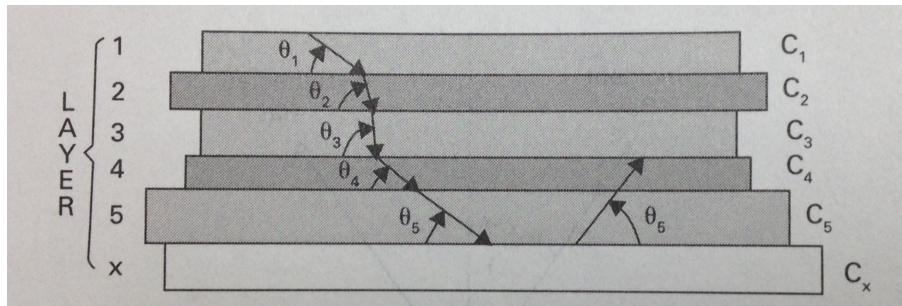


Figure 2.2: Snell's Law applied to multiple layers

Source: C.M. Payne, *Principles of naval weapon systems*, Naval Institute Press, vol. 1, p. 164, 2006

2. *Scattering of signal:* When active sonar is employed, scattering occurs from any and all objects in the AO and may become a serious source of interference. For example, acoustic scattering is similar to the scattering of a car's headlights in fog. A high-intensity, small beamwidth light will penetrate the fog to some extent, but broader beam headlights will emit light in all directions, scatter back to the operator, and overwhelm that reflected light from the target direction. Thus, active sonar is required to transmit in a narrow beam to minimize this effect [19]. Furthermore, a complication is that a plethora of echoes, and therefore possible false positives, are also obtained from surrounding objects in the sea such as from schools of fish and rocks, increasing the possible error rate of the sensor, which is a measure of

performance that will be addressed in Chapter 3.

3. *Countermeasures*: Pertaining to the military environment specifically, active countermeasures can be launched by opposing naval forces in order to raise the noise level and provide a larger false target in order to either obscure the true signature of the intended target or mimic the sound signature of an unintended target.

Acoustic Sensor Limitations and this Thesis External factors may limit the sonar's range resolution and bearing resolution ability to distinguish features. These external limitations also include the size and composition of the target and the underwater conditions. Since the size of the target was predetermined and the underwater conditions pristine, the factors limiting the bearing resolution of the sonar, specifically in this work, include the set beamwidth and the three approximated ranges to the target. Thus, through minimizing these external limitations that might affect the range and bearing resolution, the establishment of an appropriate detection threshold and the ability to receive the desired intensity of sound may be maximized. Furthermore, the resolution from which that set sound intensity arrives is ultimately dependent upon the amount of signal lost en route to and back from the target [28]; this was mitigated through the controllable conditions of the aquatics facility which minimizes the possible refraction and scattering of the acoustic signal while maximizing the physical ability to set the sonar range to the target and ultimately enhance the probability to distinguish features.

2.1.4 Measures of Effectiveness

As previously discussed, the environment in which underwater sensors are deployed can prove too much for the system to operate efficiently. Aside from those environmental constraints on sensors that have been discussed, the following is a brief discussion regarding particular measures of effectiveness (MOE). These MOE are specified in terms of a level of importance significant to the community based on the criticality of the functions performed. These third, fourth, and fifth-order considerations focus on the technical disturbances that can affect a sensor's ability to provide effective data sets for researchers [5]:

1. *Dependability*: An underwater sensor's dependability can be defined as the trustworthiness of the system [36]. In the robust technical system of sonar, a researcher is dependent on the continuity performance such as the ability to project a ping and

- receive the subsequent return. Although the environmental effects of scattering may disrupt the signal process, the technical reliance of sonar through its designed architecture should be able to provide data sets pertinent to that operational environment.
2. *Sustainability*: System sustainability ensures that consumed resources such as electricity, replacement parts, or any physical resources utilized for the acquisition of data be replaceable. This is applicable because the desire is to design a system and methodology that eliminates waste of the community's time and resources caused by sub-par technical operations or environmental constraints [5].
 3. *Serviceability*: The serviceability of any desirable acoustic system refers to those characteristics of design that ensure the system can be properly serviced throughout its life cycle [5]. Considering this MOE is important in that the sonar utilized to collect data be robust yet uncomplicated to reassemble on a mobile platform upon completion of planned or unplanned maintenance. Disturbances within the operational environment, such as elevated surge rate or large objects, may collide with or push the system into danger. Should damage to the system occur, it is desirable to utilize a system that can be serviced effectively and efficiently.
 4. *Testability and Diagnostics*: Traditionally, system testing has been a manual effort performed by mission critical personnel in an attempt to identify troubleshooting methods for a system [37]. In the case of an acoustic system utilized for this work, a modular system is chosen. This modularity allows the performance of critical hardware and software trials in a laboratory setting prior to deployment in a harsh operational environment. Further, these initial trials minimize the probability of errors experienced in field work.

2.1.5 Theoretical Application

With the introduction of underwater acoustic sensors, the question of the smallest resolvable feature that the sonar may insonify arises. Should a sonar have the set frequency of 900 kilohertz (kHz), for example, the following relationship can be used to determine the wavelength of the system [28]

$$f = \frac{c}{\lambda}, \quad (2.9)$$

where f is the frequency of the sonar at 900 kHz, c is the speed of sound in the medium at 1476 meters per second based on a chlorinated environments typical salinity (approximately 3500 parts per million) and temperature (approximately sixty-five degrees Fahrenheit), and λ is the wavelength of that signal determined to be 0.0016 meters [38].

The sonar's range and bearing resolutions are limited by angular diffraction causing blurring of the signal's return. Angular diffraction is determined by the aperture within the elements of the sonar. Thus, the size of the aperture is directly related to the angular resolution of the sonar from the diameter of the aperture and signal wavelength by the Rayleigh criterion. The Rayleigh criterion can be represented by [39]

$$\theta = \frac{k \times \lambda}{D_{aperture}}, \quad (2.10)$$

where θ is the angular resolution in radians, λ is the wavelength of the signal in the water medium, $D_{aperture}$ is the diameter of the sonar aperture, and k is the constant factor derived from a Bessel function which in the case presented shall be approximated at a value of one due to a sonar's diffraction pattern [32].

Wavelength has been calculated to be 0.0016 meters. In order to determine the sonar aperture diameter, the Rayleigh criterion becomes

$$D_{aperture} = \frac{k \times \lambda}{\theta} \quad (2.11)$$

The bearing resolution for the P900 sonar at a 1 meter distance from the target is 0.0209 meters at a beam width angle of 1.2 degrees [40]. Therefore, $D_{aperture}$ is calculated to be 0.076 meters which is required data in order to determine the minimum distance between pylons and feature thickness that may be distinguished.

Sonar systems send out a pulse and listen for its return or echo. The time for the pulse energy to deploy and return is determined by the distance to the target. Using this understanding of sonar and the concepts within the Rayleigh criterion, the distance between pylons and the concept of range resolution can be represented by

$$D_w = \frac{R \times \lambda}{D_{aperture}}, \quad (2.12)$$

where D_w is the smallest resolvable distance between two objects, and R is the range of the sonar to the platform [41].

As an example, the sonar may be placed at a fixed distance of 5 meters from the rig. Solving for D_w , the smallest resolvable distance that the sonar may insonify is then calculated to be 0.105 meters. Therefore, if the gap spacing or features in the rig are less than 0.105 meters in width, the sonar will not be able to distinguish them at this sonar range to target.

2.2 Underwater Electro-Optical Sensors

The Mark (Mk) I, or more affectionately known as the human eyeball, was the first optical sensor utilized by man [28]. However, with the underwater community's desire to further their view and understanding of the ocean's depths, the study of underwater EO sensors has emerged. Unfortunately, the opacity of salt water to light is extreme, making the job of collecting optical images in the ocean, for example, a daunting task. Similar to the steady advances in underwater sonar technologies, the current improvements in electronics and sensing technology incorporated with those advances in signal and underwater image processing have since enabled spectacular underwater EO sensing methodologies to emerge [25].

2.2.1 Operational Description

The basic physics of light propagation in water greatly influences the performance of underwater optical imaging systems. As in sonar systems, underwater optical imaging systems are classified into two areas: passive and active. For the purposes of this thesis, we shall consider the discussion and comparison of active systems alone. Active optical systems utilize an operator-generated light source such as the use of continuous artificial illumination in an underwater camera system. This is an advantage similar to active sonar in that active EO systems may direct the incident light into very narrow beams, be monochromatic, and be used in very short periods if required. Further, active EO systems allow underwater imaging at greater distances and enhanced contrast than through the sole use of sunlight

based, passive systems [25].

Underwater EO systems in its various forms are currently being used by the U.S. Navy. In order to enhance the detection of submarines, mines, and other underwater traffic, a vast ocean-floor optical sensor array utilizing minute phase shifts of light are being configured for deployment, particularly around public shipyards [42]. This EO system allows for the sensor array to detect phase shifts in the light waves caused by the sound propagation of underwater objects and vehicles as they pass above the sensor. The advantages of utilizing EO systems in this case are the system's sensitivity to changes in sound and the reliability of its all-optical components. The sensor arrays and signal-transmission media, for example, are constructed from plastics which do not corrode or short-circuit when submerged, thus alleviating an important maintenance concern of the Navy. Further, silica-based optical sensors are also being utilized on submarines that again alleviated the need to place non-EO systems external to the pressure hull minimizing the previous preventative maintenance system (PMS) requirements [43].

2.2.2 Noise and Limitations

Strand states that environmental noise sources are the factors that primarily limit the performance of underwater EO imaging and associated systems [44]. In the open-water environment, EO imaging systems may have sensory ranges in excess of greater than 30 meters, while within a congested littoral zone the same systems may obtain a range reduced to far less. Blue-water environmental limitations include:

1. *Backscatter noise*: Photons undergo scattering before reaching the target; this scattering is observed by the receiver, resulting in convoluted images.
2. *Forward scatter noise*: Forward scattering of photons that are reflected from the target. Due to scattering, the resulting image appears as though the photons were reflected from an incorrect target location; this leads to the loss of image resolution.
3. *Attenuation*: Attenuation is dependent on the wavelength of the signal and increases with frequency [45]. The loss of the photon signal is due to the photons being absorbed or scattered out of the receiver's field of view (FOV) which limits the signal strength at the receiver [46].

Further limitations include the fact that conventional underwater imaging systems, which consist of expensive video cameras and floodlights, are limited to ranges of one to one and a half beam attenuation lengths of approximately one to two meters caused by the effects of backscatter noise. Thus, EO do not allow for the range and bearing resolution needed to expedite target identification and the associated detail recognition in the congested, littoral environments simulated in this work [44].

2.2.3 Underwater Sensor Conclusion

In the controlled aquatic environment utilized in this work, an underwater EO system may have proven equally, if not more, effective. However, the emphasis of this work is the establishment of a methodology to distinguish the finer features in congested, littoral environments; these are the same environments in which EO systems are limited based on the effects of backscatter noise. Thus, in order to simulate this AO of interest, the decision was made to utilize equipment that had previously demonstrated the ability to distinguish features at ranges greater than merely one or two meters from the target. Furthermore, based on previous work conducted with Center for Autonomous Vehicle Research (CAVR), the determination was made to undertake this endeavor with a single, readily available, and proven acoustic sensor rather than purchasing multiple new, expensive, and unproven EO equipment and expending precious time learning how to operate the hardware and software associated with it.

2.2.4 Sensor Summary

Whether it be through the use of sonar or EO, the ability to produce accurate underwater maps is challenging. The return, or echo, of the active propagation includes data pertaining to the underwater environment. However, the interpretation of the extracted data in a sonar image may be surrounded by noise and clutter which influences the ability to distinguish features of interest. Typically, data obtained in consecutive scans vary slightly even when observing a static target; this is due to echoes returning to the sonar's receiving array are not direct reflections from the target. These factors further complicate the initial detection, subsequent classification, tracking, and map production unless prior knowledge of the operational environment is available to interpret the sonar inputs [47].

Similar limitations are experienced when using EO techniques. The propagation of light in

seawater suffers from constraints such as absorption and scattering resulting in the decay of the light wave. Thus, only a percentage of the incident radiation reaches deeper ocean depths with much less reaching targets in littoral zones. Ultimately, the scenes produced by EO techniques are devoid of vision features desirable for map production [47].

2.3 Environment

Localization is the ability for modern underwater robots to deploy and track its motion and pose in the operating environment [48]. Localization techniques take many forms. To construct an enhanced algorithm and methodology for detecting specific features from the underwater environment for the community's benefit, three of the current approaches for localization and navigation in the underwater environment are reviewed followed by a brief discussion regarding the establishment and benefit of a defined ground truth.

2.3.1 Dead Reckoning and INS

Accurate navigational data is critical for safe operation and recovery of an AUV. Dead reckoning is the navigational process of determining a current position by using a previously determined position and continuing ahead based upon the known speed and time on the particular course. Traditionally used by sailors, the method of dead reckoning may now be utilized in limited AUV applications. It may be used to reduce the need for sensing technology, such as GPS, which reduces the cost and complexity of systems at the expense of performance. However, the problem with this technique is that it is inaccurate and the presence of any significant current will add a velocity component to the AUV which may not be detected by the speed sensor. Within the littorals, currents become significant which can result in inaccurate position and distance estimates when operating at slow speeds. This limits the accuracy of the dead reckoning technique [49].

A potential upgrade to dead reckoning, inertial navigation systems (INS) is an autonomous navigational tool that provides information regarding velocity and position to the AUV based on inertial sensors and through dead reckoning [50]. Once the initial conditions are known, an integration of acceleration provides the AUV with velocity information while the second integration provides the AUV with position inputs. The INS consists of an inertial measurement unit; this inertial sensor suite consists of accelerometers, which measure

the linear motion in three orthogonal directions, and gyroscopes, which measure the angular motion of the AUV. The components of a typical unit is represented in Figure 2.3. The two additional modules consists of a pre-processing unit and a mechanization module; the system as a whole is represented in Figure 2.4. Once underway, the velocity and positioning signals are pre-processed and filtered in order to mitigate faults before transferring to a mechanization algorithm that converts the signals into updated attitude and position information [50]. Although the accelerations of the AUV are integrated twice in time to determine the updated position, the drift rates for INS can be significant and may cause errors. Further, the INS system can be difficult to set up along with increased cost and power consumption that have historically made INS systems undesirable for AUV applications [49].

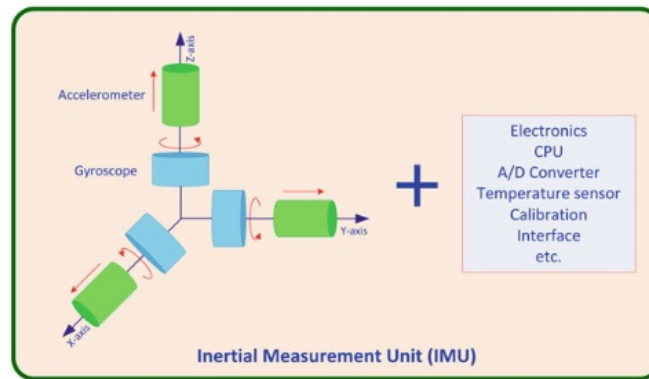


Figure 2.3: Inertial measurement unit

Source: Bowditch, "Chapter 7: Dead Reckoning", Bowditch, 1995. [Online]. Available: <http://fer3.com/arc/imgx/bowditch1995/chapt07.pdf>

The concern with dead reckoning and INS based solution is that position error increases as the AUV travels; this will be based on the ocean currents, the forward velocity of the AUV, as well as the capabilities of sensors. The maximum AUV travel time between surfacing for a position update will then be dictated by dead reckoning inertial navigation accuracy. Poor dead reckoning will dictate a high frequency of surfacing and minimize the time to collect data sets. Also, AUVs operating within the littorals risk collision with surrounding surface vessels when resurfacing for position fixes. For deep water operations, the time and energy required for an AUV to surface are again unfavorable which may result in lost data pertinent to the application of further map enhancement [49].

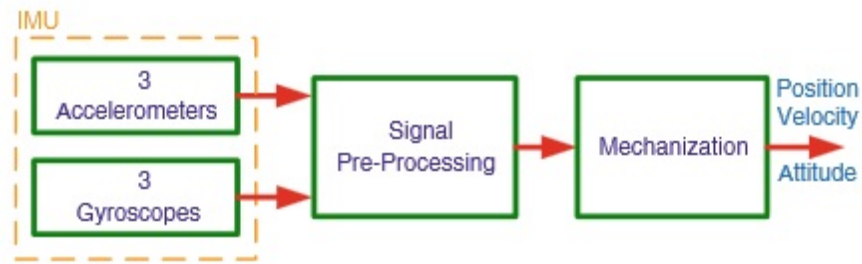


Figure 2.4: Inertial navigation system

Source: Bowditch, "Chapter 7: Dead Reckoning", Bowditch, 1995. [Online]. Available: <http://fer3.com/arc/imgx/bowditch1995/chapt07.pdf>

2.3.2 Acoustic Beacons

Acoustic energy propagates effectively in the ocean. This ability allows for acoustic transponders to be used as beacons in order to guide an AUV without the need for resurfacing to obtain a GPS fix. One specific acoustic beacon system that has been employed is the long baseline (LBL). This system utilizes external transducer arrays which serve as aids to navigation. Transponders are deployed within an AO and then surveyed to accurately measure position. The AUV generates an acoustic signal which is returned by each beacon as it is received. The AUV position is determined by measuring the sound wave travel time between the vehicle and each beacon, the sound speed profile, and the physical geometry of the beacon array. With this information, the relative distances between the AUV and each array node can be calculated. The two primary techniques are:

1. Compute fixes through the intersection point of spheres from the beacons in the array, and
2. Integrate the raw time of flight (TOF) data into a Kalman filter.

A variant of this beacon system is referred to as hyperbolic navigation. In this system, the AUV acts passively and instead listens to an array of beacons whose geometry is known. Each beacon pings in a relative sequence at a unique frequency. By knowing which beacon pings when and the geometry of the array, the AUV can reconstruct where it must re-position to in order to hear the sequence. This system has the advantage of saving energy during active pinging and allows for increased survey time and data sets for updated mapping [49].

Two specific challenges in acoustic beacon systems occur; these are the errors of array geometry and the sound speed profile. Positioning error occurs due to improper survey of the beacon positions. Modern, self-calibrating beacons enable the surveying task to only one beacon with the others determining their own positions relative to the first. However, this increases the possibility of position errors due to the errors in assumed local sound speed [49].

Difficulty in acoustic navigation may also be caused through the error in assumed sound speed profile. This results in a distance bias in calculations that generates errors resulting in incorrect TOF values and position fixes. LBL may work efficiently in deep water and with close array separations; however, over longer distances in shallower water complex propagation effects and an increased frequency of false position fixes occurs [49].

2.3.3 Ground Truth

The ability to define the ground truth data allows for the calibration of sonar and assists in the understanding of what is actually being observed or missed. More specifically, ground truth involves a process in which detections in the sonar image are compared to what is physically present in order to verify the sonar detections. For example, in the case of a sonar frame, ground truth aids in determining the accuracy of the detection performed by sensing software, and allows for the classification of the detections, including both the error rates of the sensor and of the detection algorithms [10]. Figure 2.5 represents an example of the first algorithm being applied and the defined ground truth (presented by the grey rectangles) which allows a researcher the ability to compare and verify the sonar detections.

Defining the ground truth enables the interpretation and analysis of what is being sensed [10]. Using image processing, ground truth involves the process in which pixel intensity in a sonar image is compared to the physical location of the rig.

1. Figure 2.6 is an example of the a specified sonar image which populates to begin the process of defining the ground truth.
2. The researcher may now select two points to define the orientation or the rig; this step typically involves placing the cross-hairs on what appears to be the ends of the rig. Once the two points have been selected, the tool produces a solid line connecting

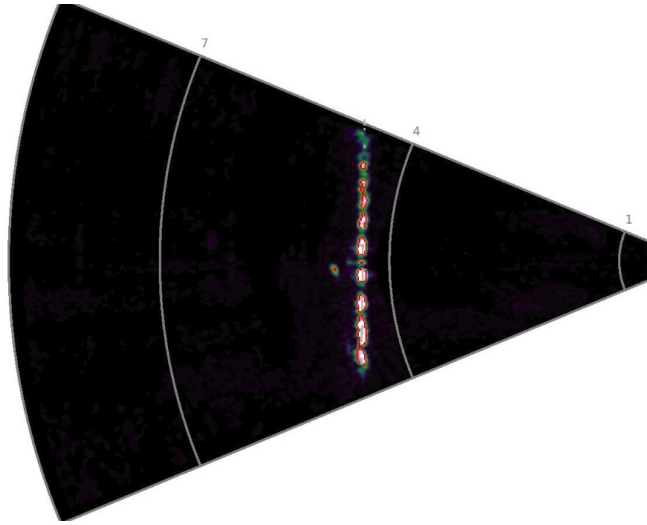


Figure 2.5: Ground truth compared to sonar detections

- the two points establishing the initial rig alignment and is represented in Figure 2.7.
3. The next step allows the researcher to select the starting point of the rig; this step is represented in Figure 2.8.
 4. The orientation of the rig is now defined once the rig features are plotted and is represented in Figure 2.9.

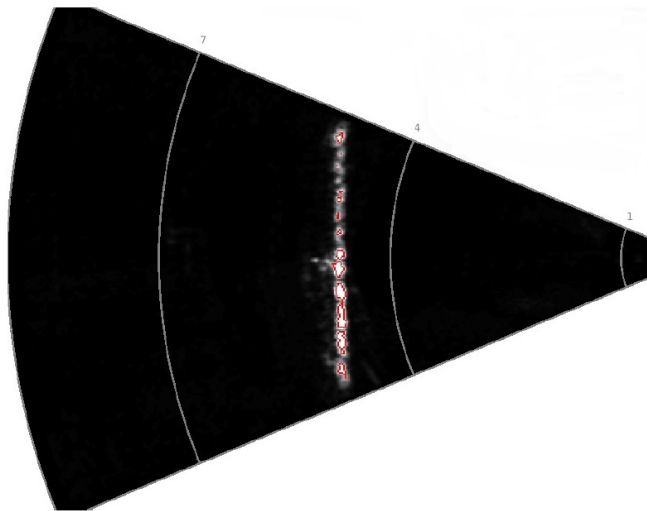


Figure 2.6: Step 1 of the ground truth overlay

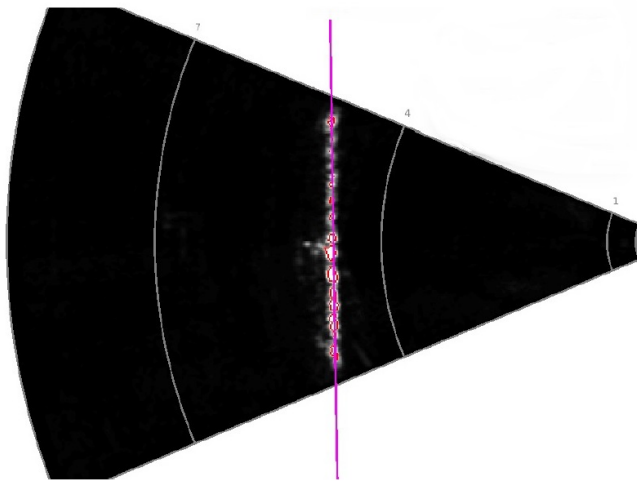


Figure 2.7: Verification of rig outline alignment

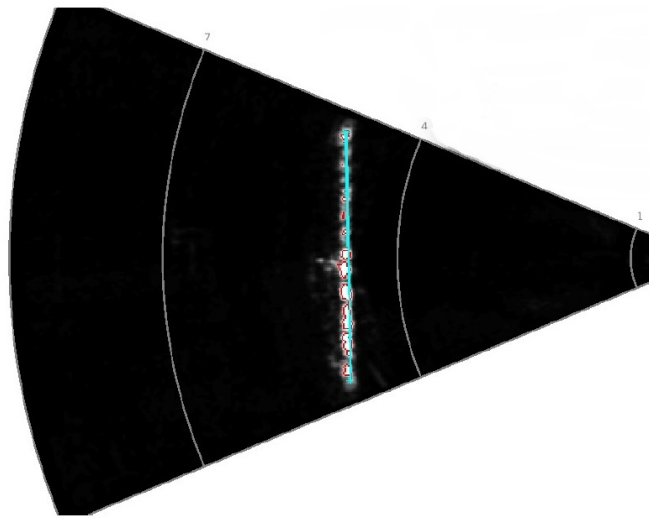


Figure 2.8: Defined starting point

2.3.4 Environment Conclusion

The environment refers to knowing what a researcher is looking at (ground truth) and from where (localization). During this thesis work, the physical location of the target was approximately known relative to the sensor while the ground truth data was obtained based the design and construction of the rig. Although dead reckoning, INS, and acoustic beacons

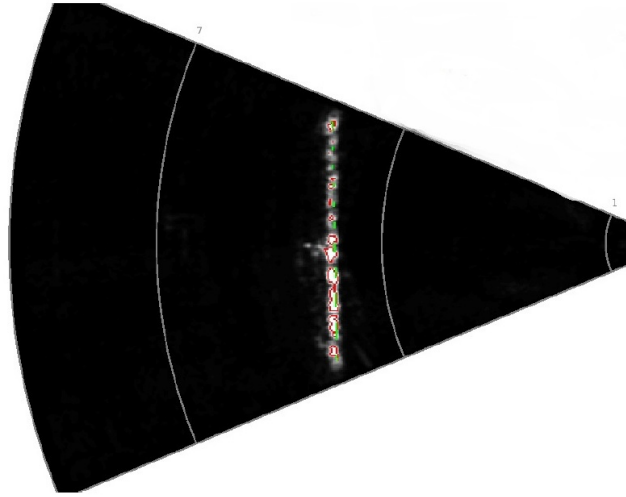


Figure 2.9: Ground truth defined

have proven localization benefits in missions involving autonomous vehicles, these navigational aids do not provide the understanding to what a researcher is physically looking at. By applying a defined ground truth, this work was able to know not only what was being observed, but from an approximate physical location as well. Furthermore, the application of constructing an enhanced image processing algorithm and methodology for detecting specific features in congested environments is then simplified when utilizing ground truth. Once the defined ground truth was established, sonar images may easily be compared to what is physically present in order to verify the sonar detections.

2.4 Perception

Image processing algorithms are the tools used in this work to extract useful information from measurements obtained in the environment from the sonar data. Two proposed processing algorithms, developed by Dr. Noel du Toit, were compared to demonstrate the proposed methodology. The geometry of the insonified rig is specified and used to define the ground truth of the features in the sonar image frame.

2.4.1 Algorithm I

What follows is a step by step discussion of Algorithm I. Figure 2.10 represents the raw image produced through the sonar signal processing.

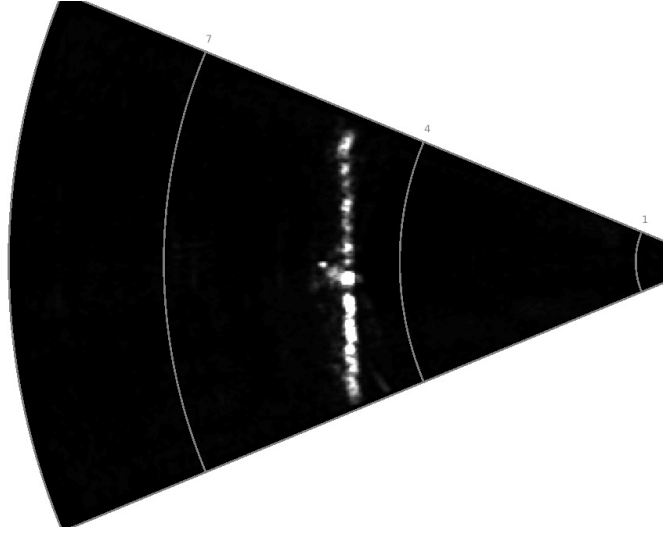


Figure 2.10: Raw image

1. The first step in Algorithm I is to apply Gaussian blurring to the original sonar image. The technique of Gaussian blurring involves the blurring or smoothing of an image through the use of a Gaussian function which reduces the noise associated with the image [51]. This smoothing effect of the image enhances the visual representation of the rig as well as the intensity return; this is obtained through the use of the Matrix Laboratory (MATLAB) command, *imgaussfilt*. The *BLUR WINDOW* parameter defines to what extent the Gaussian filter will be applied [52]. The *BLUR SIGMA* parameter is defined based on the desire of the researcher. Gaussian blurring is referred to as a low-pass filtering method which allows for the suppression of those undesirable high-frequency details, such as noise and edges, on the sonar image yet also preserving the desirable low-frequency aspects [?]. This is shown in Figure 2.11.

```
% defining the control parameters including the blur factor  
% and standard deviation  
BLUR_WINDOW = 3;  
BLUR_SIGMA = 0.3 * ((BLUR_WINDOW - 1) * 0.5 - 1) + 0.8;
```

```
% applying Gaussian filtering which filters the sonar image with a
% 2D Gaussian smoothing kernel with the standard deviation of sigma
img_filt = imgaussfilt(img_8,BLUR_SIGMA,'FilterSize',BLUR_WINDOW);
```

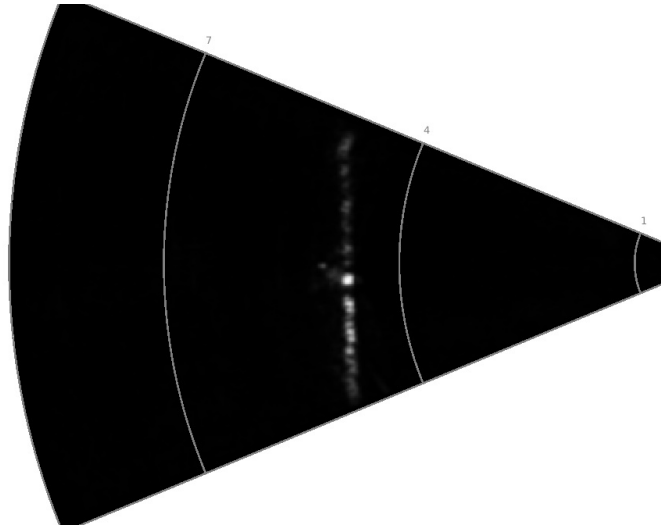


Figure 2.11: The effects of Gaussian blurring

2. The second step in the algorithm is to define the intensity threshold which creates a binary image of potential features and mitigates the presence of noise. The researcher may vary the pixel luminance threshold from 0 to 1 which defines the sensitivity of the algorithm; in this case the threshold is set at 0.15 and is shown in Figure 2.12. The purpose of this step is to mitigate the noise of the surrounding environment while displaying only the desirable features of the target.

```
img_segm = im2bw(img_filt, .15);
```

3. The third step is to erode or diminish the binary image that is produced through the use of the command, *imerode* [53]; the result is shown in Figure 2.13. The purpose of this step is to determine the minimum value of each pixel's surroundings which allows the viewer to distinguish features as opposed to a viewing a compilation [54]. This step also provides the effect of removing very small returns which are often associated with spurious returns.

```
img_err = imerode(img_segm, seD);
```

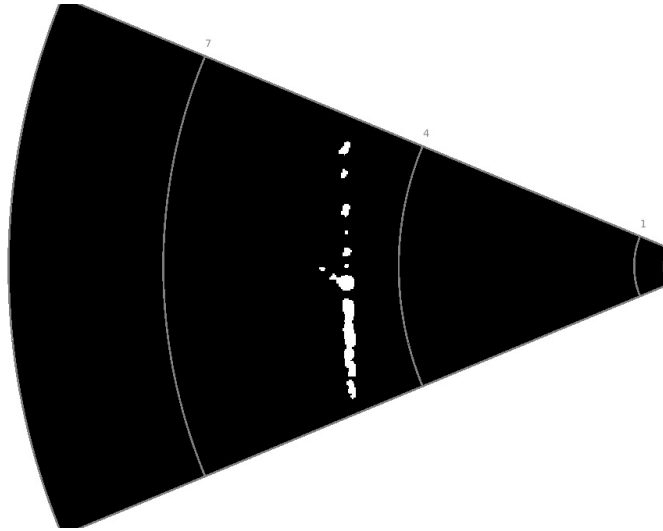


Figure 2.12: Thresholding applied

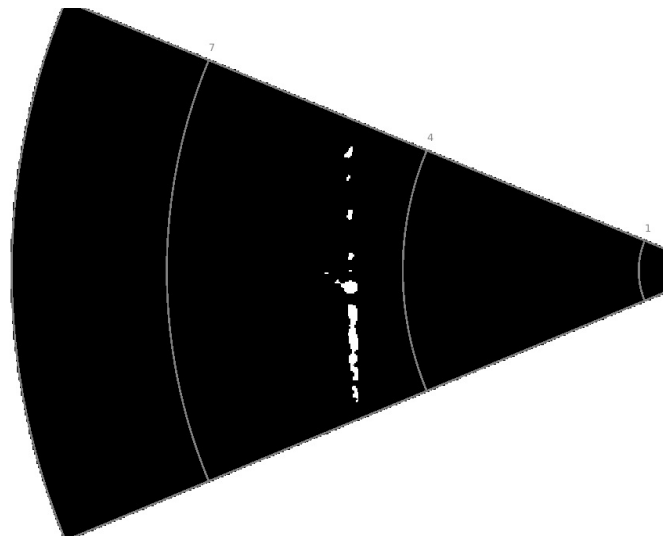


Figure 2.13: Eroded image

4. The fourth step in this image processing involves the establishment of the outlines surrounding those intensity returns. The results are shown in Figure 2.14.

2.4.2 Algorithm II

What follows is a step by step discussion of Algorithm II.

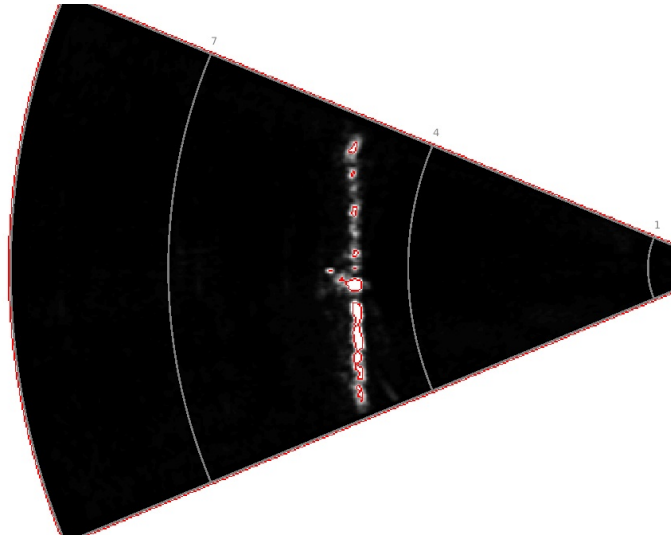


Figure 2.14: Algorithm I final image

1. Similar to Algorithm I, the first step in Algorithm II is to apply Gaussian blurring to the original sonar image. The next step is to detect and highlight the edges of the intensity returns. Using the *edge* command, edge detection is a technique used to find those boundaries associated with the intensity returns from the sonar. *Edge* takes the original intensity image as its input and returns a binary image of the same size defining a value of 1 where the function finds edges and a 0 where it does not [55]. This is shown in Figure 2.15.

```
% edge detection
[~, threshold] = edge(img_filt, 'sobel');
fudgeFactor = 3.0;
img_edge = edge(img_filt, 'sobel', threshold * fudgeFactor);
```

2. The next step is to dilate or enlarge the binary image produced through the command, *imdilate* [56]. This command widens or enlarges the returns for visual ease of the researcher and shown in Figure 2.16.

```
% dilate image
img_dil = imdilate(img_edge, [se90 se0]);
```

3. As in Algorithm I, the third step is to erode the binary image and then grab the

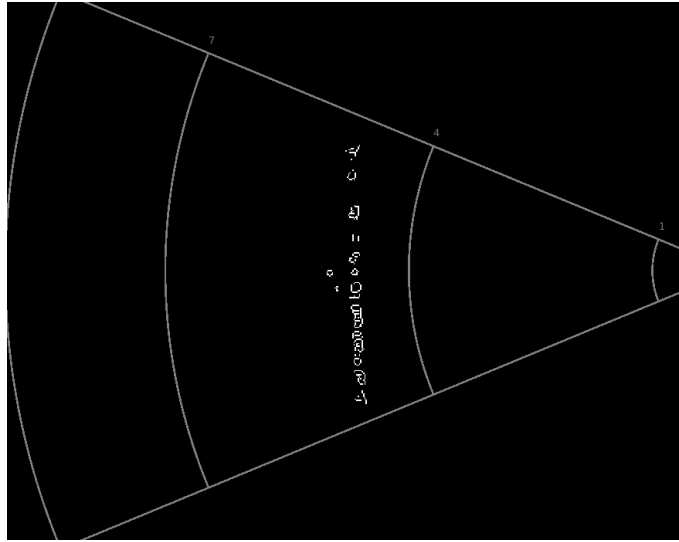


Figure 2.15: Image example of edge detection

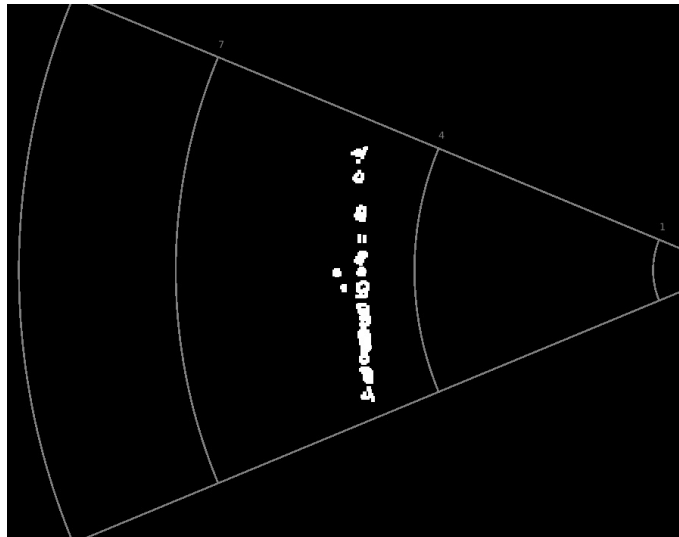


Figure 2.16: Example of dilating an image

outlines to produce the final sonar image; this line of code is presented below as well as the resulting features plotted in red shown in figure 2.17.

```
img_outline = bwperim(img_err);
```

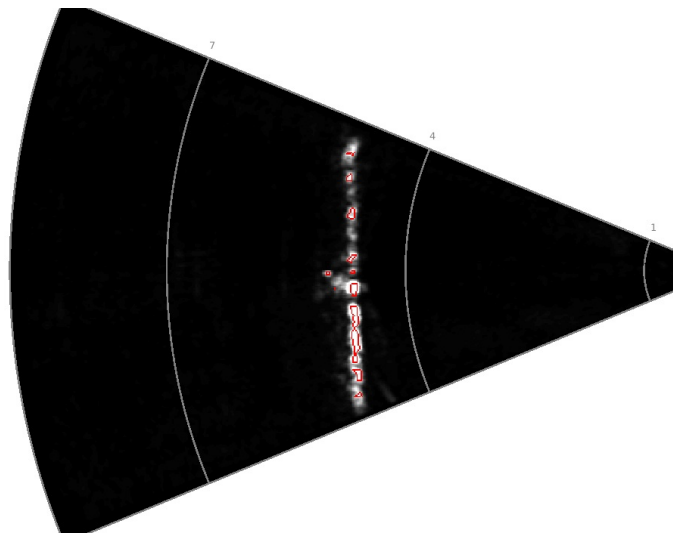


Figure 2.17: Final product through the use of Algorithm II

THIS PAGE INTENTIONALLY LEFT BLANK

CHAPTER 3:

EXPERIMENTAL DESIGN

What must be considered when designing an experiment that allows for the accurate representation of the underwater environment? The underwater community's capability gap is the inability to distinguish accurately features, specifically those too small to detect using common methods, within congested environments. The trifecta introduced in Chapter 2 drove the experimental design and identification of targets that the underwater community, specifically naval divers, tend to encounter in the littorals. Thus, two distinct targets were constructed to provide the ground truth element while an AUV carried a high frequency sonar providing the sensor element.

1. The motivation for Platform Golf is to evaluate the ability to observe and extract information of spaces between objects (i.e., gaps).
2. The motivation for Platform Tango is to evaluate the ability to detect equally spaced features of increased thickness.

What follows is a brief description regarding specific environment and sensor considerations.

1. *Size of a target:* The objective of this work is to establish a methodology in order to determine which features are distinguished or not in a complex underwater environment. Distinguishing those smaller underwater features through sonar signal processing and then detecting them through image processing is challenging, particularly those features that are set on the sea floor where high levels of clutter and noise exists. Additionally, smaller targets are more difficult to insonify due to the target's low TS [19].
2. *Sensor localization:* The initial insonification of the entire target was conducted which then provided the knowledge of the structure location. From that knowledge, the ability now existed to eliminate the concerns of sensor localization and ground truth for most trials; this was based upon the sonar range from the target and accurate knowledge of the target geometry.
3. *Field of View:* The high frequency sonar utilized in this work provides a horizontal

FOV of 45 degrees. Using the calculated frame length of 3.048 meters, a standoff distance of approximately 3.65 meters is required in order to insonify the entire width of the platform. Should this distance decrease, the ability to insonify the entire frame would be lost. However, the ability to resolve within the target will be enhanced due to the dependence of the bearing resolution on range.

3.1 Rig Design

The design of the targets or rigs utilized in this work were driven by a systems engineering approach, considering what the stakeholders needs are in distinguishing objects within the littoral zone. A brief description regarding the system effectiveness and possible rig construction involved three specific considerations.

1. *Usability of the target:* The emphasis is on the ease of rig use for data collection.
2. *Capability of the target:* The focus is on the ability to achieve desired outcomes through measurable features such as the size and thickness of the target features.
3. *Repeatability of the target:* The concern is with future trials and quantified ability of the target to continue to function during and after trials within an aquatic environment [5].

These system effectiveness factors would not be complete without also considering the cost of producing such a rig. The community need for a generalized platform requires low-cost building materials that would be widely available for all researchers and one representative of today's modern maritime applications [5]. Achieved Availability (AA) can be described as the probability that an item or system will successfully operate when utilized under specific, measurable, and controlled conditions [5]. Thus, the two prototypes for data collection were constructed with Polyvinyl Chloride (PVC) piping and secured using a strong liquid adhesive providing convenience and versatility. The following describes the additional justifications associated with this material selection for the experimental rig:

1. PVC pipes are corrosion resistant.
2. PVC pipes are built to include watertight joints that allow joint tightness and are easily assembled.
3. PVC pipes are easy reusable and recyclable.
4. PVC pipes are relatively inexpensive [57].

Once the construction material was identified, there was still the issue of determining what size of features and at what range to the target the forward-looking sonar (FLS) would be able to insonify. Ultimately the question remained, is there a quantitative or measurable relationship between the diameter of the submerged pipe used and the range of the sonar's signal to the target? To answer this question, the assumptions made were that the relative position of the sonar to the rig may be controlled, and that the FOV of the FLS cannot be varied. Therefore, the assumption is that the greater the sonar FOV, theoretically, the greater the viewable height and width that the FLS can observe based on a fixed vehicle pose.

With this FOV assumption in place, the next step was to determine the smallest resolvable distance between two objects or smallest feature width that the sonar could distinguish, and then construct the rig based off those calculations. The first step was to consider how the set sonar frequency affected the ability to distinguish features. Frequency is the measure of how many sonar pulses the FLS outputs into the water each second [19]. The sonar that was utilized in this work for the acquisition of data was the BlueView P900 forward looking, high resolution sonar seen in its unmounted state in Figure 3.1; this sonar is a 900 kHz system. This sonar system is referred to as blazed array sonar. A blazed array sonar utilizes a multi-beam signal with each individual signal having variations encoded within its unique frequency [58]. These particular variations allow the blazed array signal to contain more information and be more versatile in its directional orientation. Thus, the hope in choosing this sensor and frequency was that at 900 kHz the system might have a high probability to resolve the smaller features of the rig with a higher resolution than that of a lower frequency sonar [19].

In order to determine the height and width of the two rigs, an investigation of the horizontal and vertical sonar FOVs was conducted. Using the theory presented in Chapter 2, if the spacing between the top and bottom support is less than 0.79 meters, the sonar will not be able to distinguish between these two objects. Further, should the spacing between the vertical supports be less than 0.078 meters, the sonar will not be able to distinguish between these two objects. Therefore, while ensuring that the platforms are producible by other researchers and considering stability and portability of the platforms, both rigs are 1.5 meters by 3 meters. This proves to be justifiable, and convenient, in that locally available PVC lengths are pre-cut to this order. Figure 3.2 shows the completion of Platform Golf



Figure 3.1: BlueView P900 sonar

Source: Teledyne SeaBotix. (2015). P900 Series. [Online]. Available: <http://www.blueview.com/products/2d-imaging-sonar/pseries-archives/p900-series/>

while Figure 3.3 shows the completion of Platform Tango based on these considerations.

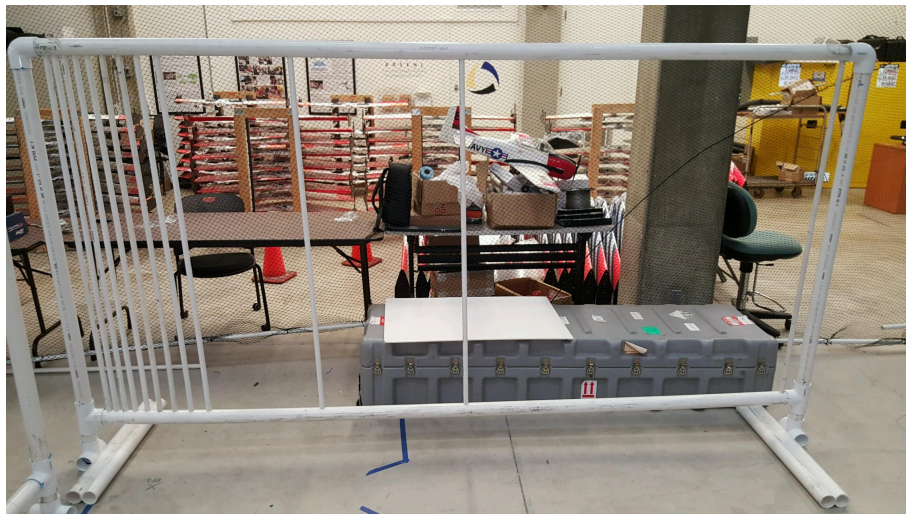


Figure 3.2: Finished Platform Golf in CAVR bay

Platform Golf was built to represent the space engineered between pylons with measurements of the gaps being 0.007 (0.27), 0.01 (0.39), 0.018 (0.70), 0.023 (0.90), 0.03 (1.18), 0.037 (1.45), 0.043 (1.69), 0.049 (1.92), 0.457 (17.99), 0.614 (24.17), and 1.42 (55.90) meters (inches). Platform Tango represents the variations in thickness of stationary objects



Figure 3.3: Finished Platform Tango in CAVR bay

with specific outer diameter measurements of the pylons being 0.009 (0.35), 0.0215 (0.84), 0.0267 (1.05), 0.033 (1.29), 0.048 (1.88), 0.067 (2.63), 0.101 (3.97), 0.134 (5.27), 0.168 (6.61), and 0.202 (7.95) meters (inches). The total cost of required building material is presented in Table 3.1.

3.2 ACQUAS

The obtained data sets were compiled through the use of an Agile Close-Quarters Underwater Autonomous System (ACQUAS) supplied by CAVR at Naval Postgraduate School (NPS) seen in Figure 3.4. ACQUAS itself is a miniature ROV manufactured and distributed by Teledyne SeaBotix [59]. The vehicle is a modular system allowing for the incorporation of multiple sensors based on its data interface and connectors. ACQUAS has also been outfitted with an INS and DVL for navigation purposes, as well as the active sonar system previously described. The ACQUAS platform is designed to conduct underwater operations as a fully autonomous system with a tether within the littoral zone and coastal waters in depths ranging to 304.8 meters seawater (MSW). This extensive range in depth allows ACQUAS to fulfill specific military and civilian mission needs that include:

Table 3.1: Building Material Information

<i>Part</i>	<i>Quantity</i>	<i>Cost per Unit</i>	<i>Cost</i>
2" x 10' PVC40-DWV PE Pipe	4	\$7.92	\$31.68
1-1/2" x 10' PVC40-DWV Pipe	1	\$6.70	\$6.70
1/4" x 5' PEX Pipe	2	\$1.86	\$3.72
Milwaukee Bi-metal Hole Saw 8 PC Kit	1	\$48.84	\$48.84
Milwaukee 1-1/4" Bi-metal Hole Saw	1	\$8.47	\$8.47
Milwaukee 1-3/4" Bi-metal Hole Saw	1	\$9.75	\$9.75
3/4" x 10' PVC40 PE Pipe	1	\$2.34	\$2.34
1" x 10' PVC40 PE Pipe	4	\$3.93	\$15.72
1/2" x 10' PVC40 PE Pipe	8	\$2.03	\$16.24
2" PVC Tee	8	\$1.98	\$15.84
16 oz PVC Cement Wet/Dry	1	\$10.95	\$10.95
2" PVC El 90D	8	\$1.98	\$15.84
Total Cost			\$ 183.36

1. Sea-floor survey and inspection;
2. Sub-sea equipment installation, inspection, manipulation, and maintenance;
3. Salvage and recovery operations;
4. Marine observation [14]

The standard ACQUAS is an updated approach to small yet highly capable inspection AUV systems. Until recently, vectored vehicles start in the 49.9 kilogram weight category. ACQUAS weighs a mere 18.1 kilograms in air and has a length of 0.62 meters. This reduced weight and convenient size allow for effortless deployment and handling. ACQUAS is modular and can be configured to meet unique mission needs. Configurations include:

1. Six Brushless Direct Current (DC) thrusters
2. Two x 1,080 Lumen Light Emitting Diode (LED) arrays
3. Four video channels including high definition
4. Four high speed data channels
5. Three high speed Ethernet channels [59]

Similar to most satellite-guided vehicles operating on the water's surface, ACQUAS may utilize GPS in order to obtain positional fixes. When submerged, however, ACQUAS requires an alternative method in order to accurately navigate within the ocean depths, such as the use of an integrated navigation solution [59].



Figure 3.4: Modified (tethered, autonomous) SeaBotix ACQUAS

3.3 Measures of Performance

Measures of performance (MOP) are defined as the process of analyzing critical factors impacting the system or its development [60]. Within the consideration of this experimental design, the performance parameters involve physical properties of the sensor as well as the processing algorithms [61]. The following describes the two MOPs critical to the designs within this system of systems (SoS) and will be further discussed in Chapter 4.

1. *Probability of detection:* This thesis is concerned with the community's current inability to know what is seen or missed with modern sonar and processing algorithms. Using a binary methodology, the sensor can be considered operationally effective should it distinguish the target's features.
2. *Error rate of the sensor:* The methodology within this work will aim to determine the precise error rate of the fixed environment. Further explanation shall be presented within Chapter 4; however, the methodology within this work shall consist of acquiring the acoustic data, establishing certain intensity thresholds, and then layering the physical dimensions of the target atop the sonar frame in order to calculate the error

rate per frame. This will enable a more accurate understanding of what features may have been missed in the environment.

3.4 Data Collection Methodology

The data acquired for this thesis originated from trials conducted with Platforms Golf and Tango, ACQUAS, and the P900 FLS. The targets were initially deployed within a small basin along the US Coast Guard Pier in Monterey, CA. This isolated area was expected to be ideal for placement of the light weight platforms and ACQUAS based upon measurable factors that included depth within the basin and the environment typical to the usage of commercial sonar. However, increased surge prevented successful data collection efforts at this test site. The AO is visually represented in Figure 3.5 by the Google Earth screen shot.



Figure 3.5: Location of Initial - US Coast Guard Pier Monterey, CA

Source: Google Maps. (2015). US Coast Guard Pier. [Online]. Available:

<https://www.google.com/maps/@36.6090694,-121.8940931,153m/data=!3m1!1e3>

In light of this initial setback, a more controllable or benign setting was sought out at the Stevenson School aquatics facility in Pebble Beach, CA. At this location the research focused on the P900's ability to observe and extract information of spaces between objects and to detect equally spaced features of increased thickness. The AO is visually represented in Figure 3.6 by the Google Earth screen shot.

The research emphasis was placed on the establishing a method that future researchers may reconstruct to evaluate their own results. The P900 FLS was first mounted onto the AUV and placed at a distance that allowed the sensor to insonify the entire rig, Platform Tango. Contrary to the conditions within Monterey Bay during the previous mission, the conditions within the Stevenson School aquatics facility were pristine.



Figure 3.6: Location of Contingency - Stevenson School aquatics facility Pebble Beach, CA

Source: Google Maps. (2015). Stevenson School. [Online]. Available: <https://www.google.com/maps/place/Stevenson+School/@36.5822573,-121.9522788,153m/data=!3m1!1e3!4m2!3m1!1s0x808de71e2f1b6fbd:0xcb6ee2b6c4d3b19f>

The overall methodology of this data extraction was devised to place the vehicle in three perpendicular positions facing the platforms. For the initial insonification of the entire structure, the vehicle was strategically positioned at approximately 5 meters, mid-range, as seen in Figure 3.7. This implies that the vertical pylons will be completely insonified for the width of the sensor's array and that there will be areas of no insonification between sounding lines. The horizontal cross frames should not be in the field of view. Once this first data set was collected, the vehicle was then maneuvered to the left of the platform and stopped once in line with the frame support as seen in Figure 3.8. The operator then maneuvered the vehicle laterally to the opposite support and then reset the AUV to the original pose, centered at approximately 5 meters from the target. The next step in the methodology was to rotate the vehicle along its axis without performing any lateral movement. This task would have been difficult during surges encountered in the Monterey Bay but was relatively effortless in the gentle pool environment as seen in Figure 3.7.

Being satisfied with the mid-range trials, the vehicle was then positioned at a distance approximately 7 meters from the target. The idea behind this relocation aft was to test the sensor's ability to maintain the insonification of the smaller diameter features at larger ranges. Once satisfied at this new long-range position, a data set was collected. Following

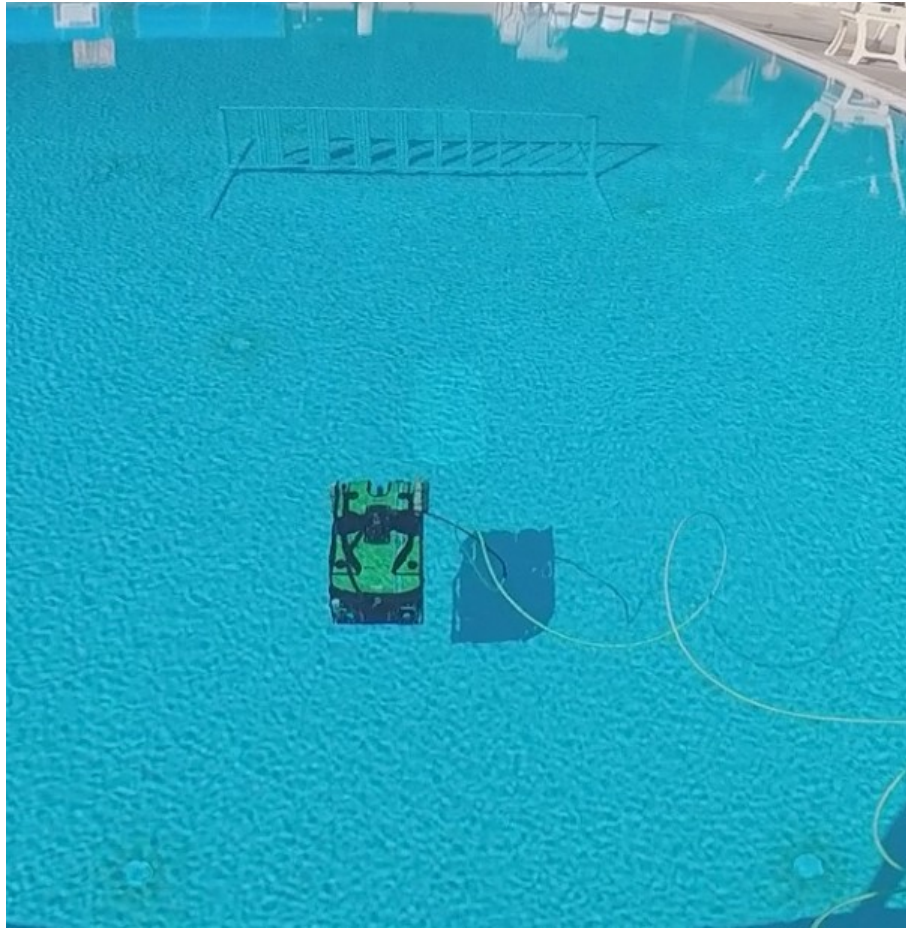


Figure 3.7: Initial setup position of the vehicle on Platform Tango

the completion of the long-range pose, the vehicle was then positioned within 1.5 meters, short-range, of the platform. Similar to the extended distance of the AUV, this closer position would attempt to answer the question of bearing and range resolution between objects that were systematically placed near or adjacent to each other. In other words, could a sensor distinguish between similar objects spaced at extremely close intervals? The short-range data set collected here consisted of the vehicle transitioning laterally and then back to center after one complete pass of the frame. With the conditions and trials progressing with relative ease, Platform Tango was removed and replaced with Platform Golf. Once Platform Golf was secured to the base of the pool, the methodology conducted consisted of a mid-range lateral movement, long-range forward facing movement, a mid-range sweeping movement, and a short-range lateral movement of the vehicle as seen in

Figures 3.8, 3.9, and 3.10.



Figure 3.8: ACQUAS positioned to begin lateral data extraction on Platform Tango



Figure 3.9: ACQUAS sweeping Platform Tango



Figure 3.10: ACQUAS data extraction on Platform Golf

THIS PAGE INTENTIONALLY LEFT BLANK

CHAPTER 4:

ANALYSIS

4.1 Sonar Theory Applied to the BlueView P900

Given the theory presented in Chapter 2, what is reasonable to expect in the experimental results for the sonar used in this work: the BlueView P900 sonar? Chapter 2 described the theory of sonar, which can now be used to explicitly calculate the sizes of features that is expected to be detectable as a function of range. Second, a discussion of the possible errors that can occur during sonar signal processing is presented.

1. The vehicle and sonar were placed at the minimum range of 1.5 meters from the rigs during two of the trials. Applying this range to the theory presented in Chapter 2, the expected smallest resolvable distance that the sonar may distinguish between objects is 0.0313 meters. If the horizontal spacing between the pylons or the thicknesses of the pipes are less than 0.0313 meters, the sonar will not be able to distinguish them.
2. The vehicle and sonar were placed at the mid-range of five meters from the rigs during five of the trials. Applying this range to the theory presented in Chapter 2, the expected smallest resolvable distance that the sonar may distinguish between objects is 0.104 meters. If the horizontal spacing between the pylons or the thicknesses of the pipes are less than 0.104 meters, the sonar will not be able to distinguish them.
3. The vehicle and sonar were placed at a long range of seven meters from the rigs during two of the trials. Applying this range to the theory presented in Chapter 2, the expected smallest resolvable distance that the sonar may distinguish between objects is 0.146 meters. If the horizontal spacing between the pylons or the thicknesses of the pipes are less than 0.146 meters, the sonar will not be able to distinguish between them.

The potential errors that can occur in the produced sonar images are:

1. *False positives*: the sonar detects an object when there is no physical feature present. A sample of a false positive is circled in green in Figure 4.1: suggesting that there are additional features adjacent to and behind the seventh rig feature which is an

inaccurate representation.

2. *True negatives*: the sonar fails to detect an object when there is a physical feature present to detect [51]. A sample of a true negative is circled in red in Figure 4.1: providing an example in which the third smallest diameter pipe is not insonified by the sonar; this is a fault in the processing because it is known that the platform and pipe are present yet not detected.
3. *Compilations*: the sonar combines the returns from distinct objects into a single return. A sample of compilation is circled in yellow in Figure 4.1: the smallest diameter pipe of Platform Tango is not detected but rather the signal return combines the support frame and the pipe.

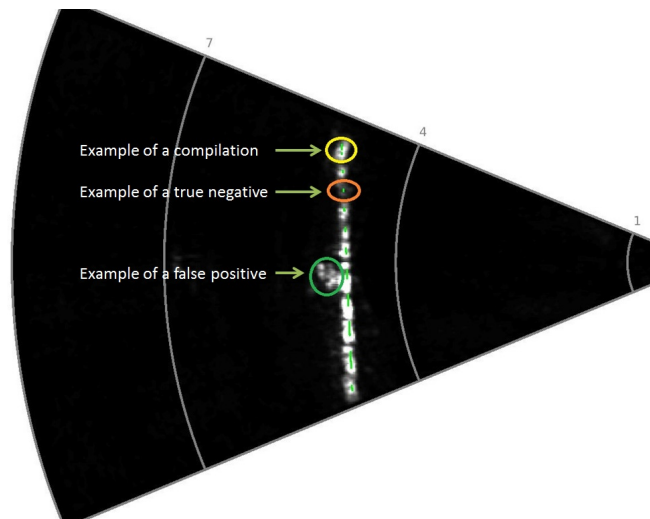


Figure 4.1: Example of errors within sonar signal processing

4.2 Sonar Image Interpretation

Image processing extracts the feature data through the use of various operations on the images; this is the process that was demonstrated earlier in Chapter 2. Typically, image processing requires that features be well defined in the sonar images, either through factors such as pixel intensity or texture variation, in order to reliably distinguish them from their surroundings. Not only can image processing be used to detect these features or targets, it may also use the information to classify or recognize the targets and track them [62]. Once the image processing algorithms have been applied, the probability of detection can

be calculated by comparing the detected features to the ground truth data. The probability of detection is a measure of how likely detection of a feature is to occur and is a function of both the obtained sonar image and the image processing algorithm used.

The goal of the image processing algorithms is to reliably extract information from the sonar images. However, this is complicated due to various factors that arise such as low update rates and the low resolution of images; both are due to the physics of utilizing acoustic signals. Furthermore, sonar images tend to have high noise content, complicating the image processing task. In general, a higher sensitivity level of the image processing algorithm, the higher the probability of detection. This comes at the expense of detecting more clutter or false positives in the sonar image [51]. Conversely, a low sensitivity level of the image algorithm, the lower probability of detection. This comes at the benefit of the reduced number of false positives produced in the sonar image. Three distinct but related objectives with sonar image processing can be identified; these are the detection, classification, and tracking of underwater targets [63].

1. *Detection*: Detection is the discovery of underwater objects. The detection of small features, specifically, through the use of image processing is critical for building accurate representations of complex underwater environments. Based on the algorithm sensitivity level, the image processing will detect a varying number of features.
2. *Classification*: Classifying is the act of categorizing the detected underwater objects. For example, the texture or pixel intensity variations of the objects on the sonar image may be used to classify the detected objects as opposed to merely discovering a number of objects in the frame. Generally, the classification of an object is based on its type or shape. For example, the classification type may include arranging the detected objects based on material composition or whether they remain static or dynamic. Classifying an object based on its shape is also common. In the case of mine warfare, distinguishing the shapes of underwater mines aid in determining their explosive capability [19]. The information used to classify an object differs from that of merely detecting an object. Although the element of classifying objects is not within the scope of this thesis, it is an important underwater environmental objective and one that should be considered for future work.
3. *Tracking*: The process of tracking an underwater target may be described as repeatedly recognizing an object. In order to track an object, that object must first be

detected and classified. Based on the sensitivity of the algorithm, the ability to track the classified object then becomes time dependent. For example, submarines first detect and classify the targets they encounter and will repeatedly plot the position of the contact over a period of time. Although the process of tracking objects is not within the scope of this thesis, it is also an important underwater environmental objective that should be considered for future work.

4.3 Results

Based on the image processing of Algorithm I and II, an analysis of the generated outputs is presented below. In order to determine the error rate of the sonar, the average number of false positives, true negatives, and compilations were calculated per data set by comparing the generated sonar images to the ground truth. In order to determine the overall probability of detection, the average number of detection's for each feature was calculated for each data set.

Furthermore, based on the theory in Chapter 2, the expectation was that:

1. The smallest resolvable distance the sonar may distinguish is 0.0313 meters or greater when the sonar was 1.5 meters from the target. This forecast suggests that the smallest five gaps in Platform Golf (0.007 to 0.03 meters) will not be distinguishable while remaining gaps shall. Within Platform Tango, only the smallest three features (0.009 to 0.0267 meters) will be indistinguishable.
2. The smallest resolvable distance the sonar may distinguish is 0.104 meters or greater when the sonar was five meters from the target. This forecast suggests that the smallest eight gaps in Platform Golf (0.007 to 0.049 meters) will not be distinguishable while the remaining gaps shall. Within Platform Tango, the smallest six features (0.009 to 0.067 meters) will not be distinguishable while the remaining thicker features will.
3. The smallest resolvable distance the sonar may distinguish is 0.146 meters or greater when the sonar was seven meters from the target. This forecast again suggests that the smaller eight gaps in Platform Golf will be indistinguishable while the remaining larger gaps (0.457 to 1.42 meters) shall. Within Platform Tango, only the two thickest features (0.168 and 0.202 meters) shall be distinguishable while the smaller features

will not be.

4.3.1 Forward Insonification at 5 meters standoff - Platform Tango

Based on the data compiled and analysis of 207 sonar images, the sonar signal processing produces an average of 2.92 false positives per image, 0.22 true negatives per image, and 37% of the pylons blend together and are indistinguishable from each other. The extracted information from Algorithm I conclude that 56% of the features are distinguishable throughout the data set while 53% are distinguishable from Algorithm II. Based on these results, the following conclusions are drawn:

1. The sonar signal processing produces more false positives than true negatives; this is shown, for example, in Figure 4.2 which provides a visual representation of the raw sonar image with rig overlay. Possible reasons include the physical nature of acoustic signals and super-position of the reflection of the signal off the pipes, i.e., acoustic interference.
2. The percentage of compilations are likely due to the close vicinity of the end pipes to the support frame as well as the amount of noise surrounding the larger diameter pipes.
3. Overall, the average probability of features detected are very similar between Algorithm I (56%) and II (53%) until observing the three larger features. These three features tend to be observed as compilations much more so than any of the other features possibly due to the increased amount of noise surrounding pipes that are closely positioned to each other.
4. Figure 4.3 provides a visual representation of Algorithm I applied to this data set overlaid with the ground truth data. The comparison between the ground truth and the sonar signal processing reveals the compilation effect seemingly resulting from larger features spaced closely together. Also, the third feature is not distinguished through the signal processing; this is a clear example of a true negative.
5. Figure 4.4 provides a visual representation of Algorithm II applied to this data set overlaid with the ground truth data. The comparison between the ground truth and the sonar signal processing reveals the compilation effect seemingly resulting from the larger features being closely spaced together. Also, the third feature is not distinguished through the signal processing which is an example of a true negative.

Further, there is a distinct false positive appearing behind the seventh feature that could be the result of a higher quantity of noise surrounding this feature as opposed to the other features.

6. Figure 4.5 provides a visual comparison of the average probability of detection based on the feature thicknesses. The conclusions drawn from this comparison are that the first and third feature are not distinguishable by the sonar signal processing. Further, the second through the sixth feature are consistently detected and align with the ground truth overlay. The seventh through the tenth features are large and the probability of detecting these features diminish greatly. Overall, the rig features have a greater probability of being detected when utilizing Algorithm I.
7. The smallest diameter feature of the rig was the 0.009 meter PVC pipe. Based on the theory, the signal and image processing confirmed that this feature was not distinguishable in that it appeared as a compilation with the adjacent support frame.
8. The largest diameter feature of the rig was the 0.203 meter PVC pipe. When viewing the raw sonar images, the 0.203 meter pipe was detected and the image processing algorithms were able to extract data. However, this larger feature typically appeared as a compilation rather than being a stand-alone object; generally, this also proved to be the case of the 0.10, 0.13, and 0.16 meter features.
9. By positioning the sonar at the standoff distance of five meters and in the middle of the rig, the resulting signal and image processing produced false positives and compilations behind the fifth and sixth feature. For future work, it might be of interest to position the sonar at various fixed positions throughout the length of the rig in order to determine the uniqueness of this occurrence.
10. The 0.0267 meter feature is classified as a true negative in the majority of the sonar images; this occurrence is curious and should be investigated in future work. However, based upon the theory in Chapter 2, the expected inability to distinguish this feature proves accurate.

These figures apply to the signal and image processing while the vehicle maintained a fixed pose at a range of five meters from Platform Tango.

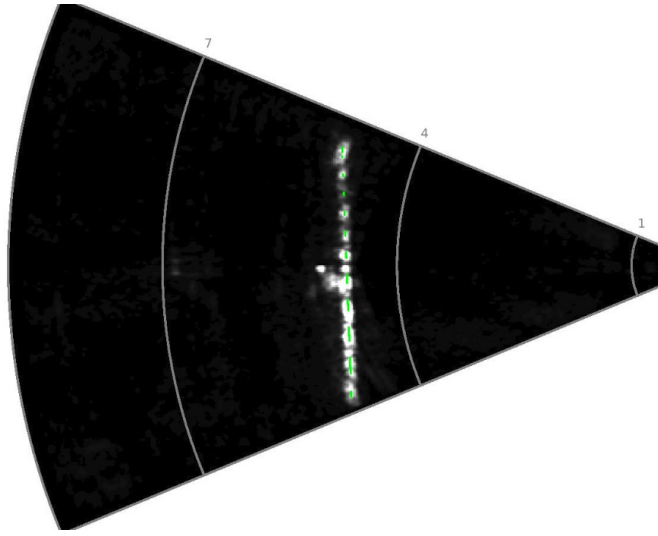


Figure 4.2: Raw sonar image - forward insonification at 5 meter standoff; Platform Tango

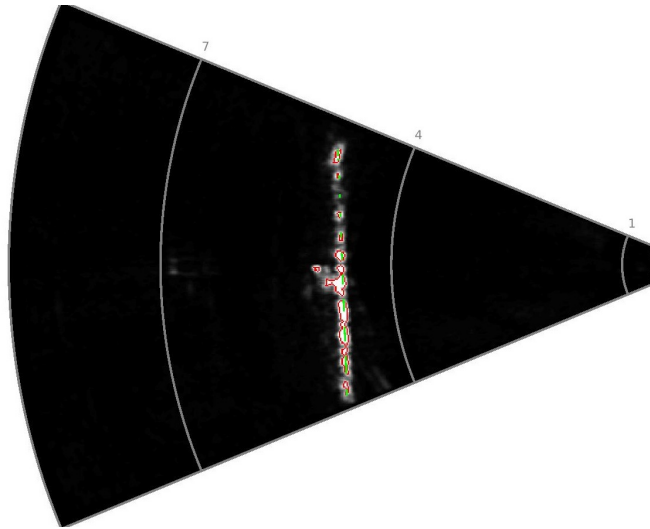


Figure 4.3: Example of Algorithm I based on the applied forward insonification at 5 meter standoff; Platform Tango

4.3.2 Lateral Movement at 5 meters standoff - Platform Tango

Based on the data compiled and analysis of 234 sonar images, it can be inferred that the sonar signal processing produces 1.46 false positives per image, 0.71 true negatives per image, 25% of the pylons blend together and are indistinguishable from each other. The

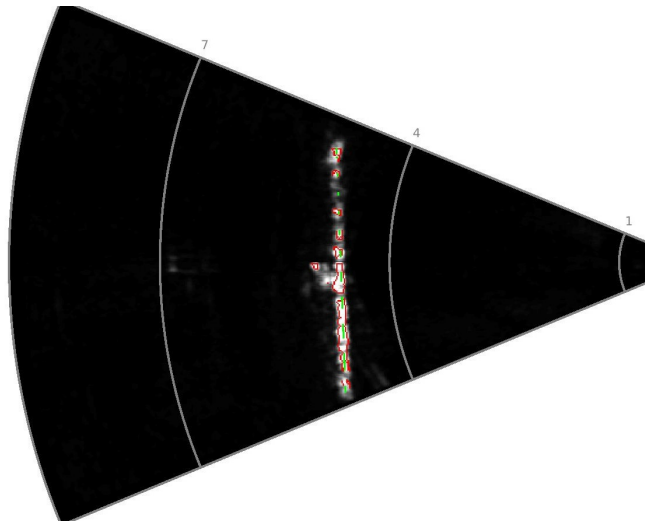


Figure 4.4: Example of Algorithm II based on the applied forward insonification at 5 meter standoff; Platform Tango

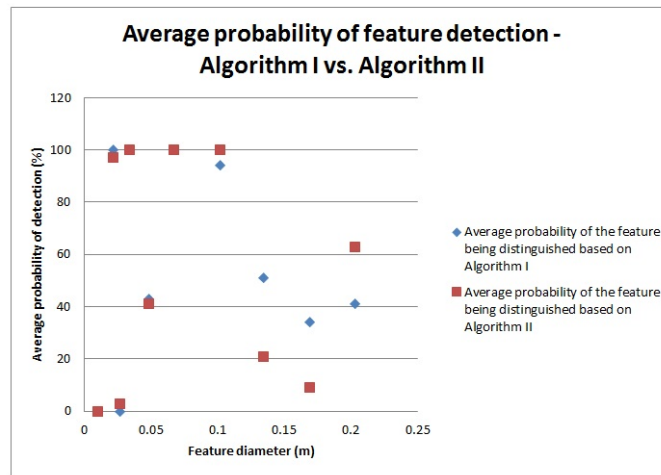


Figure 4.5: Average probability of feature detection based on the applied forward insonification at 5 meter standoff; Platform Tango

extracted information from Algorithm I conclude that 64% of the features are distinguishable throughout the data set while 57% are distinguishable from Algorithm II. Based on these results, the following conclusions are drawn:

1. The sonar signal processing produces more false positives than true negatives; this

is shown in Figure 4.6 which provides a visual representation of a raw sonar image. The sonar signal processing produces more false positives than true negatives; this is shown in Figure 4.2 which provides a visual representation of the raw sonar image. The number of false positives are less than those of the previous data set while the number of true negatives increases. Due to the vehicle moving laterally to acquire the data, it may be assumed that more data was obtained providing a clearer picture of the actual target against the environment.

2. Figure 4.7 provides a visual representation of Algorithm I applied to this data set overlaid with the ground truth data. The comparison between the ground truth and the sonar signal processing reveals that the larger features are more distinguishable when the sonar is positioned closer to it than when the sonar is at the other end or in the middle of the platform. Although features nine and ten still appear as a compilation, it is easier to assume that there might be two distinct objects adjacent to each other as opposed to one massive object in the location.
3. Figure 4.8 provides a visual representation of Algorithm II applied to this data set overlaid with the ground truth data. The comparison between the ground truth and the sonar signal processing also reveals that the larger features are more distinguishable when the sonar is positioned closer to it than when the sonar is at the other end or in the middle of the platform. The same effect is observed when the sonar is positioned next to the smaller features of the rig.
4. Figure 4.9 provides a visual comparison of the average probability of detection based on the feature thicknesses. The conclusions drawn from this comparison are that the first and third feature are not distinguishable by the sonar signal processing. The remaining features have a much greater probability of being detected with Algorithm I providing the better average probability of detecting features.
5. As was noted in the previous section, by maintaining the sonar between the fifth and sixth features, false positives were produced along with compilations that included the sixth feature, specifically. As the vehicle conducted a slow lateral movement parallel to the rig, individual features become more distinguishable as the sonar passed in front of them. Referring to Figure 4.7, Algorithm I was able to extract data and produce an image that more clearly defined the larger features as opposed to the compilations previously viewed in the earlier data set. Algorithm II also produced an enhanced image providing well defined feature determination; this may be seen in

Figure 4.8.

6. Although the larger features proved to be distinguishable by positioning the sonar in front of the feature, the smaller features remained indistinguishable. In Figure 4.9, both algorithms were not able to extract data from the first (0.009 meters) and third (0.026 meters) feature; both of which fall below or at the expected smallest resolvable width of a feature. The remaining features were distinguishable through both algorithms; all of which were greater than the expected resolvable width of a feature except for the second feature (0.021 meters).

As the sonar conducted the lateral movement, various features were not insonified through the sonar signal processing. Thus, the image processing was not able to extract data from those features. The figures that follow reflect solely what is observed in the sonar images and extracted data based on the algorithms.

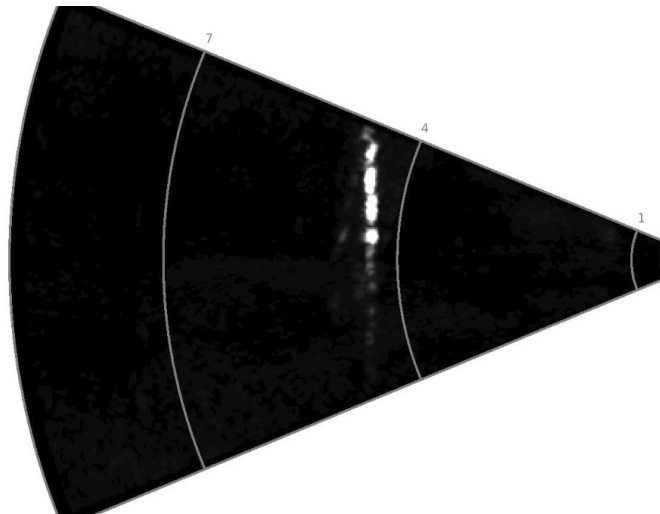


Figure 4.6: Example of raw sonar image based on the applied lateral movement at 5 meters standoff; Platform Tango

4.3.3 Sweeping Movement at 5 meters standoff - Platform Tango

Based on the data compiled and analysis of 186 sonar images, it can be inferred that the sonar signal processing produces 1.30 false positive per image, 1.02 true negative per image, and 26% of the pylons blend together and are indistinguishable from each other. The extracted information from Algorithm I conclude that 60% of the features are distinguish-

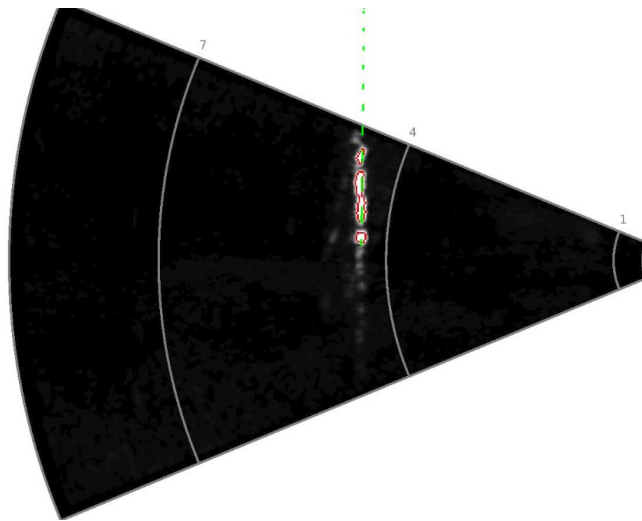


Figure 4.7: Example of Algorithm I based on the applied lateral movement at 5 meters standoff; Platform Tango

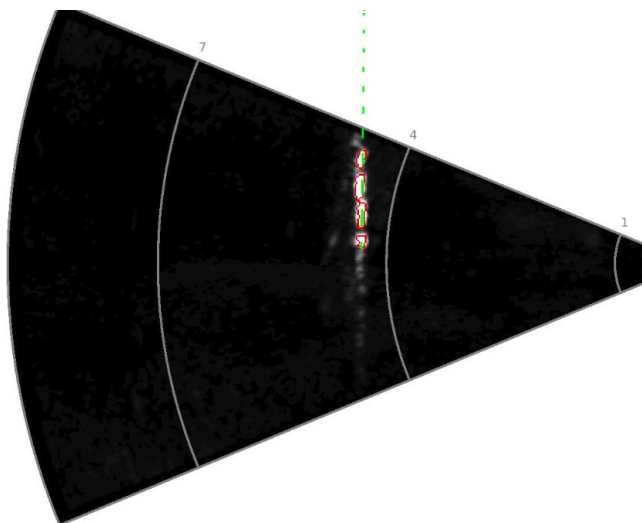


Figure 4.8: Example of Algorithm II based on the applied lateral movement at 5 meters standoff; Platform Tango

able throughout the data set while 62% are distinguishable from Algorithm II. Based on these results, the following conclusions are drawn:

1. The sonar signal processing produces many false positives; this is shown in Figure 4.6 which provides a visual representation of a raw sonar image.

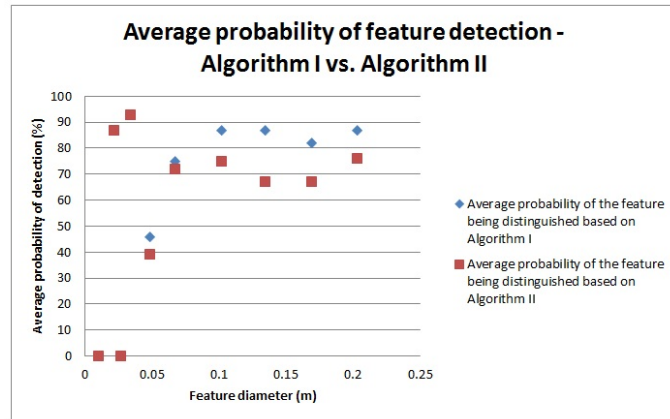


Figure 4.9: Average probability of feature detection based on the applied lateral movement at 5 meters standoff; Platform Tango

2. Figure 4.12 provides a visual representation of Algorithm I applied to this data set overlaid with the ground truth data. This particular example reveals a large compilation as the sonar is conducting a sweeping motion to acquire data. Based on this image, the inability to distinguish features is presented.
3. Figure 4.13 provides a visual representation of Algorithm II applied to this data set overlaid with the ground truth data. This particular example also reveals a large compilation as the sonar is conducting a sweeping motion to acquire data. Based on this image, the inability to distinguish features is presented.
4. Figure 4.14 provides a visual comparison of the average probability of detection based on the feature thicknesses. The conclusions drawn from this comparison are that the smaller images have a higher probability of being detected. These results are similar to those presented in the first and second data set because the sonar is generally unable to distinguish the larger features when insonifying at the perpendicular pose, while the inability to insonify features exist when features do not fall within the sonar's FOV.

Based on the figures presented in this chapter, it would be easy to conclude that not only were the individual features indistinguishable, but the rig as a whole. These compilations of the features do not provide a clear picture nor do they aid in determine the establishment of the ground truth, either. However, the sonar is able to distinguish features when conducting slow sweeping movements; this is shown in Figure 4.10. In Figure 4.10 features are distin-

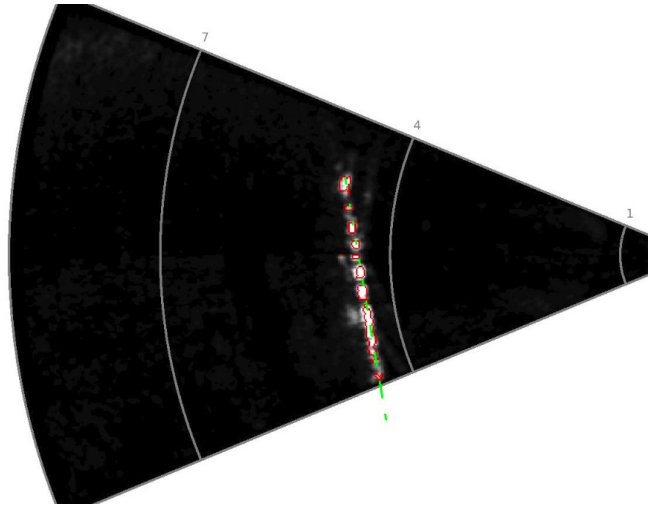


Figure 4.10: Sonar image based on image processing of Algorithm II applied to the sweeping movement at 5 meters standoff; Platform Tango

guishable although particular features compile together and other features are completely missed by the signal processing; this is due to the target not being in the sonar's FOV.

As the sonar conducted the sweeping movement, various features were not insonified through the sonar signal processing. Thus, the image processing was not able to extract data from those features. The figures that follow reflect solely what is observed in the sonar images and extracted data based on the algorithms.

4.3.4 Forward Insonification at 7 meters standoff - Platform Tango

Based on the data compiled and analysis of 165 sonar images, it can be inferred that the sonar signal processing produces 0.18 false positives per image, 1.8 true negatives per image, and 17.6% of the pylons blend together and are indistinguishable from each other. The extracted information from Algorithm I conclude that 49% of the features are distinguishable throughout the data set while 31% are distinguishable from Algorithm II. Based on these results, the following conclusions are drawn:

1. The sonar signal processing produces more true negatives than false positives; this is shown in Figure 4.15 which provides a visual representation of a raw sonar image. The signal processing also produces a lesser number of compilations while also pro-

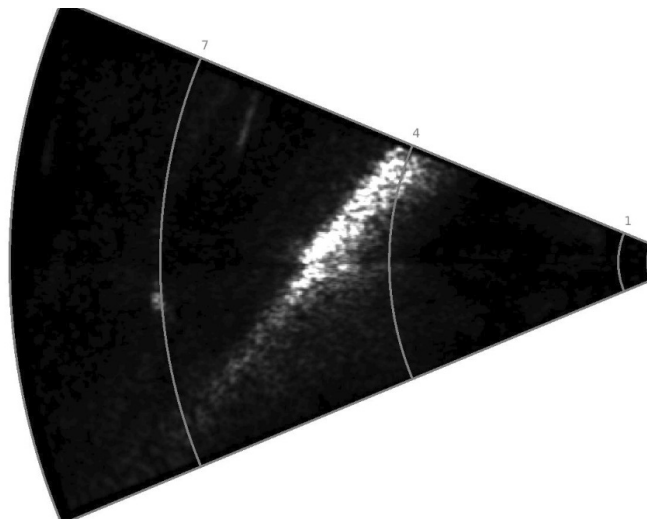


Figure 4.11: Example of raw sonar image based on the applied sweeping movement at 5 meters standoff; Platform Tango

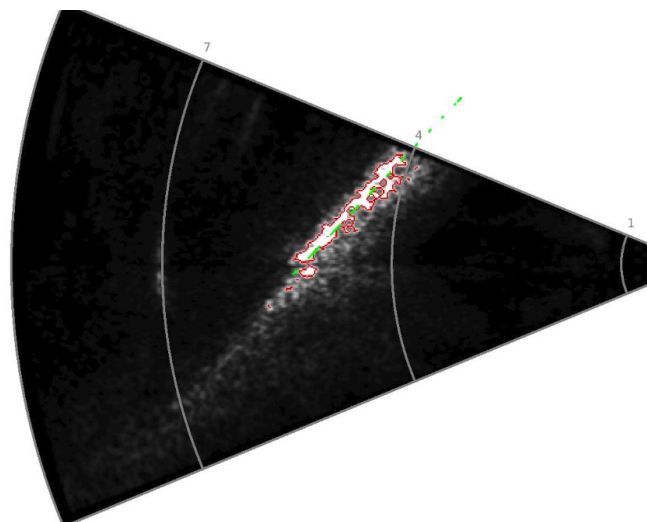


Figure 4.12: Example of Algorithm I based on the applied sweeping movement at 5 meters standoff; Platform Tango

ducing a minimal number of returns where the smaller features would presumably be.

2. Figure 4.16 provides a visual representation of Algorithm I applied to this data set overlaid with the ground truth data. At this increased range, features two through five now appear as true negatives while the those compilations previously seen in the

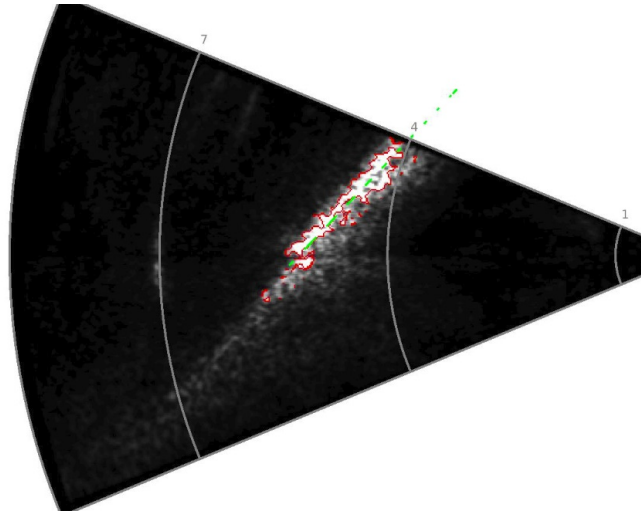


Figure 4.13: Example of Algorithm II based on the applied sweeping movement at 5 meters standoff; Platform Tango

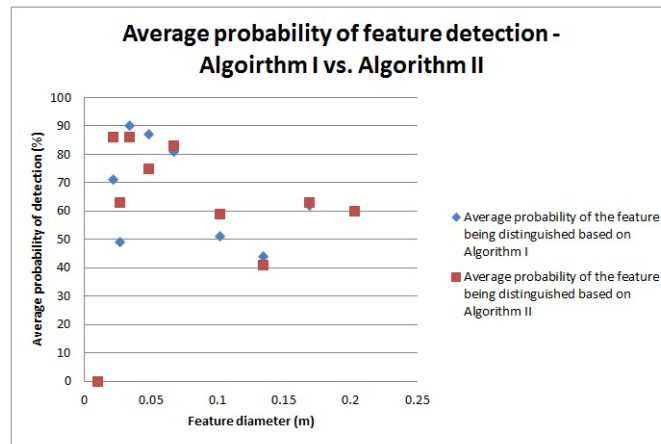


Figure 4.14: Average probability of feature detection based on the applied sweeping movement at 5 meters standoff; Platform Tango

larger figures do not appear.

3. Figure 4.17 provides a visual representation of Algorithm II applied to this data set overlaid with the ground truth data. At this increased range, features two and three appear as the only true negatives while a compilation appears around features six, seven, and eight.
4. Figure 4.18 provides a visual comparison of the average probability of detection

based on the feature thicknesses. The conclusions drawn from this comparison are that Algorithm I is more successful in detecting features than Algorithm II. As the diameter of the feature increases, the ability of Algorithm II to detect the feature decreases at a rapid rate. While there is some decrease in the ability to detect the larger features, the ability of Algorithm I maintains a higher efficiency.

5. The smallest expected resolvable width the sonar may distinguish is 0.12 meters or greater when the sonar is seven meters from the target. Based on this theory, the sonar should only be able to distinguish the three largest features of 0.13, 0.17, and 0.20 meters. However, Figure 4.16 presents a conflicting result to the theory. The first 5 features (0.009 to 0.048 meters) were expected to not be distinguishable by the algorithm and is the case. Interesting, features six (0.067 meters) and seven (0.102 meters) are detected through the signal processing, data is extracted through the image processing, and presented as individual features. The three largest feature are also distinguishable, as expected.
6. Figure 4.17 presents a similar result through the use of Algorithm II. However, the second algorithm is unexpectedly able to extract data from the fourth (0.034 meters) and fifth (0.048 meters) features as well as the subsequent features.
7. Overall, Algorithm I has the higher average probability of distinguishing the rig features because Algorithm II extracts data that appears more so as compilations than individual features.

4.3.5 Forward Insonification at 1.5 meters standoff - Platform Tango

An attempt was made to extract the data of the features at close range. Although the sonar was able to insonify the target, the ability to distinguish features and define the ground truth proved unattainable through an analysis of 72 sonar images; this is seen in Figure 4.19. The ground truth was unable to be defined based on the signal and image processing.

4.3.6 Lateral Movement at 5 meters standoff - Platform Golf

Based on the data compiled and analysis of 180 sonar images, it can be inferred that the sonar signal processing produces 0.89 false positives per image, 0.20 true negatives per image, and 74% of the gaps blend together and are indistinguishable from each other. The extracted information from Algorithm I conclude that 45% of the gaps are distinguishable

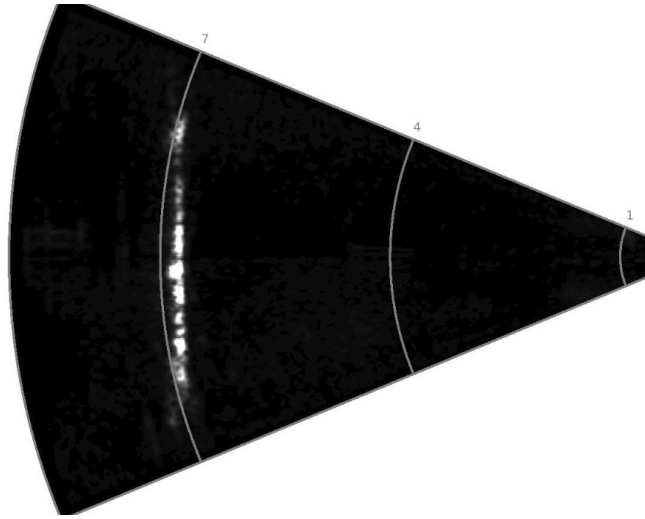


Figure 4.15: Example of raw sonar image based on the applied forward insonification at 7 meters standoff; Platform Tango

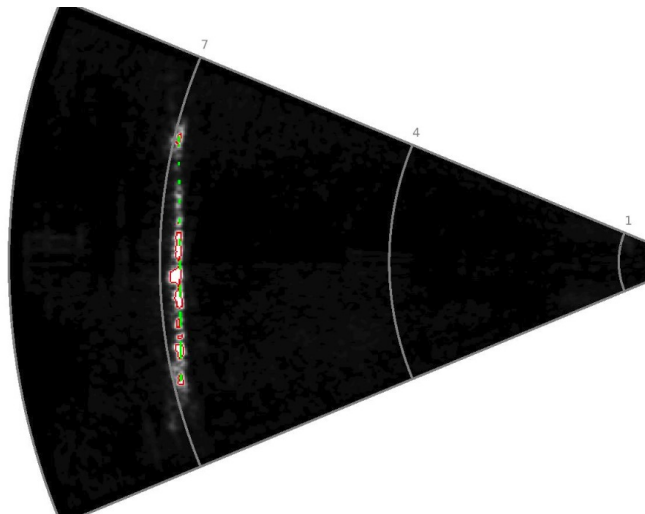


Figure 4.16: Example of Algorithm I based on the applied forward insonification at 7 meters standoff; Platform Tango

throughout the data set while 59% are distinguishable from Algorithm II. It is also interesting to note that the image processing in Algorithm II detects the stability piping at the base of the rig shown in all three of the provided sonar images. Based on these results, the following conclusions are drawn:

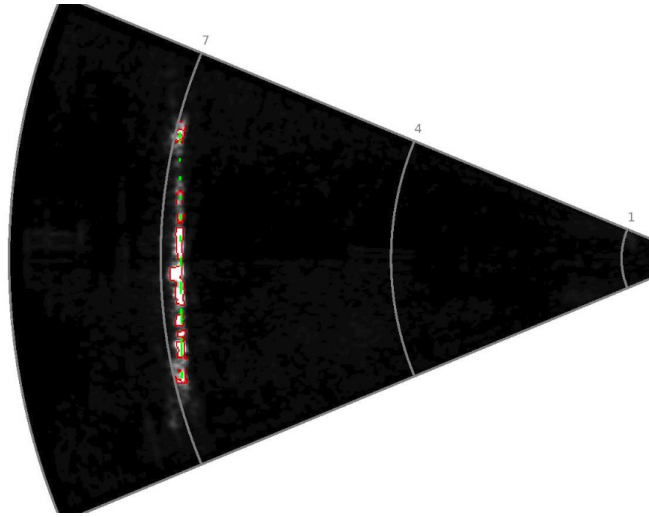


Figure 4.17: Example of Algorithm II based on the applied forward insonification at 7 meters standoff; Platform Tango

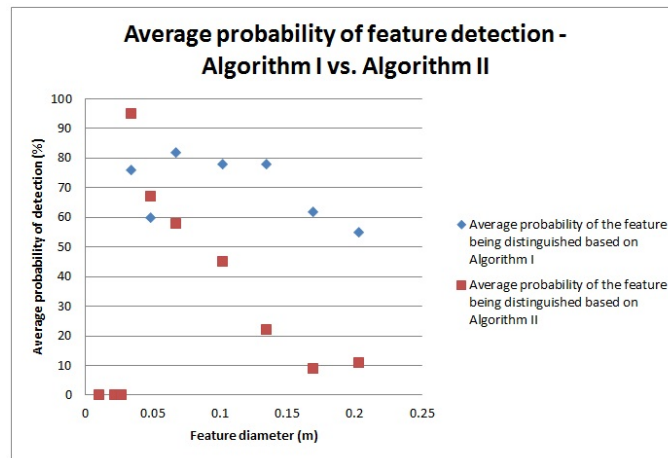


Figure 4.18: Average probability of feature detection based on the applied forward insonification at 7 meters standoff; Platform Tango

1. The sonar image appears as one compilation; this is shown in Figure 4.21 which provides a visual representation of a raw sonar image. The pixel intensity return appears to have faint features that may resemble the smaller gap spacing, but these gaps are not able to be distinguished based on the signal processing.
2. Figure 4.22 provides a visual representation of Algorithm I applied to this data set overlaid with the ground truth data. The comparison between the ground truth and

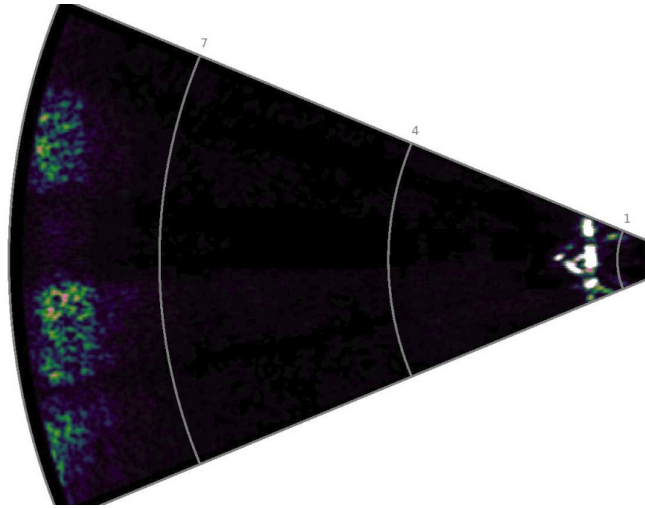


Figure 4.19: Example of raw sonar image based on the applied forward insonification at 1.5 meters standoff; Platform Tango

- intensity returns show that the support frame and the first gap become compiled while the following gaps appear as true negatives.
3. Figure 4.23 provides a visual representation of Algorithm II applied to this data set overlaid with the ground truth data. The edge detection ability of Algorithm II provides a rough outline of the rear stability piping while also aids in extracting the data of features that Algorithm I could not.
 4. Figure 4.24 provides a visual comparison of the average probability of detection based on the gap spacing. Overall, Algorithm II dominates the probability of gap detection. Although both algorithms are not able to distinguish the small gap spacing, both have a high probability of detecting the larger gap spacing.
 5. Based on the gap spacing in Platform Golf, it was expected that only the three largest gaps would be distinguishable. Figure 4.22 validates this expectation in that the smaller eight gaps are indistinguishable while the ninth is. Figure 4.20 provides an example of the data extracted in this data set from Algorithm I compared to the defined ground truth. From viewing Figure 4.20, the expectation in distinguishing the smaller gaps is minimal compared to those larger than 0.086 meters wide.
 6. Algorithm II is able to extract data resulting in a higher probability of detection than compared to that of Algorithm I. Although both are not able to distinguish the first eight gaps, Algorithm II provided gap spacings which were typically clear of false

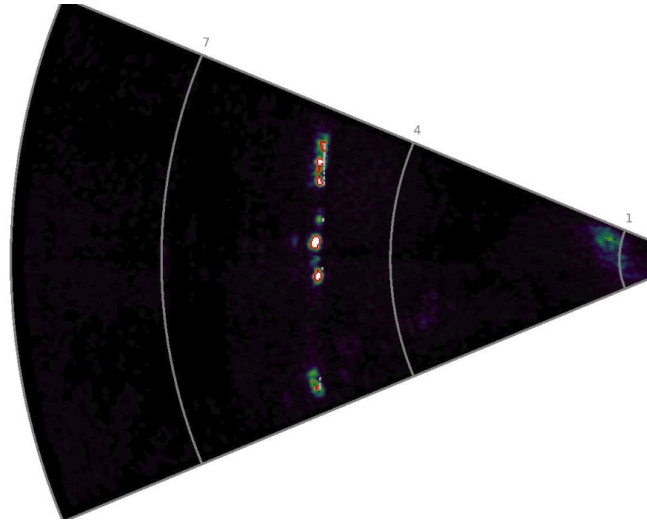


Figure 4.20: Sonar image with ground truth defined based on the applied lateral movement at 5 meters standoff; Platform Golf

positives such as those observed in using Algorithm I; this is shown in Figure 4.20.

As the sonar conducted the lateral movement, various gaps were not insonified through the sonar signal processing. Thus, the image processing was not able to extract data from those gaps. The values in the following tables reflect solely what is observed in the sonar images and extracted data based on the algorithms.

4.3.7 Forward Insonification at 7 meters standoff - Platform Golf

Based on the data compiled and analysis of 156 sonar images, it can be inferred that the sonar signal processing produces 0.19 false positives per image, 1.98 true negatives per image, and 77% of the gaps blend together and are indistinguishable from each other. The extracted information from Algorithm I conclude that 17% of the gaps are distinguishable throughout the data set while 20% are distinguishable from Algorithm II. Based on these results, the following conclusions are drawn:

1. The sonar image appears as two compilations; this is shown in Figure 4.25 which provides a visual representation of a raw sonar image.
2. Figure 4.26 provides a visual representation of Algorithm I applied to this data set overlaid with the ground truth data. The smaller gap spacing is not distinguishable

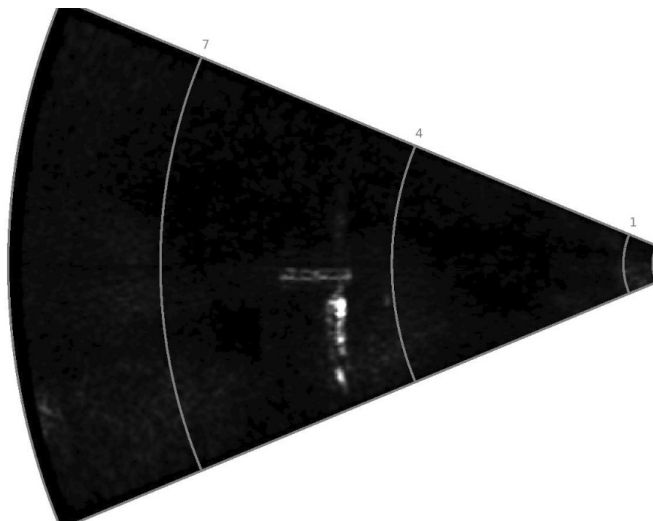


Figure 4.21: Example of raw sonar image based on the applied lateral movement at 5 meters standoff; Platform Golf

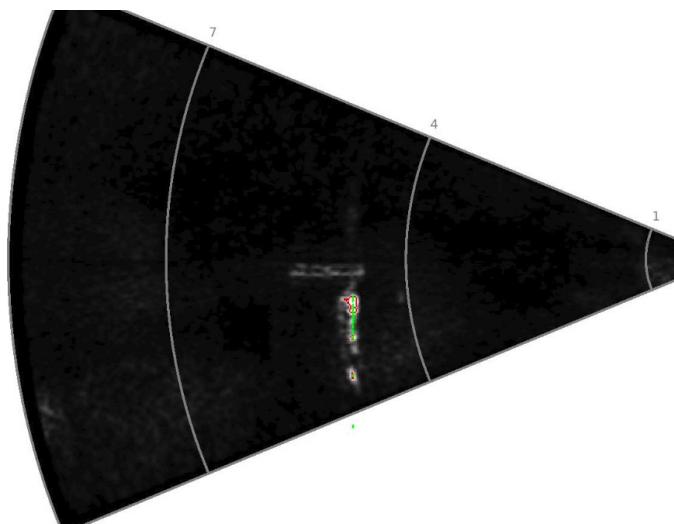


Figure 4.22: Example of Algorithm I based on the applied lateral movement at 5 meters standoff; Platform Golf

by the image processing. Based on this figure, the image appears to be simply two gaps as opposed to the eleven of the ground truth.

3. Figure 4.27 provides a visual representation of Algorithm II applied to this data set overlaid with the ground truth data. Similar to Algorithm I, Algorithm II is not able

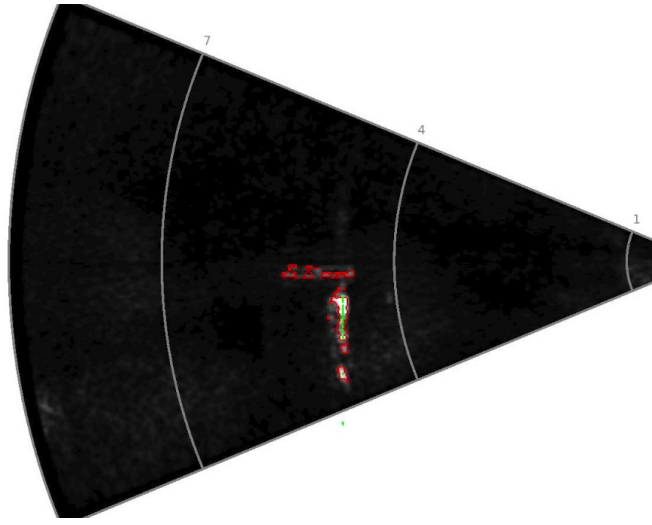


Figure 4.23: Example of Algorithm II based on the applied lateral movement at 5 meters standoff; Platform Golf

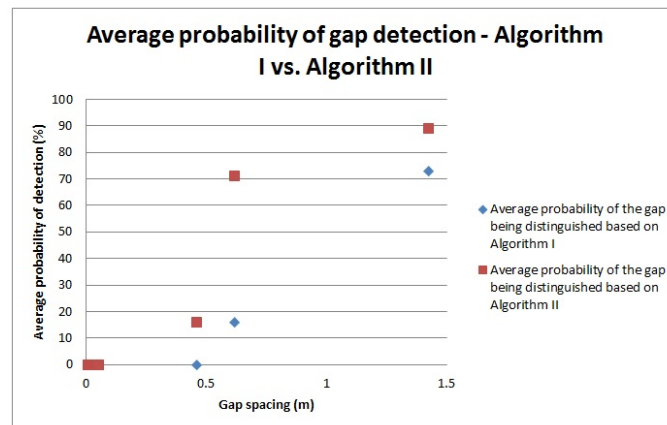


Figure 4.24: Average probability of gap detection based on the applied lateral movement at 5 meters standoff; Platform Golf

to extract the data of small gaps within the ground truth. Although the majority of the small gaps appear to be detected as a single compilation, the gaps are not distinguishable. Again, the algorithm appears to extract data of two gap spacings as opposed the eleven of the ground truth.

4. Figure 4.28 provides a visual comparison of the average probability of detection based on the gap spacing. Both algorithms could not detect the variations of the

- smaller eight gaps while Algorithm II provided a higher probability in detecting the larger gap spacings.
5. The smallest expected resolvable gap spacing the sonar may distinguish is 0.12 meters or greater when the sonar is seven meters from the target. Based on Figure 4.25, the smaller gap spacings are not distinguishable by the signal processing, as expected; however, neither are the larger gap spacings. The image appears to be simply two gaps as opposed to the eleven of the ground truth.
 6. The defined ground truth shown in Figure 4.26 compared to the two compilations suggest that not only are the smaller gaps indistinguishable but also not detectable by the signal processing. Further, this image presents one large false positive near the middle of the rig.
 7. These results are consistent throughout both algorithms; however, Algorithm II provides the higher probability of detection based on the feature edge detections observed in images, such as in Figure 4.27, which suggest gaps between the intensity returns.

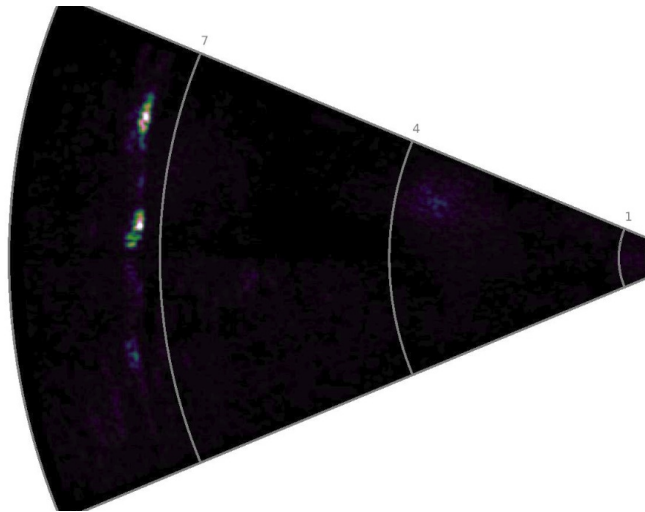


Figure 4.25: Example of raw sonar image based on the applied forward insonification at 7 meters standoff; Platform Golf

4.3.8 Sweeping Movement at 5 meters standoff - Platform Golf

Based on the data compiled and analysis of 96 sonar images, it can be inferred that the sonar signal processing produces 1.03 false positive per image, zero true negatives per

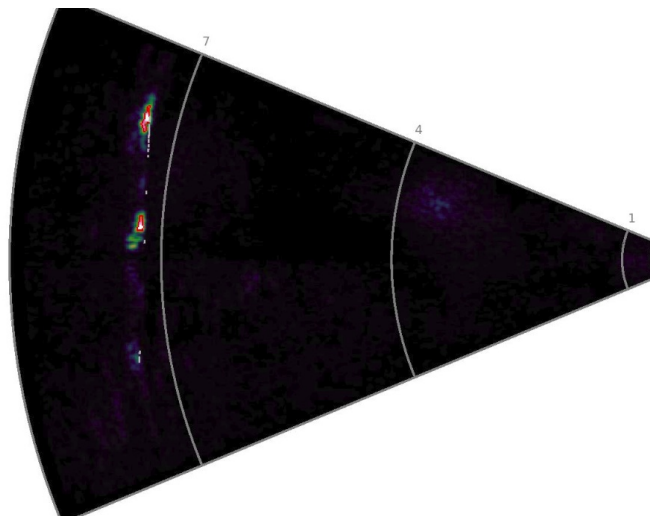


Figure 4.26: Example of Algorithm I based on the applied forward insonification at 7 meters standoff; Platform Golf

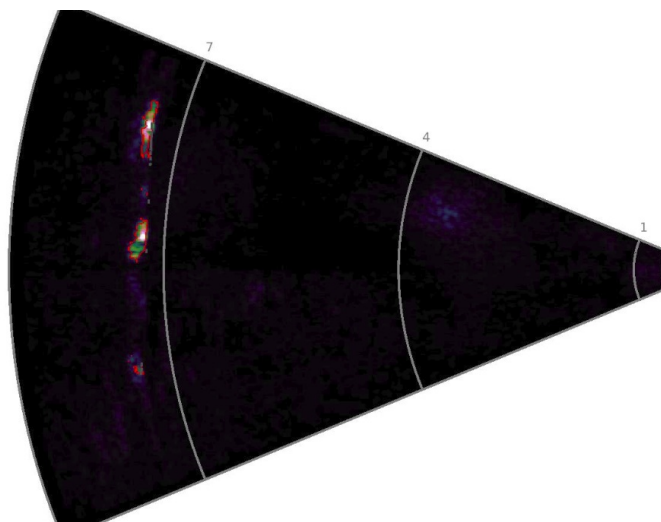


Figure 4.27: Example of Algorithm II based on the applied forward insonification at 7 meters standoff; Platform Golf

image, and 49% of gaps blend together and are indistinguishable from each other. The extracted information from Algorithm I conclude that 53% of the gaps are distinguishable throughout the data set while 81% are distinguishable from Algorithm II. Based on these results, the following conclusions are drawn:

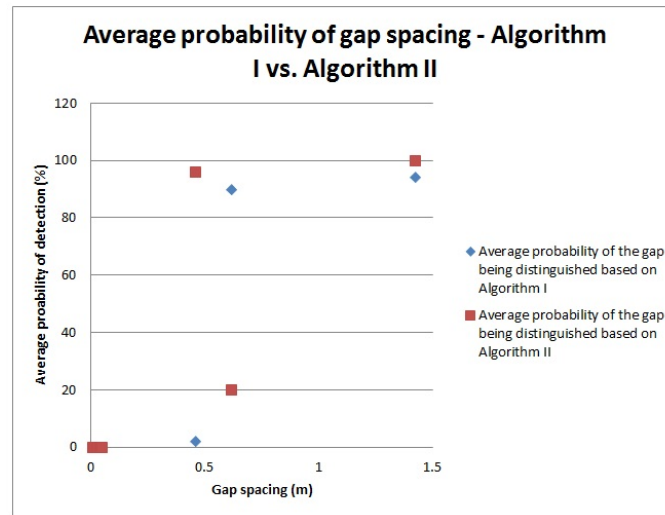


Figure 4.28: Average probability of gap detection based on the applied forward insonification at 7 meters standoff; Platform Golf

1. Figure 4.30 provides a visual representation of a raw sonar image. Based on the position of the sonar, the signal processing provides a clear distinction of the larger gaps in the rig.
2. Figure 4.31 provides a visual representation of Algorithm I applied to this data set overlaid with the ground truth data. The algorithm is able to extract data pertaining to the larger gaps of the rig. The algorithm is also able to clearly extract the data concerning the vertical pipes in the rig. This is an excellent example of the algorithm's ability to extract the gap data.
3. Figure 4.32 provides a visual representation of Algorithm II applied to this data set. The edge detection ability of the algorithm provides two false positives and a compilation of the support and adjacent pipe. Figure 4.32 represents the ability of the image processing to extract the data of the larger gap but does not clearly represent the second largest gap spacing.
4. Figure 4.33 provides a visual comparison of the average probability of detection based on the gap spacing. Algorithm II provides the higher probability of detecting the gap spacing. Although the algorithms are able to extract the data of the larger spacings, they are unable to detect those of the smaller gaps.

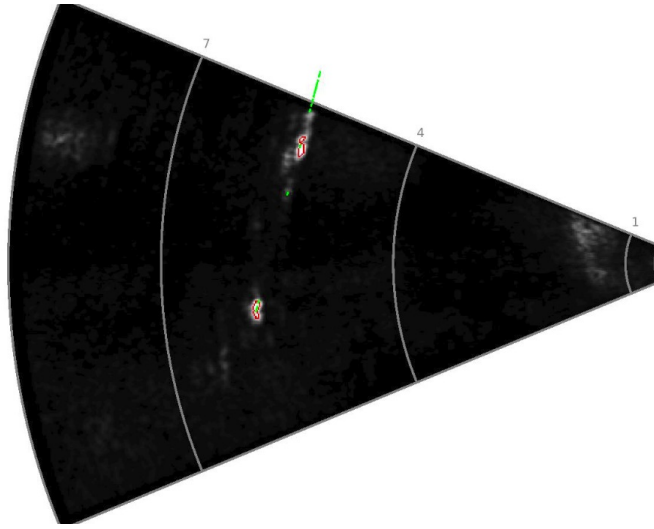


Figure 4.29: True negatives produced via Algorithm I based on the applied sweeping movement at 5 meters standoff; Platform Golf

Figure 4.31 provides an excellent example of the defined ground truth to that of the image processing in Algorithm I. As expected based on the theory in Chapter 2, the two largest gaps are clearly distinguished. Further, there appear no presence of false positives, true negatives, or compilations that may cloud the interpretation of this figure. Based on a comparison of Algorithm I and II, Algorithm II provides a higher average probability of detection due to various environmental factors observed in Algorithm I images such as those true negatives observed in Figure 4.29.

As the sonar conducted the sweeping movement, various gaps were not insonified through the sonar signal processing. Thus, the image processing was not able to extract data about those gaps. The values in the following tables reflect solely what is observed in the sonar images and extracted data based on the algorithms.

4.3.9 Lateral Movement at 1.5 meters standoff - Platform Golf

Based on the data compiled and analysis of 117 sonar images, it can be inferred that the sonar signal processing produces 1.76 false positives per image, zero true negatives per image, and 50% of the gaps blend together and are indistinguishable from each other. The extracted information from Algorithm I and Algorithm II conclude that 52% of the gaps are

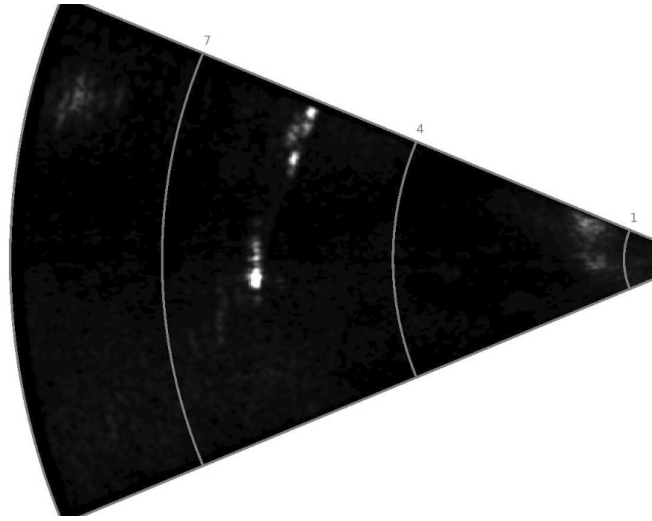


Figure 4.30: Example of raw sonar image based on the applied sweeping movement at 5 meters standoff; Platform Golf

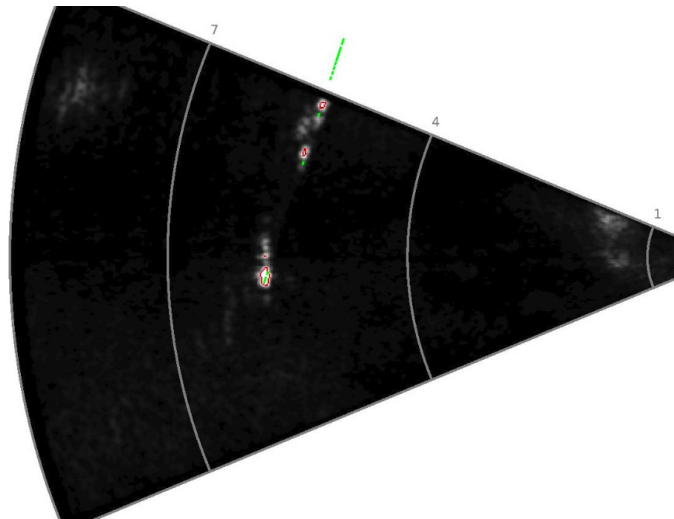


Figure 4.31: Example of Algorithm I based on the applied sweeping movement at 5 meters standoff; Platform Golf

distinguishable throughout the data set. Based on these results, the following conclusions are drawn:

1. Figure 4.34 provides a visual representation of a raw sonar image. The signal processing is able to detect the pipes of the frame, but not distinguish between the small

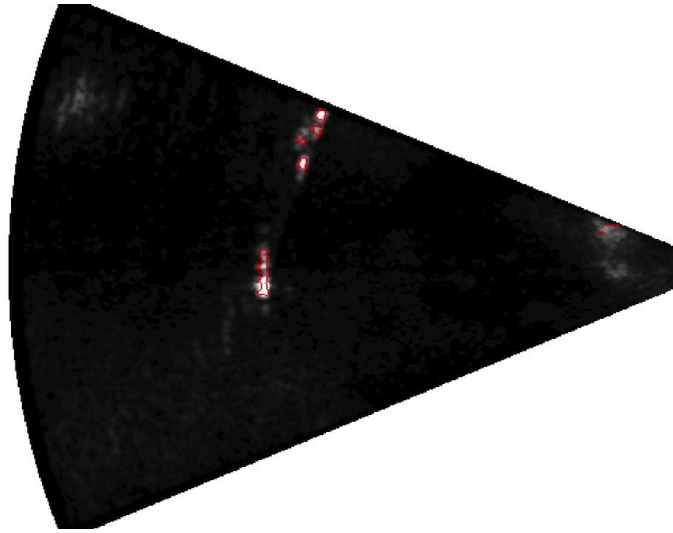


Figure 4.32: Example of Algorithm II based on the applied sweeping movement at 5 meters standoff; Platform Golf

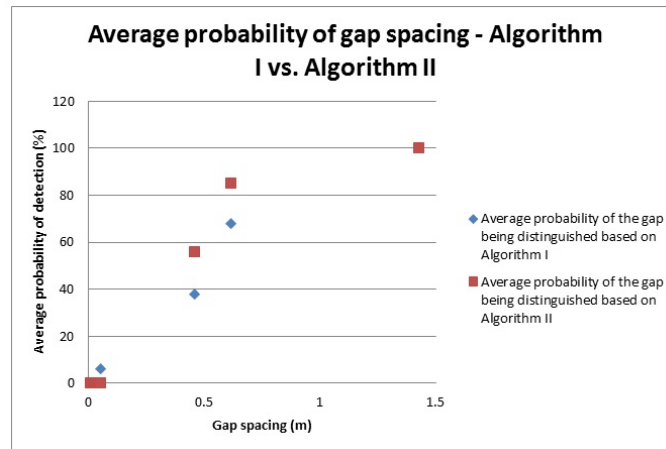


Figure 4.33: Average probability of gap detection based on the applied sweeping movement at 5 meters standoff; Platform Golf

- gap spacing. There are also two false positives that appear; the first appears behind the pipes and the other is adjacent to the support frame.
- Figure 4.35 provides a visual representation of Algorithm I applied to this data set overlaid with the ground truth data. The algorithm provides data resembling a compilation of the small gaps spacings while also producing a false positive behind the

- smaller gaps. At this range, the image processing is able to extract data from one of the pipes that had not been previously extracted at the greater ranges; this produces a clear and detectable gap spacing.
3. Figure 4.36 provides a visual representation of Algorithm II applied to this data set overlaid with the ground truth data. Similar to Algorithm I, the algorithm provides data resembling a compilation of the small gaps spacings while also producing a false positive behind the smaller gaps. At this range, the image processing is able to extract data from one of the pipes that had not been previously extracted at the greater ranges; this produces a clear and detectable gap spacing.
 4. Figure 4.37 provides a visual comparison of the average probability of detection based on the gap spacing. Interestingly, the probability of detection of both algorithms were practically identical. At the shorter range from the target, the signal and image processing were still not able to distinguish the small gap spacing. As the vehicle moved laterally, the sonar FOV could not insonify the pipes and thus the gap spacing appeared as open water; this is especially shown in the algorithm's ability to detect the largest gap spacing. However, the probability of detecting the eighth, ninth, and tenth gaps were high as the vehicle was positioned relative to these spacings.

The smallest expected resolvable gap spacing the sonar may distinguish is 0.025 meters or greater when the sonar is 1.5 meters from the target. Based on Figure 4.35 and Figure 4.36, the eight smaller gaps appear as one large compilation with false returns populating adjacent to the compilation. The expectation was that from the fifth feature on the signal processing and algorithms would distinguish the gaps; however, this is not the case. Further, as the vehicle continues to move parallel to the rig toward the larger gaps, the probability of detection increases until reaching the largest gap; this is due to the sonar's FOV which inhibits such a wide insonification of the target.

As the sonar conducted the lateral movement, various gaps were not insonified through the sonar signal processing. Thus, the image processing was not able to extract data from those gaps. The values in the following tables reflect solely what is observed in the sonar images and extracted data based on the algorithms.

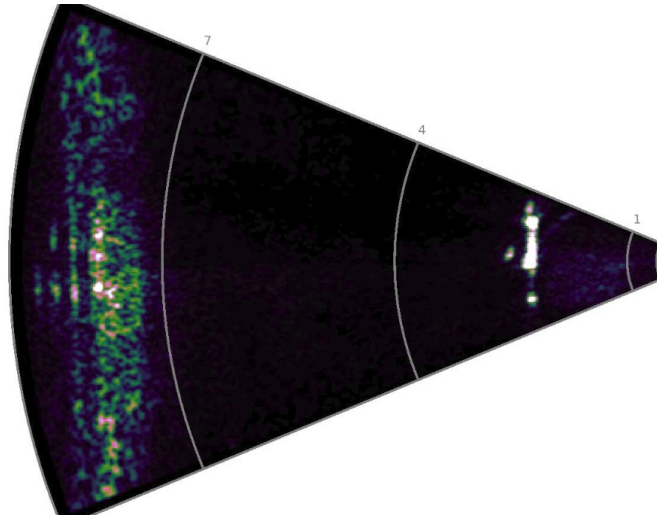


Figure 4.34: Example of raw sonar image based on the applied lateral movement at 1.5 meters standoff; Platform Golf

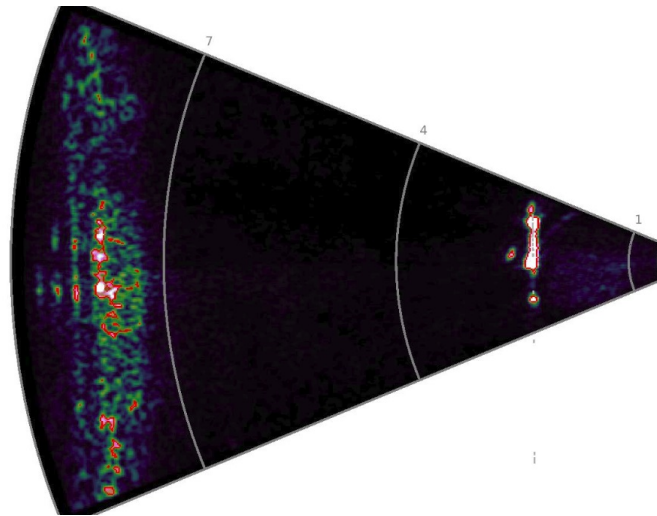


Figure 4.35: Example of Algorithm I based on the applied lateral movement at 1.5 meters standoff; Platform Golf

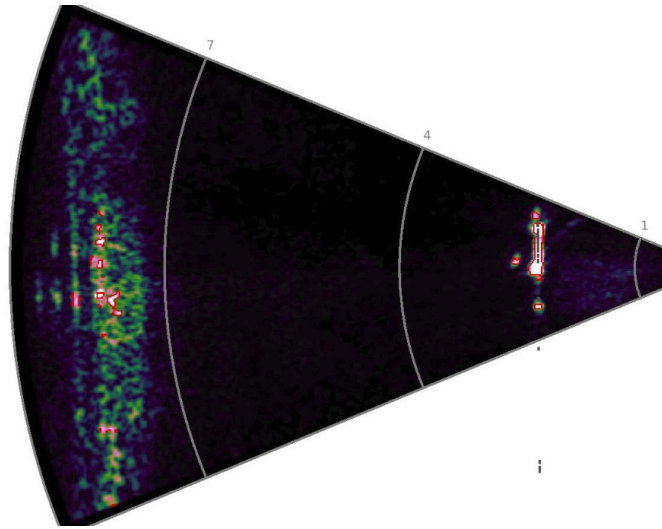


Figure 4.36: Example of Algorithm II based on the applied lateral movement at 1.5 meters standoff; Platform Golf

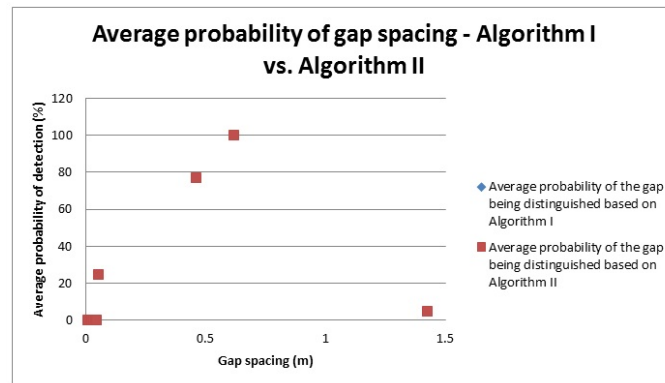


Figure 4.37: Average probability of gap detection based on the applied lateral movement at 1.5 meters standoff; Platform Golf

THIS PAGE INTENTIONALLY LEFT BLANK

CHAPTER 5:

CONCLUSION

The objectives within this work focused on the following:

1. Present to the underwater community the limitations surrounding high frequency sonar, specifically its inability to distinguish between features in congested environments.
2. Present a methodology that incorporates a defined ground truth, sonar and image processing to evaluate and compare approaches for feature detection.

In order to complete the above objectives, the approach involved the following:

1. Investigate the history of sonar, its evolution, and application throughout history.
2. Adopt the SE Waterfall model to identify stakeholders who require a method to accurately distinguish features in complex underwater environments.
3. Construct two underwater rigs that provided the ground truth platform to be insonified.
4. Consider the fundamentals of perception in the underwater environment and present unique image processing algorithms that allow for the comparison of sonar images to the ground truth data.
5. Conduct in-water trials to obtain raw sonar data by positioning the vehicle at different ranges and movements.
6. Apply both image processing algorithms to the raw sonar data and compare to the ground truth to determine the probability of detection and error rate of the sonar.

5.1 Summary

Based on the results of the trials, the following conclusions are presented:

1. The sonar signal processing and algorithms are not able to distinguish the 0.0098 meter diameter feature of Platform Tango at any of the previously stated ranges, which was expected. However, the second smallest feature (0.0215 meters) of Platform Tango was consistently distinguished throughout the trials when the vehicle was po-

- sitioned at a range to insonify the whole rig, at five and seven meters. This was additionally unexpected based on the shortest vehicle range of 1.5 meters when the expected feature to be distinguished was 0.0313 meters or greater.
2. Algorithm I provides the greater average probability of detecting individual features (57%). However, upon reviewing all results presented by the algorithm, positioning the vehicle and sonar is not necessarily conducive to distinguishing all the expected features. For example, the features typically compile at the 1.5 meter range. This occurrence might be the result of acoustic interference between features spaced adjacent to each other, as seen in Platform Golf, or that of numerous larger features not spaced far enough apart (seen in Platform Tango).
 3. Algorithm II provides the greater average probability of detecting gap spacing (53%). Presumably, this is due to the algorithm specifics and especially, erosion. By eroding the image in this manner, the minimum value assigned to each pixel's surroundings allows the researcher to distinguish the features as opposed to a viewing a compilation. This is important regarding the gap spacing in Platform Golf where same sized features were positioned at minimal distances which were expected to provide numerous more compilations during image processing.
 4. False positives occur more frequently when the sonar maintains a range to target of five meters than at any other range or movement.

The goal of this work was to provide the underwater community with a methodology to compare the data extraction and representation of complex underwater environments using different sensors and image processing algorithms. Based on the results of this work, there remains an inability to accurately distinguish congested spacing and small features. However, through the systems engineering process (SEP), this work presented an initial attempt to address the pressing capability need for the establishment of a standardized methodology that not only evaluates acoustic sensors but also provides evaluation of the associated processing algorithms. This work is therefore the initial baseline to address this community requirement.

5.2 Near-Term Improvements

This thesis suggests the establishment of a methodology to standardize the comparison of the processing of data acquired by high frequency sonar. It included two distinct al-

gorithms in order to distinguish congested features and gaps similar to those objects of interest found throughout the undersea environment. The specific focus on the use of the P900 FLS showed promise for accurate underwater bearing and range resolution of a target and leads to the discussion of future work using additional high frequency sensors to distinguish underwater features. However, there are always areas within any experiment or methodology for improvement. Such categories of improvement could be suggested in the following areas:

1. image processing
2. platform design
3. sensor selection
4. environmental considerations

5.2.1 Image Processing

As seen throughout the perception process, the algorithmic results appear very similar for the two approaches evaluated. In order to perhaps alleviate such confusion as to which algorithm produces which images, redefining the color scheme or dimensions of the rig overlay is suggested. Further, the ability to annotate the leading edge of the platform exist through MATLAB. An additional suggestion would be to establish the leading edge view of the platform verses the top-down view in order to enhance the algorithms' abilities to distinguish platforms.

Further, Algorithm I distinguished the smaller features of Platform Tango more efficiently than Algorithm II while Algorithm II provided better resolution of the small gaps in Platform Golf. Based on the specifics of the separate algorithms, and to provide a more complete algorithm, the following suggestions are provided for future work.

1. Blending the two algorithms: Increasing the intensity threshold in order to further mitigate the presence of noise then utilizing edge detection to find those boundaries associated with the intensity returns from the sonar. This process may allay the potential errors than can occur in the produced sonar images.
2. Omit the dilate command: The large percentage of compilations observed in the sonar images after applying the second algorithm may be due to enlarging the features. The features were not spaced drastically apart and thus this image processing

technique may have presented complications that could have been avoided.

5.2.2 Platform Design

In an attempt to justify and construct a platform or target for data extraction, a number of constraints immediately presented themselves. In particular, the idea of placing a target in the salt water environment minimized the material that could be considered. Not wanting to battle corrosion, PVC immediately provided a solution for any structure and had demonstrated to be effective in the previous work conducted at NASA Extreme Environment Mission Operations (NEEMO) XX. Although this material proved effective in the fight against corrosion, the structural deviations and weight necessitate discussion.

1. **Structural errors** within the fabrication of thinner diameter pipes were immediately noticeable. Prior to purchase, it was not evident that these smaller diameter pipes were not completely erect and were bowed near the center. Once these pipes were vertically inserted into the supporting frames, the use of very thin, yet strong, commercial fishing line was required in order to maintain the gap spacing between piping. Figure 5.1 provides an image of that correction.
2. **Weight** of a single PVC pipe is not a substantial factor. However, it can be substantially more in a massive quantity when compared to producing a similar structure using metal ductwork which is thin and lightweight. This factor did not prove to be restricting until the trials were concluded and the need to fish the rig out of the pool arose. This increased weight is limiting and can complicate deployment and extraction. As was experienced in both AOs, the large and heavy platforms, especially Platform Tango, required the teamwork of two or three able bodied personnel to lower, secure, and then retrieve the platforms.

Further consideration should also address localization and ground truth. Although the experimental approach was sufficient when the entire structure could be insonified, the process was not effective when viewing the sweeping data sets when the endpoints of the rig were not visible. Thus, it may behoove future work to incorporate a rig design where the relative position of the sonar to the rig can be explicitly controlled.



Figure 5.1: Example of corrected gap reestablishment in Platform Golf

5.2.3 Sensor Selection

The sonar selected for the data extraction was the P900 FLS specifically based upon its availability and demonstrated technical performance. However, the availability of different or additional sensors may have demonstrated the same or greater effectiveness in distinguishing data. Traditionally, higher frequency sonars provide a clearer image resolution, but it needs to be close to the target of interest. Conversely, low frequency sonar has the ability to travel farther in order to insonify targets but at a lower image resolution.

Although the use of EO sensors were presented, perhaps the next iteration of this work would be to utilize both tools. As the mission of this work is to further enhance the underwater community's ability to distinguish congested features, a fusion of both sonar and EO sensor systems may be beneficial to the research.

5.2.4 Environmental Considerations

The aquatics facility at Stevenson School provided the ideal environment for this initial work. However, the majority of underwater operations occur in the open ocean or littoral

environment typical to the operational deployment of sonar systems. Those opportunities presented themselves throughout the course of this thesis but were limited due to the heavy surge and fast tidal changes within the Monterey Bay. Although these preliminary trials themselves were conducted in a very consistent location, future work might consider performing such tests during a different season or ensure enough time allotted for low-tide work versus high-tide movement.

5.3 Recommendation for Future Work

The most important recommendation for future work is to enhance the image processing algorithms. The processing algorithms utilized in this thesis were established as the baseline for extracting data in very congested underwater environments. However, the surrounding medium in which the data was extracted was benign and without much noise and clutter; this is not a realistic setting in which the underwater community typically operates. It can then be assumed that in an open water environment, the amount of false positives, true negatives, and compilations would increase significantly. Therefore, it may behoove researchers to improve on the algorithm threshold establishment that might mitigate the amount of noise compiled on the sonar images [17].

APPENDIX: EXAMPLE FIGURES AND DATA ANALYSIS TABLES

A.1 Data Set 11-51-36 Sample Analysis

The following figures and data tables apply to the signal and image processing while the vehicle maintained a fixed pose at a range of approximately seven meters from Platform Tango.

Figure A.1 provides an example of an initial raw sonar image followed by two examples of the image processing applied to image 0 in this data set; Figure A.2 and Figure A.3.

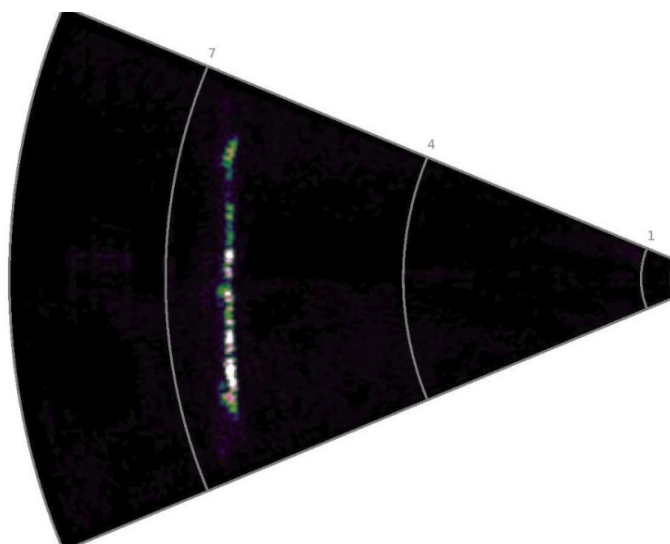


Figure A.1: Example of raw sonar image 0 - forward insonification at 7 meter standoff - Platform Tango

Figure A.4 provides an example of an initial raw sonar image followed by two examples of the image processing applied to image 50 in this data set; Figure A.5 and Figure A.6.

Figure A.7 provides an example of an initial raw sonar image followed by two examples of the image processing applied to image 303 in this data set; Figure A.8 and Figure A.9.

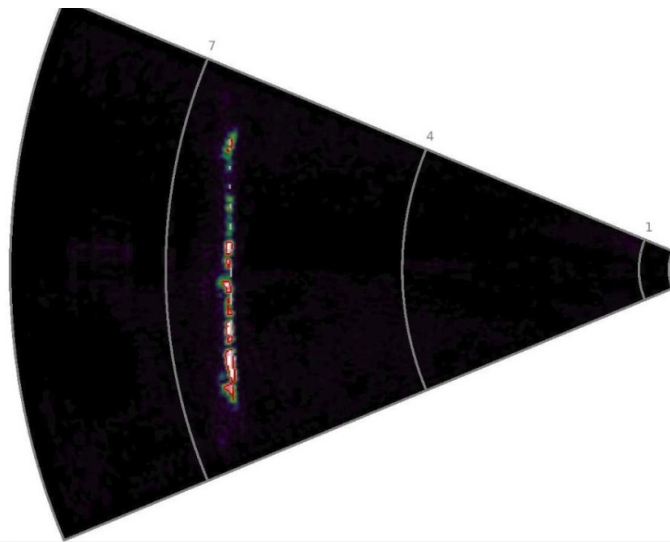


Figure A.2: Example of Algorithm I applied to image 0 - forward insonification at 7 meter standoff - Platform Tango

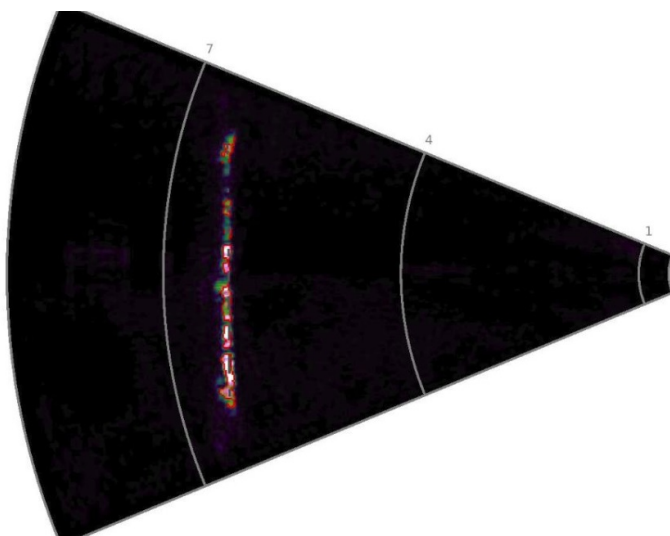


Figure A.3: Example of Algorithm II applied to image 0 - forward insonification at 7 meter standoff - Platform Tango

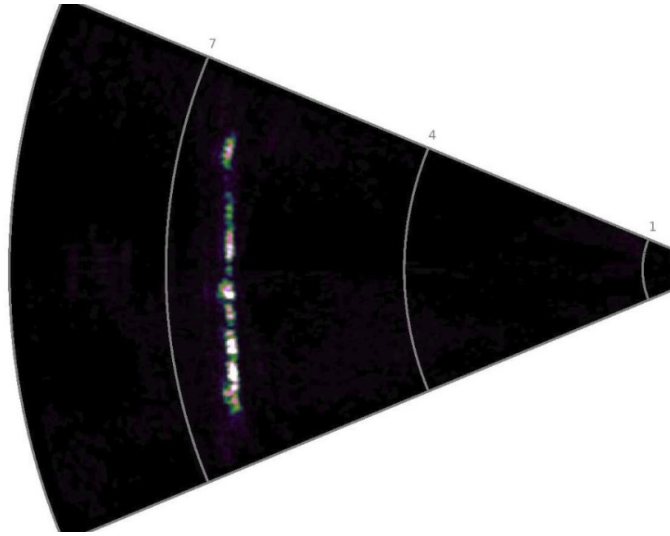


Figure A.4: Example of raw sonar image 50 - forward insonification at 7 meter standoff - Platform Tango

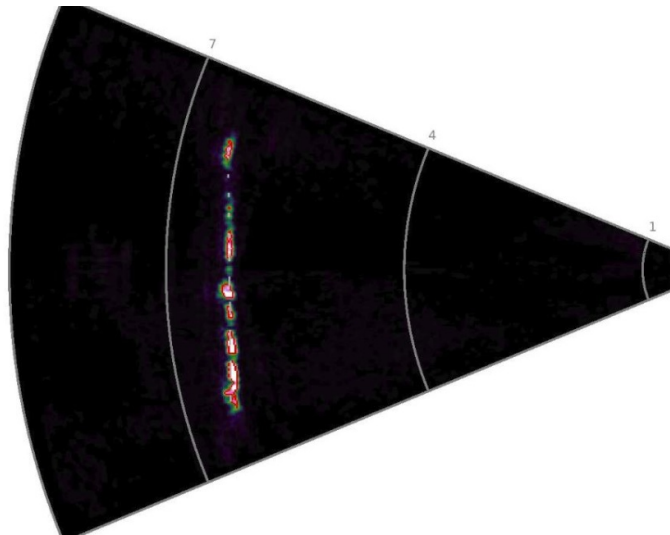


Figure A.5: Example of Algorithm I applied to image 50 - forward insonification at 7 meter standoff - Platform Tango

A.2 Data Set 12-09-07 Sample Analysis

The following figures and data tables apply to the signal and image processing. The vehicle maintained a fixed pose at a range of approximately seven meters from Platform Golf.

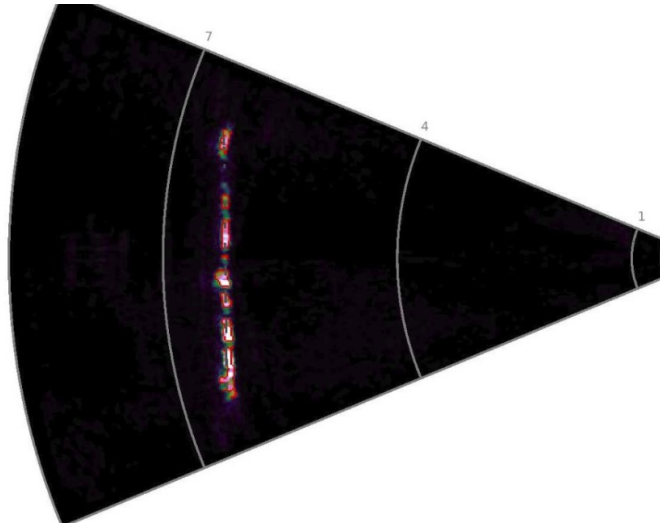


Figure A.6: Example of Algorithm II applied to image 50 - forward insonification at 7 meter standoff - Platform Tango

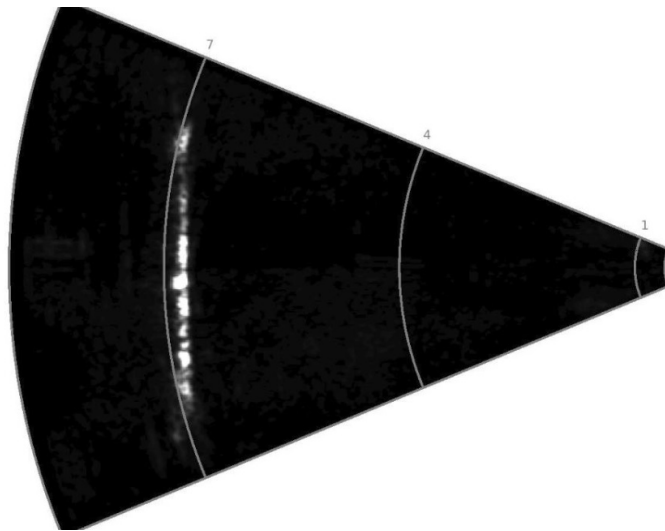


Figure A.7: Example of raw sonar image 303 - forward insonification at 7 meter standoff - Platform Tango

Figure A.10 provides an example of an initial raw sonar image followed by two examples of the image processing applied to image 0 in this data set; Figure A.11 and Figure A.12.

Figure A.13 provides an example of an initial raw sonar image followed by two examples of the image processing applied to image 25 in this data set; Figure A.14 and Figure A.15.

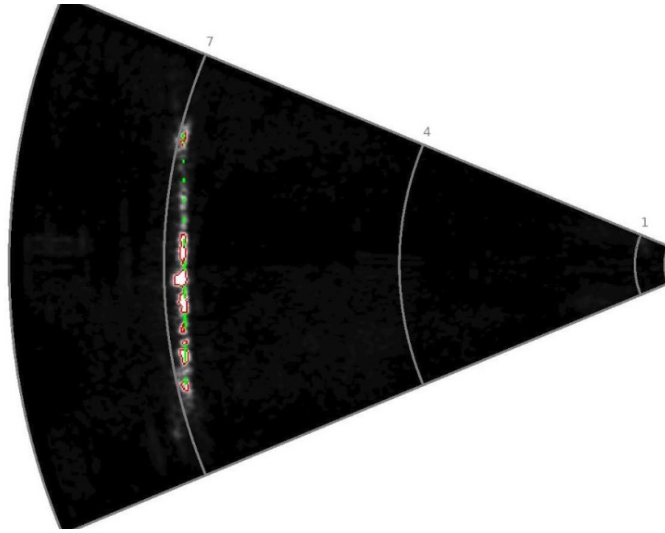


Figure A.8: Example of Algorithm I applied to image 303 - forward insonification at 7 meter standoff - Platform Tango

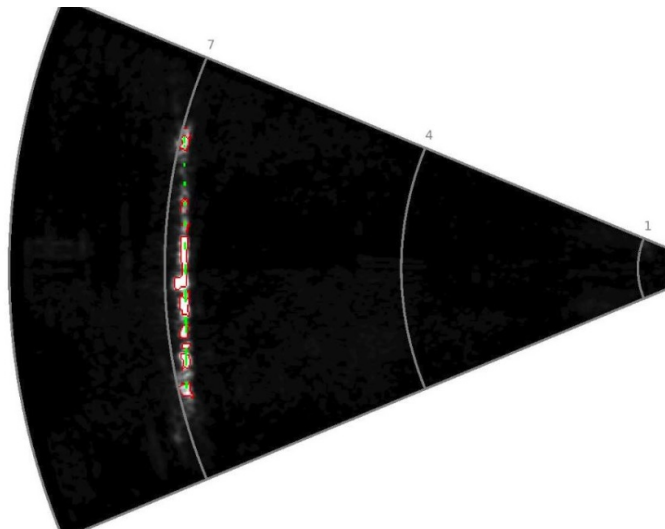


Figure A.9: Example of Algorithm II applied to image 303 - forward insonification at 7 meter standoff - Platform Tango

Figure A.16 provides an example of an initial raw sonar image followed by two examples of the image processing applied to image 50 in this data set; Figure A.17 and Figure A.18.

Table A.1: Sample of Data Set 11-51-36 Sonar Analysis

Error rate of the sonar	<i>Image 0</i>	<i>Image 50</i>	<i>Image 303</i>	<i>Average</i>
Number of false positives	1	0	0	0.18
Number of true negatives	1	1	2	1.8
Compilations	20%	20%	30%	17%

Table A.2: Sample of Data Set 11-51-36 Algorithm Analysis - binary step

Probability of detection utilizing Algorithm I	<i>Image 0</i>	<i>Image 50</i>	<i>Image 303</i>	<i>Average (%)</i>
Feature 1 with outer diameter of 0.009 meters	0	0	0	0
Feature 2 with outer diameter of 0.022 meters	0	0	0	0
Feature 3 with outer diameter of 0.027 meters	0	0	1	0
Feature 4 with outer diameter of 0.034 meters	0	0	0	76
Feature 5 with outer diameter of 0.048 meters	0	1	0	60
Feature 6 with outer diameter of 0.067 meters	1	1	1	82
Feature 7 with outer diameter of 0.101 meters	1	1	0	78
Feature 8 with outer diameter of 0.134 meters	1	1	1	78
Feature 9 with outer diameter of 0.169 meters	1	1	1	62
Feature 10 with outer diameter of 0.203 meters	1	1	1	55
Probability of detection utilizing Algorithm II	<i>Image 0</i>	<i>Image 50</i>	<i>Image 303</i>	<i>Average (%)</i>
Feature 1 with outer diameter of 0.009 meters	0	0	0	0
Feature 2 with outer diameter of 0.022 meters	0	0	0	0
Feature 3 with outer diameter of 0.027 meters	0	0	0	0
Feature 4 with outer diameter of 0.034 meters	1	1	1	95
Feature 5 with outer diameter of 0.048 meters	1	0	1	67
Feature 6 with outer diameter of 0.067 meters	1	1	0	58
Feature 7 with outer diameter of 0.101 meters	0	1	0	45
Feature 8 with outer diameter of 0.134 meters	1	1	0	22
Feature 9 with outer diameter of 0.169 meters	1	0	0	9
Feature 10 with outer diameter of 0.203 meters	1	0	0	11

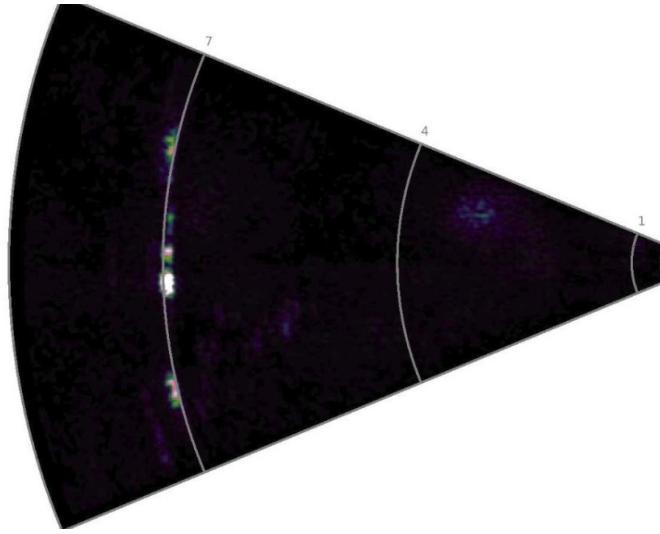


Figure A.10: Example of raw sonar image 0 - forward insonification at 7 meter standoff - Platform Golf

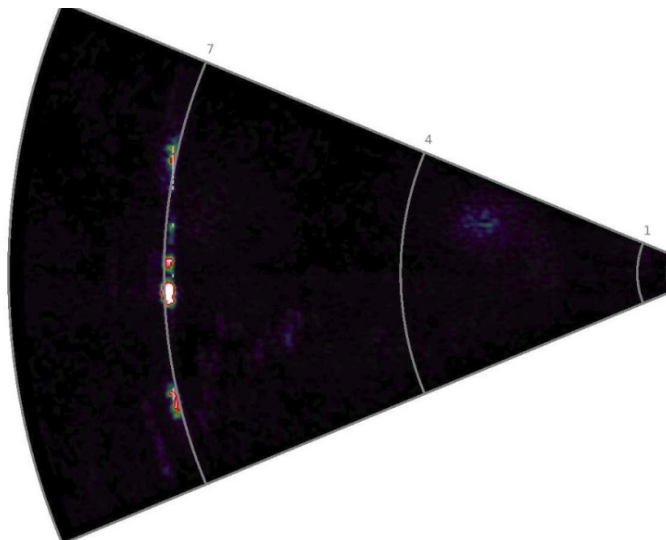


Figure A.11: Example of Algorithm I applied to image 0 - forward insonification at 7 meter standoff - Platform Golf

Table A.3: Sample of Data Set 12-09-07 Sonar Analysis

Error rate of the sonar	<i>Image 0</i>	<i>Image 25</i>	<i>Image 50</i>	<i>Average</i>
Number of false positives	1	0	0	0.19
Number of true negatives	6	1	1	1.98
Compilations	72%	81%	81%	77%

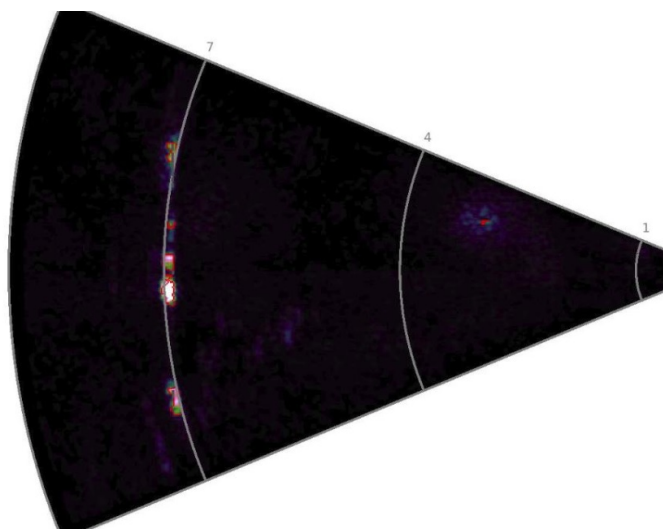


Figure A.12: Example of Algorithm II applied to image 0 - forward insonification at 7 meter standoff - Platform Golf

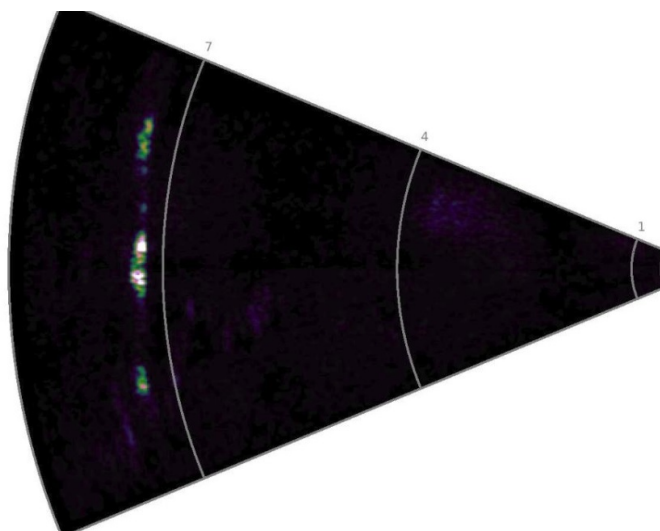


Figure A.13: Example of raw sonar image 25 - forward insonification at 7 meter standoff - Platform Golf

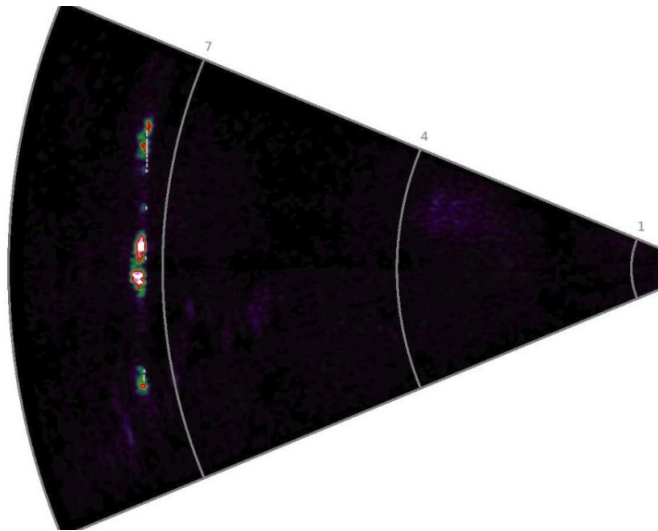


Figure A.14: Example of Algorithm I applied to image 25 - forward insonification at 7 meter standoff - Platform Golf

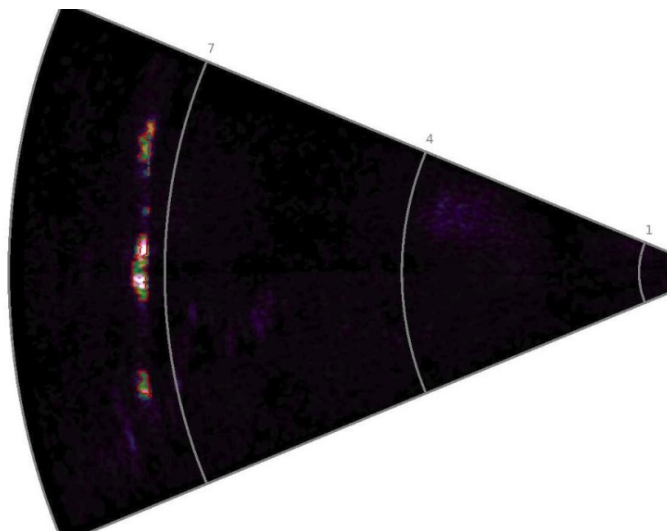


Figure A.15: Example of Algorithm II applied to image 25 - forward insonification at 7 meter standoff - Platform Golf

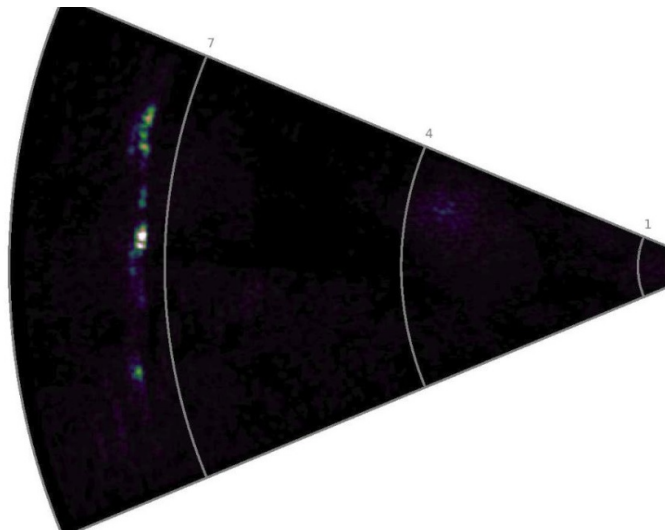


Figure A.16: Example of raw sonar image 50 - forward insonification at 7 meter standoff - Platform Golf

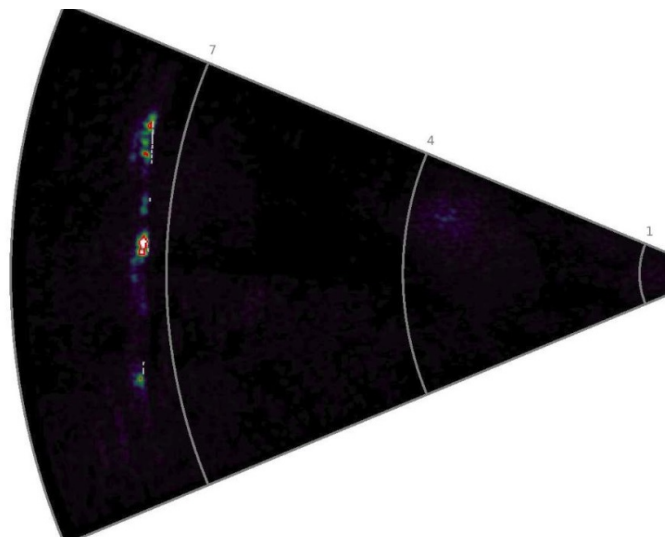


Figure A.17: Example of Algorithm I applied to image 50 - forward insonification at 7 meter standoff - Platform Golf

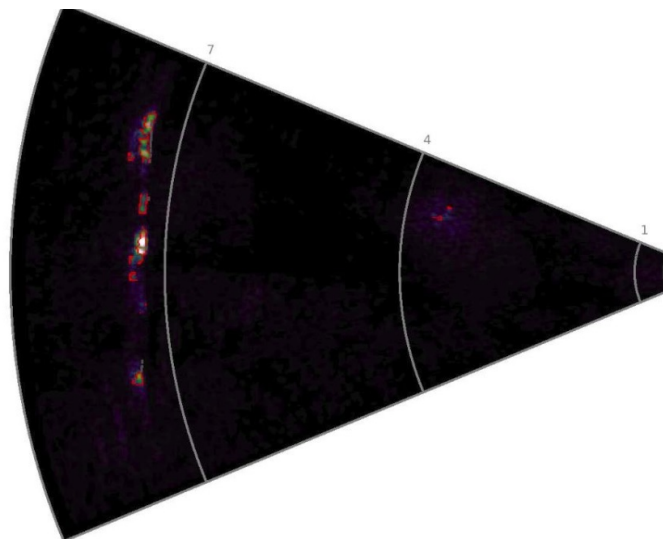


Figure A.18: Example of Algorithm II applied to image 50 - forward insonification at 7 meter standoff - Platform Golf

Table A.4: Sample of Data Set 12-09-07 Algorithm Analysis - binary step

Probability of detection utilizing Algorithm I	<i>Image 0</i>	<i>Image 25</i>	<i>Image 50</i>	<i>Average (%)</i>
Gap 1 with spacing length of 0.008 meters	0	0	0	0
Gap 2 with spacing length of 0.01 meters	0	0	0	0
Gap 3 with spacing length of 0.018 meters	0	0	0	0
Gap 4 with spacing length of 0.023 meters	0	0	0	0
Gap 5 with spacing length of 0.03 meters	0	0	0	0
Gap 6 with spacing length of 0.037 meters	0	0	0	0
Gap 7 with spacing length of 0.043 meters	0	0	0	0
Gap 8 with spacing length of 0.049 meters	0	0	0	0
Gap 9 with spacing length of 0.46 meters	0	0	0	2
Gap 10 with spacing length of 0.61 meters	1	0	1	90
Gap 11 with spacing length of 1.42 meters	1	1	1	94

Probability of detection utilizing Algorithm II	<i>Image 0</i>	<i>Image 25</i>	<i>Image 50</i>	<i>Average (%)</i>
Gap 1 with spacing length of 0.008 meters	0	0	0	0
Gap 2 with spacing length of 0.01 meters	0	0	0	0
Gap 3 with spacing length of 0.018 meters	0	0	0	0
Gap 4 with spacing length of 0.023 meters	0	0	0	0
Gap 5 with spacing length of 0.03 meters	0	0	0	0
Gap 6 with spacing length of 0.037 meters	0	0	0	0
Gap 7 with spacing length of 0.043 meters	0	0	0	0
Gap 8 with spacing length of 0.049 meters	0	0	0	0
Gap 9 with spacing length of 0.46 meters	1	0	1	96
Gap 10 with spacing length of 0.61 meters	1	0	0	20
Gap 11 with spacing length of 1.42 meters	1	1	1	100

List of References

- [1] S. De and A. Tomer, “Mapping the floor,” *Science*, vol. 42, pp. 31–34, 2005.
- [2] R. Eustice, H. Singh, J. J. Leonard, M. Walter, and R. Ballard, “Visually Navigating the RMS Titanic with SLAM Information Filters.” in *Robotics: Science and Systems*, Cambridge, MA, 2005, pp. 57–64.
- [3] R. J. Vaccaro, “The past, present, and the future of underwater acoustic signal processing,” *Signal Processing Magazine, IEEE*, vol. 15, no. 4, pp. 21–51, 1998.
- [4] N. Friedman, *US Submarines Through 1945: An Illustrated Design History*, 1st ed. Naval Institute Press, 1995.
- [5] B. S. Blanchard and W. J. Fabrycky, *Systems Engineering and Analysis*, 5th ed., 2011.
- [6] S. Negahdaripour, H. Sekkati, and H. Pirsiavash, “Opti-acoustic stereo imaging: On system calibration and 3-D target reconstruction,” *Image Processing, IEEE Transactions on*, vol. 18, no. 6, pp. 1203–1214, 2009.
- [7] C. T. Corporation, “Underwater acoustic habitat technical memorandum,” Concurrent Technologies Corporation, Tech. Rep., 12 2005. [Online]. Available: http://www.nwfsc.noaa.gov/research/divisions/cb/ecosystem/marinemammal/documents/underwater_acoustic_habitat.pdf
- [8] A. Singh, “Review article digital change detection techniques using remotely-sensed data,” *International journal of remote sensing*, vol. 10, no. 6, pp. 989–1003, 1989.
- [9] H. M. South, D. C. Cronin, S. L. Gordon, and T. P. Magnani, “Technologies for sonar processing,” *Johns Hopkins APL Technical Digest*, vol. 19, no. 4, p. 459, 1998.
- [10] J. Pickles, *Ground truth: The social implications of geographic information systems*, 1st ed. Guilford Press, New York, 1995.
- [11] H. J. S. Feder, J. J. Leonard, and C. M. Smith, “Adaptive mobile robot navigation and mapping,” *The International Journal of Robotics Research*, vol. 18, no. 7, pp. 650–668, 1999.
- [12] Y. Petillot, I. T. Ruiz, and D. M. Lane, “Underwater vehicle obstacle avoidance and path planning using a multi-beam forward looking sonar,” *Oceanic Engineering, IEEE Journal of*, vol. 26, no. 2, pp. 240–251, 2001.

- [13] L. Stutters, H. Liu, C. Tiltman, and D. J. Brown, "Navigation technologies for autonomous underwater vehicles," *Systems, Man, and Cybernetics, Part C: Application and Review, IEEE Transactions on*, vol. 38, no. 4, pp. 581–589, 2008.
- [14] P. Jasiobedzki, S. Se, M. Bondy, and R. Jakola, "Underwater 3D mapping and pose estimation for ROV operations," in *OCEANS 2008*. IEEE, 2008, pp. 1–6.
- [15] A. Y. Shcherbina, G. G. Gawarkiewicz, C. A. Linder, and S. R. Thorrold, "Mapping bathymetric and hydrographic features of Glover's Reef, Belize, with a REMUS autonomous underwater vehicle," *Limnology and Oceanography*, vol. 53, no. 5part2, pp. 2264–2272, 2008.
- [16] R. I. Brown, "System for underwater GPS navigation," Mar. 2 2004, U.S. Patent 6,701,252.
- [17] J. T. Juriga, "Terrain aided navigation for REMUS autonomous underwater vehicle," master's thesis, NPS, Monterey, CA, 6 2014. [Online]. Available: <http://oai.dtic.mil/oai/oai?verb=getRecord&metadataPrefix=html&identifier=ADA608055>
- [18] S. Williams, G. Dissanayake, and H. Durrant-Whyte, "Towards terrain-aided navigation for underwater robotics," *Advanced Robotics*, vol. 15, no. 5, pp. 533–549, 2001.
- [19] A. D. Waite and A. Waite, *Sonar for Practicing Engineers*, 3rd ed. London: Wiley, 2002.
- [20] S. C. Truver, "Taking Mines Seriously," *Naval War College Review*, vol. 65, no. 2, 2012.
- [21] J. M. Sáez, A. Hogue, F. Escolano, and M. Jenkin, "Underwater 3D SLAM through entropy minimization," in *Robotics and automation, 2006. ICRA 2006. Proceedings 2006 IEEE international conference on*. IEEE, 2006, pp. 3562–3567.
- [22] C. Stachniss, U. Frese, and G. Grisetti. (2015). OpenSLAM: Give your algorithm to the community. [Online]. Available: <https://openslam.org/>
- [23] J. Leitner, D. G. Dansereau, S. Shirazi, and P. Corke, "The Need for Dynamic & Active Datasets." [Online]. Available: <http://blawg.juxi.net/papers/ws/dynamic-active-datasets.pdf>
- [24] J. D. Tardós, J. Neira, P. M. Newman, and J. J. Leonard, "Robust mapping and localization in indoor environments using sonar data," *The International Journal of Robotics Research*, vol. 21, no. 4, pp. 311–330, 2002.

- [25] J. S. Jaffe, K. D. Moore, J. McLean, and M. P. Strand, "Underwater optical imaging: Status and prospects," *Oceanography*, vol. 14, no. 3, pp. 66–76, 2001.
- [26] C. Kunz and H. Singh, "Map building fusing acoustic and visual information using autonomous underwater vehicles," *Journal of Field Robotics*, vol. 30, no. 5, pp. 763–783, 2013.
- [27] M. Stojanovic and J. Preisig, "Underwater acoustic communication channels: Propagation models and statistical characterization," *Communications Magazine, IEEE*, vol. 47, no. 1, pp. 84–89, 2009.
- [28] C. M. Payne, *Principles of naval weapon systems*, 1st ed. Naval Institute Press, 2006.
- [29] R. Jacob, "Sonar signal processing - a perspective," in *Development of Time-Frequency Techniques for Sonar Applications*. Cochin University of Science and Technology, 2010, ch. 3, pp. 33–48. [Online]. Available: <http://dyuthi.cusat.ac.in/jspui/bitstream/purl/2677/3/Dyuthi-T0729.pdf>
- [30] K. V. Mackenzie, "Discussion of sea water sound-speed determinations," *The Journal of the Acoustical Society of America*, vol. 70, no. 3, pp. 801–806, 1981.
- [31] D. H. Johnson and S. R. DeGraaf, "Improving the resolution of bearing in passive sonar arrays by eigenvalue analysis," *Acoustics, Speech and Signal Processing, IEEE Transactions on*, vol. 30, no. 4, pp. 638–647, 1982.
- [32] L. Rayleigh, "XXXI. investigations in optics, with special reference to the spectro-scope," *The London, Edinburgh, and Dublin Philosophical Magazine and Journal of Science*, vol. 8, no. 49, pp. 261–274, 1879.
- [33] A. Ksienski, R. B. McGhee *et al.*, "A decision theoretic approach to the angular resolution and parameter estimation problem for multiple targets," *Aerospace and Electronic Systems, IEEE Transactions on*, no. 3, pp. 443–455, 1968.
- [34] W. C. Knight, R. G. Pridham, and S. M. Kay, "Digital signal processing for sonar," *Proceedings of the IEEE*, vol. 69, no. 11, pp. 1451–1506, 1981.
- [35] D. T. Blackstock, *Fundamentals of physical acoustics*, 1st ed. John Wiley & Sons, Austin, 4 2000.
- [36] J.-C. Laprie, *Dependability: Basic concepts and terminology*. Springer, 1992. [Online]. Available: http://link.springer.com/chapter/10.1007/978-3-7091-9170-5_1page-1

- [37] S. Deb, K. R. Pattipati, V. Raghavan, M. Shakeri, and R. Shrestha, “Multi-signal flow graphs: A novel approach for system testability analysis and fault diagnosis,” *Aerospace and Electronic Systems Magazine, IEEE*, vol. 10, no. 5, pp. 14–25, 1995.
- [38] V. Del Grosso and C. Mader, “Speed of sound in pure water,” *the Journal of the Acoustical Society of America*, vol. 52, no. 5B, pp. 1442–1446, 1972.
- [39] M. Born and E. Wolf, *Principles of optics: Electromagnetic theory of propagation, interference and diffraction of light*, 7th ed. Cambridge University Press, Cambridge, 1999.
- [40] Brian L. Zoebisch, private communication, 2015.
- [41] K. W. Eliceiri, “Molecular Expressions: Exploring the World of Optics and Microscopy [http: microscopy. fsu. edu](http://microscopy.fsu.edu),” *Biology of the Cell*, vol. 96, no. 6, pp. 403–405, 2004.
- [42] M. Kabatek, M. R. Azimi-Sadjadi, and J. D. Tucker, *An underwater target detection system for electro-optical imagery data*. IEEE, 2009.
- [43] D. Davis. (2002). Navy using optical sonar sensors to enhance submarine detection and alleviate maintenance problems. [Online]. Available: <http://www.militaryaerospace.com/articles/print/volume-13/issue-2/news/navy-using-optical-sonar-sensors-to-enhance-submarine-detection-and-alleviate-maintenance-problems.html>
- [44] M. P. Strand, “Underwater electro-optical system for mine identification,” in *SPIE’s 1995 Symposium on OE/Aerospace Sensing and Dual Use Photonics*. International Society for Optics and Photonics, 1995, pp. 487–497.
- [45] L. K. Boss and P. A. Jumars. (2003). SMS-491: Physical solutions of everyday problems in aquatic sciences. [Online]. Available: http://misclab.umeoce.maine.edu/boss/classes/SMS_491_2003/Week_10.htm
- [46] J. T. Sackos, B. D. Bradley, R. O. Nellums, and C. F. Diegert, “Emerging versatility of a scannerless range imager,” in *Aerospace/Defense Sensing and Controls*. International Society for Optics and Photonics, 1996, pp. 47–60.
- [47] S. Majumder, S. Scheduling, and H. F. Durrant-Whyte, “Multisensor data fusion for underwater navigation,” *Robotics and Autonomous Systems*, vol. 35, no. 2, pp. 97–108, 2001.
- [48] S. Wang, L. Chen, H. Hu, Z. Xue, and W. Pan, “Underwater localization and environment mapping using wireless robots,” *Wireless personal communications*, vol. 70, no. 3, pp. 1147–1170, 2013.

- [49] J. J. Leonard, A. A. Bennett, C. M. Smith, and H. J. S. Feder, "Autonomous underwater vehicle navigation," in *IEEE ICRA Workshop on Navigation of Outdoor Autonomous Vehicles, Leuven, Belgium, May*. Citeseer, 1998.
- [50] A. Nouredin, T. B. Karamat, and J. Georgy, "Inertial Navigation System," in *Fundamentals of Inertial Navigation, Satellite-based Positioning and their Integration*. Springer, 2013, pp. 125–166.
- [51] P. Corke, *Robotics, vision and control: Fundamental algorithms in MATLAB*, 73rd ed. Springer Science & Business Media, Berlin, 2011.
- [52] Stack Exchange. (2015). Gaussian Blur in Matlab and Connection to Image Resolution. [Online]. Available: <http://dsp.stackexchange.com/questions/16716/gaussian-blur-in-matlab-and-connection-to-image-resolution>
- [53] Mathworks. (2015). Documentation: imerode. [Online]. Available: <http://www.mathworks.com/help/images/ref/imerode.html>
- [54] S. Eddins. (2015). Dilation, erosion, and the morphological gradient. [Online]. Available: <http://blogs.mathworks.com/steve/2006/09/25/dilation-erosion-and-the-morphological-gradient>
- [55] Mathworks. (2015). Documentation: Edge Detection. [Online]. Available: <http://www.mathworks.com/discovery/edge-detection.html>
- [56] Mathworks. (2015). Documentation: imdilate. [Online]. Available: <http://www.mathworks.com/help/images/ref/imdilate.html>
- [57] N. A. P. Corporation. (2015). Benefits of PVC Pipe. [Online]. Available: <http://www.northamericanpipe.com/technical-info/benefits-of-pvc-pipe>
- [58] M. W. Uhle, "Design of an autonomous underwater vehicle to evaluate the blazed array sonar and simultaneous localization and mapping algorithms," Ph.D. dissertation, Massachusetts Institute of Technology, 2007.
- [59] Teledyne SeaBotix. (2015). vLBV and vLBC vectored Little Benthic Vehicles. [Online]. Available: <http://www.seabotix.com/products/vlbv300.htm>
- [60] B. Upadhaya, R. Munir, and Y. Blount, "Association between performance measurement systems and organisational effectiveness," *International Journal of Operations & Production Management*, vol. 34, no. 7, pp. 853–875, 2014.
- [61] C. M. Reed and A. J. Fenwick, "A consistent multi-user framework for assessing system performance," *arXiv preprint arXiv:1011.2048*, 2010.

- [62] J. C. Russ and R. P. Woods, “The image processing handbook,” *Journal of Computer Assisted Tomography*, vol. 19, no. 6, pp. 979–981, 1995.
- [63] H. Peyvandi, H. Roufarshbaf, M. Farrokhrooz, and S.-J. Park, *SONAR systems and underwater signal processing: Classic and modern approaches*. INTECH Open Access Publisher, 2011.

Initial Distribution List

1. Defense Technical Information Center
Ft. Belvoir, Virginia
2. Dudley Knox Library
Naval Postgraduate School
Monterey, California